REGULATION OF DOPAMINE RELEASE BY STRIATAL GABA AND ACETYLCHOLINE IN HEALTH AND DISEASE

DPhil in Physiology, Anatomy and Genetics

Emanuel Ferreira Lopes

Trinity Term 2019

St Edmund Hall, Oxford

Regulation of dopamine release by striatal GABA and acetylcholine in health and disease

Emanuel Lopes, St Edmund Hall

DPhil in Physiology, Anatomy and Genetics, Trinity Term 2019

Abstract

Dopamine (DA) signalling plays a central role in the normal functions of the basal ganglia, by helping facilitate behavioural processes such as action selection and reinforcement learning. Dysregulation of DA signalling is implicated in a diversity of neurological and psychiatric disorders including Parkinson's disease and addiction.

Striatal DA release is subject to major local influences besides action potentials generated in the soma. Striatal mechanisms have been shown to drive and gate axonal DA release. Understanding how these factors regulate DA signalling, and how they may be dysfunctional in disease states, is crucial for identifying novel disease therapies.

Firstly, this thesis will describe the role of striatal GABA in regulating DA release. The striatum is one of the most GABAergic nuclei in the brain, however, whether striatal GABA can modulate DA release is not understood. DA release, detected with fast-scan cyclic voltammetry from *ex vivo* striatal slices, was found to be inhibited by the activation of $GABA_A$ and $GABA_B$ receptors, independent of cholinergic input. GABA receptor antagonists enhanced DA release, indicating that DA release is under tonic inhibition by striatal GABA. Furthermore, ambient GABA manipulates short-term plasticity of DA release, and K^+-mediated changes in short-term plasticity require activity on GABA receptors.

I will then describe the implementation of several approaches to further our understanding of striatal ACh signalling. I will discuss the characterisation of a new mouse cross which will allow for the genetic targeting of striatal cholinergic interneurons (ChIs) within a parkinsonian disease state. These animals show normal parkinsonian deficits and are appropriate for the study of ChIs within the disease context. I will also describe the implementation and results of an immunohistochemical procedure for accessing ChI cell count and activity. This method reveals that parkinsonian mice have higher ChI counts but show less global activity. I also describe a method for detecting choline fluxes within striatal slices, as a proxy for ACh.

Finally, I will discuss a collaborative, standalone set of experiments exploring the impact of conditionally knocking out midbrain DA neuron-derived insulin-like growth factor 1 in striatal DA release. No changes in DA release were found within these animals.

The data presented in this thesis provide novel roles for GABA in the modulation of DA release. Furthermore, the implementation of several new methods for assessing changes in the cholinergic axis allow for further study of striatal ACh in both health and disease.

Table of contents

Statement of Authorship

This thesis contains no material that has been accepted for the award of any other degree in any University or other institution. All data represented in this thesis are wholly my own work, and where data has been contributed by other individuals, their contributions are noted below and within the main text.

The data represented in Chapter 3 are part of a wider study within the laboratory of Professor Stephanie Cragg, resulting in a first-authored publication:

Lopes E, Roberts B, Siddorn R, Clements M, Cragg S (2019) Inhibition of Nigrostriatal Dopamine Release by Striatal $GABA_A$ and $GABA_B$ Receptors. Journal of Neuroscience 39 (6) 1058-1065

As such, some of the data represented in Chapter 3 have been collected by Mr Bradley Roberts (DPhil student) and Ms Ruth Siddorn (MChem Student) and are provided with their full permissions. These data are identified in the corresponding figure legends.

Conference Abstracts and Manuscripts

Conference Abstracts:

Lopes E, Roberts B, Siddorn R, Cragg SJ. Modulation of nigrostriatal dopamine release by $GABA_{A/B}$ receptors. 13th International Basal Ganglia Society Meeting (2019; Biarritz, France; Poster).

Lopes E, Cragg SJ. The role of striatal GABA receptors in regulating dopamine release. 11th FENS Forum of Neuroscience (2018; Berlin, Germany; Poster).

Lopes E, Cragg SJ. The role of striatal GABA receptors in regulating dopamine release. 17th International Monitoring Molecules in Neuroscience Meeting (2018; Oxford, UK; Poster).

Manuscripts:

Roberts BM, Doig NM, Brimblecombe KR, **Lopes EF**, Ruth SE, Pasternack N, Wade-Martins R, Magill PJ, Cragg SJ (2019) Astrocytic striatal GABA transporter activity governs dopamine release and shows maladaptive downregulation in early parkinsonism. bioRxiv, 698274

Lopes EF, Roberts BM, Siddorn RE, Clements MA, Cragg SJ (2019) Inhibition of nigrostriatal dopamine release by striatal $GABA_A$ and $GABA_B$ receptors. Journal of Neuroscience 39: 1058-1065.

Pristerà A, Blomeley C, **Lopes E**, Threlfell S, Merlini E, Burdakov D, Cragg S, Guillemot F, and Ang S-L. Dopamine neuron-derived IGF-1 controls dopamine neuron firing, skill learning, and exploration. Proc Natl Acad Sci U S A. 2019 Feb 26; 116(9): 3817–3826.

Acknowledgments

I would like to take this opportunity to thank the many people who played a part in my DPhil journey. It has been one of the most rewarding and challenging experiences I have worked through, and it wouldn't be the same without everyone's help and support.

First, I would like to acknowledge all the support and encouragement provided by my supervisor, Professor Stephanie Cragg. My time as a doctoral student under Steph's supervision has been one of the most formative experiences in my life, in both a personal and professional sense. Steph's expertise, curiosity, and enthusiasm for research have helped me understand what makes a great scientist. I feel I have personally grown a lot in the lab, and a lot of it is due to Steph's mentorship.

I would like to thank all the members of the Cragg group, past and present, for all the great discussions and insights over the past four years. In particular, I would like to thank Drs Katherine Brimblecombe, Sarah Threlfell, and Mark Condon for training me in fast-scan cyclic voltammetry and for all the help and advice throughout these years. I would also like to thank Bradley Roberts, who was a great colleague to work alongside with on the GABA/DA experiments.

To all my friends and family, thank you for all the support and love over these past few years. From watching the sun set in Port Meadow, to rummaging through M&S to find the best reduced meals, to the countless meetings in cafés and pubs, this journey wouldn't be the same without you all.

I would also like to thank the Fundação de Ciência e Tecnologia for funding my DPhil and allowing me to carry out the work included in this thesis.

Finally, I would like to thank my parents, Carla and Eduardo. Your constant love and support have been a source of comfort and strength and have helped me get through the hardest of times. I grew up as you both worked on your respective PhDs, and I'm happy to report I'm almost there too.

Abbreviations

1p	Single pulse
2p	Paired pulse
AAV	adeno-associated virus
ACh	Acetylcholine
aCSF	Artificial cerebrospinal fluid
ALDH1a1	Aldehyde dehydrogenase type 1a1
Ca^{2+}	Calcium ion
$[Ca^{2+}]_o$	Extracellular concentration of calcium ions
CFM	Carbon fibre microelectrode
ChAT	Cholineacetyltransferase
ChOX	Choline oxidase
ChI	Cholinergic interneuron
ChR2	Channelrhodopsin-2
CPu	Caudate-putamen
D-APV	D-(2R)-amino-5-phosphonopentanoate
DA	Dopamine
$[DA]_o$	Extracellular concentration of dopamine
DAT	Dopamine transporter
DHβE	Dihydro-β-erythroidine
dMSN	Direct-pathway spiny projection neuron
DMSO	Dimethyl sulfoxide
EPSC	Excitatory postsynaptic current
eYFP	Enhanced yellow fluorescent protein
FCV	Fast-scan cyclic voltammetry
FSI	Fast spiking interneuron
GABA	γ-aminobutyric acid
GAT	Plasma membrane GABA transporter
GIRK	G protein-coupled inwardly-rectifying potassium channel
GPe	External segment of the globus pallidus
GPi	Internal segment of the globus pallidus
GWAS	Genome-wide association studies
HPLC	High-performance liquid chromatography
IPSC	Inhibitory postsynaptic current
IRES-Cre	Internal ribosome entry site-linked Cre-recombinase
iMSN	Indirect-pathway spiny projection neuron
K^+	Potassium ion
$[K^+]_o$	Extracellular concentration of potassium
L-DOPA	Levodopa
LED	Light-emitting diode
LTSI	Low-threshold spiking interneuron

mAChR	Muscarinic acetylcholine receptor
MCPG	α-Methyl-4-carboxyphenylglycine
NAc	Nucleus accumbens
nAChR	Nicotinic acetylcholine receptor
NPY	Neuropeptide Y
PBS-NaF	phosphate-buffered saline with sodium fluoride
PD	Parkinson's disease
PPR	Paired-pulse ratio
PV	Parvalbumin
S6RP	Ribosomal protein S6
SNc	Substantia nigra pars compacta
SNr	Substantia nigra pars reticulata
SNCA	human α-synuclein gene
Snca	mouse α-synuclein gene
SNCA-OVX	Human α-synuclein overexpressing mouse model of PD
STN	Subthalamic nucleus
STP	Short-term plasticity
TH	Tyrosine hydroxylase
TTX	Tetrodotoxin
UBE3A	Ubiquitin protein ligase E3A
VMAT2	Vesicular monoamine transporter type 2
VTA	Ventral tegmental area
WT	Wild-type

1. Introduction

This chapter aims to provide a summary of the research concerned with the interactions between dopamine (DA) and two striatal neurotransmitters: acetylcholine (ACh) and γ-aminobutyric acid (GABA) within the striatum. It will discuss the anatomy and function of the basal ganglia and striatum, before exploring the different striatal cellular populations in more detail. The anatomy and local striatal modulation of the mesostriatal DA neurons will then be discussed, before an overview of Parkinson's disease (PD) is provided.

1.1 Thesis overview

The striatum plays key roles in promoting motivated behaviours and learned actions. Nigrostriatal DA neurons release DA from immensely arborized structures, with each neuron forming ∼10^5 en passant varicosities and reaching ∼2.7% of striatum in rat (Matsuda et al., 2009). DA output is gated by numerous local axonal mechanisms and striatal neuromodulators that regulate or even drive DA release independently of midbrain activity (Sulzer et al., 2016). Understanding which mechanisms modulate axonal DA release and how they might be dysfunctional in diseases with DA dysregulation, such as PD and addictions, is critical for identifying novel therapeutic targets. (Sulzer et al., 2016).

The striatum is a predominantly GABAergic region, with a high density of projection neurons and interneurons that use this inhibitory neurotransmitter (Oorschot, 1996; Tepper et al., 2018). Striatal GABA receptors have been shown to modulate DA release, but this has not been extensively studied. Furthermore, extrasynaptic striatal GABA can accumulate to

exert a tonic inhibition of striatal neurons (Ade et al., 2008; Kirmse et al., 2008, 2009). However, whether striatal GABA receptors or the tonic GABA tone can modulate DA output has not elucidated. In this thesis, I explore the control of striatal DA release by local striatal GABA signalling **(Chapter 3)**.

Cholinergic interneurons (ChIs) play a particularly powerful role in gating and driving DA release through nicotinic ACh receptors (nAChRs) on DA axons (Jones et al., 2001b; Zhou et al., 2001; Rice and Cragg, 2004; Zhang and Sulzer, 2004; Threlfell et al., 2012). In **Chapter 4**, I will describe the setting up of several approaches to further our understanding of the striatal ACh/DA axis. Several lines of evidence suggest that ChIs may be altered in PD. I will discuss the characterisation of a new mouse cross which will allow for the genetic targeting of ChIs within a parkinsonian disease state. I will also describe the implementation and results from a new immunohistochemical procedure for ChI function and cell number. Finally, I will discuss the implementation of a method for measuring ACh fluxes indirectly by detecting choline within acute striatal slices.

Chapter 5 is a standalone chapter, where I explore the impact of conditionally knocking out midbrain DA neuron-derived insulin-like growth factor 1 (IGF-1) on striatal DA release. Peripheral hormones such as IGF-1 have been demonstrated to modulate neuronal function and development. However, it is not known whether these roles extend to DA axons. The background information for this chapter will be covered in detail within **Chapter 5**.

1.2 The striatum and the basal ganglia

The basal ganglia are a group of subcortical nuclei consisting of the striatum (caudate and putamen in primates), the internal and external segments of the globus pallidus, (GPi and GPe, respectively) the subthalamic nucleus (STN), and the substantia nigra pars reticulata and pars compacta (SNr and SNc, respectively). Classically, the basal ganglia have been widely studied within the context of motor function (Graybiel et al., 1994; Albin et al., 1995), but more recent evidence has highlighted a role for these nuclei in many aspects of behaviour such as cognition (Middleton and Strick, 2000), action selection (Nicola, 2007; Cisek and Kalaska, 2010), and learning (Knowlton et al., 1996; Schultz, 2006; Yin and Knowlton, 2006). Furthermore, dysfunctions in basal ganglia networks are involved in a number of neurological disorders such PD, Huntington's disease, and schizophrenia (Obeso et al., 2008).

The main input nucleus of the basal ganglia is the striatum. This nucleus receives excitatory and inhibitory inputs from a large range of brain regions, such as the thalamus, cortex, and dopaminergic/GABAergic projections from the ventral midbrain (DeLong and Wichmann, 2007). Inputs from these regions are integrated within the striatum, activating signalling pathways that project through the basal ganglia nuclei. These pathways form outputs that feedback to the cortex or midbrain, or project to regions including the hypothalamus, thalamus, and superior colliculus **(Figure 1.1)**. The topographic arrangement of these inputs into the striatum and maintenance throughout the nuclei of the basal ganglia forms a set of parallel loops that each support specific behavioural and cognitive functions (Alexander and Crutcher, 1990; Redgrave et al., 2010). However, these loops are not exclusively isolated as a degree of integration occurs at the level of the striatum and at other points in the signalling pathways (Joel and Weiner, 1994; Averbeck et al., 2014).

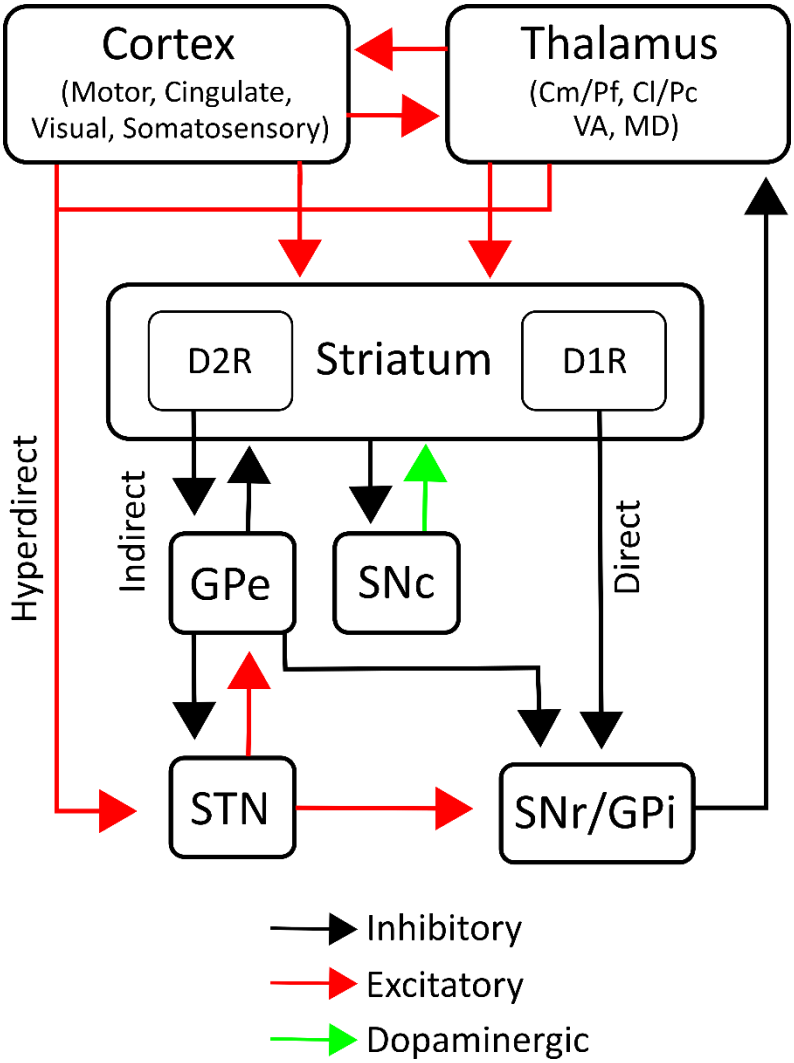

Figure 1.1 - Connectivity within the basal ganglia. A simplified representation of major signalling pathways between the cortex, thalamus, and the basal ganglia nuclei. Indirect pathway represents D_2 DA receptor (D_2R)-positive medium spiny neuron projections to GPe. Direct pathway represents D_1 DA receptor (D_1R)-positive medium spiny neuron projections to SNr/GPi. Thalamic nuclei: Cm/Pf, centromedian/parafascicular nuclei; Cl/Pc, central lateral/paracentral nuclei; VA, ventral anterior nucleus; MD, medial dorsal nucleus. Other nuclei: SNc, substantia nigra pars compacta, GPe, globus pallidus external segment; SNr/GPi, substantia nigra pars reticulata/globus pallidus internal segment; STN, sub-thalamic nucleus. Red projections are GABAergic inhibitory projections, green are glutamatergic excitatory projections and green are dopaminergic modulatory projections.

1.2.1 Anatomy and subdivisions of the striatum

As the main input region of the basal ganglia, the striatum is a complex structure that plays a role in several behaviours. The striatum can be divided based on connectivity, developmental differences, and functional differences. However, in rodents the striatum does not have clear anatomical boundaries. Instead, functional aspects of the striatum lie along gradients formed along dorsal-ventral, medial-lateral, and rostral-caudal anatomical axes (Voorn et al., 2004).

In this thesis, a distinction is drawn between the dorsal and ventral striatum, each playing distinct behavioural roles. The dorsal striatum, which consists of the caudate nucleus and putamen, has been thought to predominantly play a role in sensorimotor related functions (Knowlton et al., 1996; Packard and McGaugh, 1996; Packard, 1999; Yin et al., 2004, 2005; Quinn et al., 2013). The ventral striatum, which includes the nucleus accumbens (NAc), serves mainly as the limbic-motor interface participating in reward-based learning and motivated behaviours (Carlezon et al., 1995; Rodd-Henricks et al., 2002; Kalivas et al., 2003; Sellings and Clarke, 2003; Ikemoto, 2007).

While the cellular structure and function of the striatum is largely conserved between primates and rodents, the relative positioning of striatal structures varies significantly. In primates, the caudate nucleus and putamen are structurally and functionally distinct (Gerfen and Bolam, 2010). The caudate nucleus is found lateral of the anterior horn of the lateral ventricles, while the putamen sits more caudally, medial to the external capsule and lateral to the globus pallidus. These nuclei are separated by white matter of the internal capsule. The caudate nucleus primarily receives inputs from the prefrontal cortex, while putamen receives

primary inputs from motor and somatosensory cortex. The NAc is adjacent to the two structures, delineated by the ventromedial end of the internal capsule.

In rodents, the striatum is a continuous structure positioned ventrally of the external capsule and lateral to the dorsal horns of the lateral ventricles. The caudate nucleus and putamen are not segregated, forming one contiguous nucleus known as the caudate-putamen (CPu), and the anatomical boundaries between CPu and NAc are less evident. Despite the continuous nature of the striatal nuclei in rodents, the topographic pattern of afferent fibres remains similar to that exhibited in primates.

The striatum can also be subdivided by expression of certain biochemical markers, which corresponding to the striosome and matrix regions (Gerfen et al., 1987b, 1987a). Striosomes are characterised by high levels of μ-opioid receptor, D1-receptor, substance P and calretinin, whereas matrix regions can be distinguished by a higher expression of calbindin and acetylcholinesterase (Graybiel and Ragsdale, 1978; Besson et al., 1988; Sakamoto et al., 1992; Crittenden and Graybiel, 2011). The matrix comprises approximately 85% of the striatal complex, while the striosome represents the remaining 15%. The functional implications of these striatal subdivisions are not yet fully understood; however, they are known to differ in terms of their development, circuitry, and disease susceptibility (Graybiel and Ragsdale, 1978; Crittenden and Graybiel, 2011).

1.2.2 Cellular composition of the striatum

The largest population of neurons in the striatum are the GABAergic medium-sized spiny neurons (MSNs), also known as spiny projection neurons (SPNs), comprising approximately 95% of striatal neurons (Kemp and Powell, 1971; Graveland and Difiglia, 1985;

Smith and Bolam, 1990; Bolam et al., 2000). MSNs are the main input and output neurons in the striatum, integrating afferent inputs with local synaptic and neuromodulatory signalling, and projecting to downstream basal ganglia nuclei. The primary axons of MSNs project out of the striatum to the globus pallidus and SNr (Kawaguchi et al., 1990). These neurons also project local collateral axons (Somogyi et al., 1981) which mediate a network of inter-inhibition, such that stimulation of a given MSNs has the ability to inhibit surrounding MSNs (Tunstall et al., 2002; Guzmán et al., 2003).

MSNs switch between periods of low and high excitability known as up- and down-states (Wilson and Groves, 1981; Wilson and Kawaguchi, 1996). The resting down-state, characterised by a hyperpolarised resting membrane potential, occurs due to abundant expression of inwardly-rectifying potassium (K^+) channels (Nisenbaum and Wilson, 1995). Switching between these states is dependent on simultaneous activity in excitatory synaptic inputs (Wilson and Kawaguchi, 1996), which activate a calcium (Ca^{2+})-dependent process in the distal dendrites of MSNs (Plotkin et al., 2011). As glutamate receptors rapidly desensitise with any given synaptic contact, concurrent inputs from distinct projections produce the greatest excitatory effect on MSN activity and as such MSNs are well-adapted to integrate excitatory input from multiple sources (Carter et al., 2007).

Excitatory inputs to MSNs mainly arise in the cortex and thalamus (Nauta, 1979; Somogyi et al., 1981; Guo et al., 2015). Excitatory projections form asymmetric glutamatergic synapses onto MSNs (Doig et al., 2010) but differ regarding their subcellular targets (Dubé et al., 1988; Smith et al., 1994). Inputs from MSNs also arise from other basal ganglia nuclei, including GPe (Bevan et al., 1998; Guo et al., 2015; Saunders et al., 2016), and other brain

regions such as the hippocampus, amygdaloid complex and the dorsal raphe nuclei (Voorn et al., 2004; Wall et al., 2013; Guo et al., 2015).

Two major populations of MSN can be defined on basis of their projection targets and expression of D_1 or D_2 receptor types (Albin et al., 1989; Gerfen et al., 1990; Surmeier et al., 1996). Direct-pathway MSNs (dMSNs) express D_1-type DA receptors and send monosynaptic projections to the output nuclei of the basal ganglia, the GPi, and the SNr. Activation of dMSNs therefore inhibits neurons in the GPi and SNr and consequently disinhibits the activity in the target regions of those outputs. Indirect-pathway MSNs (iMSNs) express D_2-type DA receptors and project to the GPe, synapsing onto neurons that project to the GPi and SNr. Activation of iMSNs therefore inhibits neurons in the GPe, disinhibiting GPi neurons, and consequently inhibiting activity in target regions of basal ganglia output.

Simply put, the roles of the direct- and indirect-striatal output pathways are to promote particular actions by disinhibition of the relevant basal ganglia targets, and to inhibit possible ongoing actions by parallel inhibition of alterative targets (Alexander and Crutcher, 1990; Nelson and Kreitzer, 2014). In support of this, the selective activation of dMSNs promotes initiation and maintenance of movement, while activation of iMSNs results in freezing behaviour (Kravitz et al., 2010; Freeze et al., 2013). Additionally, selective ablation of dMSNs or iMSNs leads to hypolocomotion and hyperlocomotion, respectively, and results in impaired motor learning in both cases (Durieux et al., 2012). However, it is widely accepted that this model is largely oversimplified and does not account for all basal ganglia functions, and the role of these subpopulations is not yet fully understood.

1.2.3 Striatal GABAergic interneurons

In addition to MSNs, the remaining 5% of striatal neurons consist of a number of biochemically and physiologically distinct interneurons (Tepper and Bolam, 2004). With exception of ChIs, which signal through ACh, the remaining interneuron types are GABAergic.

The most extensively-characterised GABAergic striatal interneuron is the fast-spiking interneuron (FSI), also known as PV+ interneurons due to their expression of the calcium-binding protein parvalbumin (PV) (Kawaguchi, 1993). FSIs receive excitatory inputs from sensory and motor cortices (Ramanathan et al., 2002), and inhibitory input from PV-expressing projection neurons in the GPe (Bevan et al., 1998; Saunders et al., 2016) and ChIs (Chang and Kita, 1992). FSIs mediate a powerful rapid feed-forward inhibition of MSNs (Koós and Tepper, 1999; Koos et al., 2004). These interneurons are also unique in that they form electrical synapses with neighbouring FSIs via gap junctions, allowing for fast electrical signalling which promotes synchrony throughout the population (Kita et al., 1990; Koós and Tepper, 1999; Hjorth et al., 2009).

Another population of GABAergic striatal interneurons are the low-threshold spiking interneurons (LTSIs) that express somatostatin and neuropeptide Y (NPY). LTSIs synapse onto distal dendritic spines of MSNs (Kubota and Kawaguchi, 2000) and partake in reciprocal connections with neighbouring ChIs (Elghaba et al., 2016; Straub et al., 2016). LTSIs demonstrate prolonged plateau potentials in response to depolarisation, fire action potentials at low thresholds and exhibit autonomous firing in striatal slices (Bennett and Wilson, 1999; Beatty et al., 2012) and *in vivo* (Sharott et al., 2012). LTSIs are suggested to play an important role in goal-directed learning (Holly et al., 2019). A number of other minor populations of GABAergic interneurons have been identified in the striatum (Tepper et al.,

2018), but their physiological properties and roles within the striatum are less well-characterised.

1.2.4 Striatal cholinergic interneurons

The first striatal interneuron population to be described, ChIs are identified by their characteristically large soma and lack of dendritic spines (Kawaguchi, 1993). While distributed across the striatum, ChIs exhibit decreasing density along the anterior-posterior axis (Matamales et al., 2016). In contrast to other striatal interneuron populations, ChIs are not primarily GABAergic, and instead release ACh. However, a recent study has demonstrated that approximately half of all ChIs are capable of co-releasing GABA (Lozovaya et al., 2018).

While ChIs make up only approximately 1% of total striatal neurons, ChIs have an enormous influence throughout the striatum due to their extensive dendritic trees, dense axonal arbours, and large number of vesicle-containing varicosities (Hoover et al., 1978; Kawaguchi, 1993). ChIs autonomously fire in the absence of neuronal input due to an intrinsic pacemaker mechanism, and as such are tonically active in striatal slice preparations (Bennett and Wilson, 1999). ChIs input directly onto MSNs, with symmetric synapses distributed between the soma, dendrites, and spines (Izzo and Bolam, 1988). ChIs support corticostriatal plasticity in MSNs through activation of M4 receptors on these neurons (Pakhotin and Bracci, 2007; Pancani et al., 2014). ChIs have been suggested to operate through point-to-point synaptic transmission but are also thought to partially operate though non-synaptic volume transmission of ACh (Contant et al., 1996; Descarries et al., 1997). ACh exerts its postsynaptic effect at nAChRs, which are fast ligand-gated cation channels, and muscarinic ACh receptors (mAChRs), which are modulatory G-protein coupled receptors. Cholinergic signalling also

exerts powerful control over striatal DA release through action at nAChRs, this will be discussed in **Section 1.4.1**.

The wide-ranging effects that ChIs mediate on striatal processing have generated a great degree of interest in understanding the role of striatal ChIs in the normal functioning of the basal ganglia. ChIs encode behaviourally salient events, such as novel/unexpected and motivationally relevant events, including contextual information about action performance (Graybiel et al., 1994; Calabresi et al., 2000; Apicella, 2002, 2007; Kimura et al., 2003). In response to certain environmental stimuli, these neurons exhibit a characteristic firing pattern comprised of an initial increase in firing rate, followed by a pause, and in some occasions a rebound excitation. The behavioural role of this response is not fully understood but is temporally coincident with phasic activity in DA neurons (Morris et al., 2004), suggesting an interaction between these two neurotransmitters during signalling of reward-related events.

1.3 The mesostriatal dopamine system

Midbrain DA neurons form projections to various brain regions, including various cortical areas (such as the primary motor and sensory cortex), striatum, amygdala, hippocampus, septum, lateral habenula and sub-thalamic nucleus, among others (Yetnikoff et al., 2014). DA neurons densely innervate the striatum, and DA receptors are expressed throughout the region supporting the wide-ranging actions of DA on striatal function. This section will briefly review the anatomical characteristics and physiological properties of midbrain DA neurons, the regulation of striatal DA signalling, and the roles of mesostriatal DA signals in behaviour.

1.3.1 Midbrain dopamine nuclei

Several populations of DA neurons are found in multiple anatomical regions, and the main populations that project to the striatum are the SNc and the ventral tegmental area (VTA) (Björklund and Dunnett, 2007). The SNc is subdivided into a dorsal tier, in which DA neurons express the calcium buffer calbindin, and a ventral tier, which is calbindin-negative, leading to an increased susceptibility to degeneration in PD (Yamada et al., 1990). The dorsal tier is continuous with the VTA, in which DA neurons are also calbindin-positive (Lavoie and Parent, 1991).

While the principal cells of the midbrain nuclei are dopaminergic, these regions also contain smaller populations of GABAergic projection neurons (Nair-Roberts et al., 2008). These neurons make local connections within the midbrain (Ciccarelli et al., 2012), and project to target structures including the NAc (Van Bockstaele and Pickel, 1995). The role of these GABAergic projection neurons is not understood, but they have been shown to contribute to mesostriatal reward signalling, particularly the encoding of aversive stimuli (Tan et al., 2012; van Zessen et al., 2012).

1.3.2 Anatomy and physiology of mesostriatal DA neurons

Ventral midbrain nuclei DA neurons send axonal projections to forebrain targets. These projections are generally described in terms of three major projection pathways: the nigrostriatal pathway, projecting to the dorsal striatum; the mesolimbic pathway, projecting mainly to the NAc, amygdala, olfactory tubercle and septum; and the mesocortical pathway, projecting mainly to the cingulate, prefrontal and perirhinal cortical areas (Yetnikoff et al., 2014). These projections arise from distinct populations of DA neurons which are

differentially distributed between midbrain nuclei, although there is overlap in the anatomical locations of these groups. While DA neurons of the SNc and VTA project mainly to CPu and NAc respectively (Ungerstedt, 1971), there is some crossover as a subset of the projections to CPu arise from neurons in the VTA (Aransay et al., 2015), and similarly some projections to NAc originate in SNc (Björklund and Dunnett, 2007). This overlap is partially explained by the diverse projection targets of calbindin-positive projections from dorsal tier SNc, which include both dorsolateral CPu and NAc (Lavoie et al., 1989; Prensa and Parent, 2001).

Each DA neuron has a single thin, unmyelinated axon that projects from the shaft of a principle dendrite, rather than from the cell body (Tepper et al., 1987). These axons project through the dorsal part of the medial forebrain bundle, a loose collection of white matter projecting from the midbrain through the lateral hypothalamus to the olfactory tubercle (Ungerstedt, 1971; Nauta et al., 1978; Beckstead et al., 1979). Within the dorsal striatum, nigrostriatal DA axons branch extensively to form a dense axonal arbor, estimated to contain up to 25,000 branch points, with a total membrane length up to 780 mm in the rat (Matsuda et al., 2009; Pissadaki and Bolam, 2013). These complex and dense axonal arbors are crucial sites for the local regulation of DA release, separate from mechanisms that govern action potential generation in the midbrain.

DA neurons generate relatively broad action potentials at frequencies up to 10 Hz, with an average tonic firing rate of approximately 4 Hz (Grace and Bunney, 1984a; Clark and Chiodo, 1988; Lacey et al., 1989). This tonic firing is dependent on an intrinsic ionic pacemaking mechanism, in which Na^+ and Ca^{2+} channels gradually drive membrane to a spiking threshold (Bean, 2007; Chan et al., 2007; Puopolo et al., 2007). DA neurons also demonstrate firing bursts interspersed within the tonic activity of 2-5 spikes at 10-40 Hz

(Grace and Bunney, 1984a, 1984b), with bursts up to 100 Hz also reported (Hyland et al., 2002). Burst firing is thought to be mainly generated via activation of NMDA receptor (Charlety et al., 1991) thought to be driven by excitatory synaptic inputs from areas including the pedunculopontine nucleus (Lokwan et al., 1999; Floresco et al., 2003) and the STN (Smith and Grace, 1992; Chergui et al., 1994).

At the level of the midbrain, the firing frequency of DA neurons is correlated to DA release in the striatum (Suaud-Chagny et al., 1992). Burst firing at an average frequency of 20 Hz in populations of DA neurons has been shown to increase average extracellular levels of DA ($[DA]_o$) in striatum approximately 3-10 fold in comparison to tonic firing, depending on the duration of the burst (Dreyer et al., 2010). However, the combination of heterogeneity in the properties of DA neurons and local regulatory mechanisms within the striatum complicate the exact relationship between somatic firing rates, and striatal DA release is therefore complex and regionally variable.

1.3.3 Dopamine receptors

DA mediates its postsynaptic effects by binding and activating of DA receptors. There are five known types of DA receptors, D_1-D_5, all of which are metabotropic G-protein-coupled receptors. These receptors fall into two families; D1-type, comprising D_1 and D_5, and D_2-type, comprising D_2, D_3 and D_4 (Beaulieu and Gainetdinov, 2011). D_1-like receptors are $G_{\alpha s}$ coupled, which increases the activity of adenylyl cyclase (AC) causing increased levels of cyclic adenosine monophosphate production. D_2-like receptors are $G_{\alpha i}$ coupled, which inhibits AC and decreases cyclic adenosine monophosphate production. D_2 receptors facilitate different effects of DA signalling depending on their splice variant; the D_2S variant is expressed

presynaptically and functions as an inhibitory autoreceptor, while the D_2L variant mediates inhibitory postsynaptic effects (Usiello et al., 2000; Beaulieu and Gainetdinov, 2011). Splice variants of D_3 and D_4 receptors have also been described (Beaulieu and Gainetdinov, 2011), although their roles in striatal DA signalling have not yet been fully defined.

DA neurons express D_2 autoreceptors at the soma and at axonal release sites. Activation of somatic D_2 receptors leads to opening of G-protein linked inwardly-rectifying K^+ (GIRK) channels, which mediate a hyperpolarising outward current (Lacey et al., 1988; Beckstead et al., 2004), while at axonal release sites it has been suggested that D_2Rs mediate their actions through voltage-gated K^+ channels (Cass and Zahniser, 1991; Congar et al., 2002; Martel et al., 2011).

As mentioned previously, the two main MSN subpopulations differentially express D_1 and D_2 receptors. Consequently, the effect of DA signalling on striatal processing is to modulate the balance between these parallel processing systems.

D_1 receptor activation promotes MSN firing activity during up-states by activating L-type Ca^{2+} channels (Hernández-López et al., 1997; Vergara et al., 2003), while D_2 receptors reduce L-type currents and activate hyperpolarising K^+ currents (Hernández-López et al., 1997; Vergara et al., 2003). Additionally, activation of D_1 receptors can prolong up-states in direct-pathway MSNs, while activation of D_2 receptors shortens up-states in indirect-pathway MSNs (Plotkin et al., 2011). Therefore, DA signalling directly and differentially modulates excitability in the two main pathways.

In addition, DA can regulate the strength of excitatory inputs onto MSNs. Studies on the effect of DA on corticostriatal plasticity in slice preparations have provided inconsistent results, showing patterns of long-term potentiation and depression that are highly dependent

on cell type-specific localisation of DA and ACh receptors (Reynolds and Wickens, 2002; Calabresi et al., 2007). However, the importance of this DA-mediated modulation of corticostriatal plasticity has been demonstrated by its roles in learning and motor function (Reynolds et al., 2001; Picconi et al., 2003). This regulation of synaptic plasticity is likely to influence the transitions of MSNs between up- and down-states, providing another mechanism by which DA can modulate striatal output to downstream basal ganglia nuclei.

1.3.4 Regulation of striatal neurons by DA release

Striatal DA also regulates the activity of local interneurons. ChIs in both CPu and NAc express inhibitory D_2 receptors (Alcantara et al., 2003) that reduce ACh release (Stoof et al., 1987), an effect that appears to be more pronounced in CPu than in NAc (Henselmans and Stoof, 1991). Activation of D_2 receptors activates a hyperpolarising current in ChIs (Straub et al., 2014), reduces pacemaker frequency by modulation of voltage-gated Na^+ channels (Maurice et al., 2004), and inhibits release by limiting Ca^{2+} entry (Yan et al., 1997). Conversely, activation of D_1 receptors appears to increase striatal ACh release (Damsma et al., 1991; Imperato et al., 1992; Consolo et al., 1999), although the mechanism by which this occurs remains unclear, since only a small fraction of ChIs are thought to express D_1 receptors (Le Moine et al., 1991). D_5 receptors are widely expressed on striatal GABAergic interneurons, including PV-positive, NPY/somatostatin/NOS-positive, calretinin-positive, and ChIs (Rivera et al. 2002). Their main impact on ChIs is predominantly thought to be indirect, through enhancing GABAergic inhibition of ChIs (Yan and Surmeier, 1997; Rivera et al., 2002). A fraction of NPY/somatostatin/NOS-positive neurons are also thought to express D_1 receptors (Le Moine et al., 1991).

DA is therefore optimally positioned to mediate wide-ranging modulation of striatal processing. Therefore, determining what factors shape DA release is of considerable importance in understanding the modulatory actions of striatal DA.

Long-term plasticity of corticostriatal synapses may play a crucial role in striatal action selection reinforcement. Selectively activating specific subsets of MSNs from both pathways may differentially weight basal ganglia processing toward selection of specific actions while inhibiting alternative actions (Freeze et al., 2013; Cui et al., 2014). Changes in the weighting of excitatory inputs to the striatum, caused by modulation of long-term plasticity at synapses onto MSNs, is consequently thought to support the selection and reinforcement-based learning of actions (Yin et al., 2009).

The mechanisms underlying expression of different forms of long-term plasticity at these synapses are not fully understood. In both slice and *in vivo* preparations, different forms of plasticity have been induced depending on the experimental preparation, stimulation protocol and manipulations of DA signalling (Reynolds and Wickens, 2002; Kreitzer and Malenka, 2008). However, a common factor that has been identified is the importance of DA signalling (Calabresi et al., 1997; Wang et al., 2006; Kreitzer and Malenka, 2007), leading to the suggestion that phasic DA release gates the induction of corticostriatal plasticity which is required for reward-related reinforcement of actions (Reynolds et al., 2001; Fisher et al., 2017). This gating is thought to depend on both the timing and magnitude of striatal DA release (Arbuthnott and Wickens, 2007; Thivierge et al., 2007).

Understanding factors that govern striatal DA release in response to presynaptic activity is crucial in understanding the complex circuit-level physiology of the striatum, and the role of striatal processing in basal ganglia function.

1.3.5 Behavioural roles of striatal DA release

Early work characterising the behavioural role of DA was guided by the discovery of DA depletion in PD, which results in motor dysfunction (Ehringer and Hornykiewicz, 1960). Furthermore, early studies report increased DA neuron firing on initiation of actions (Romo and Schultz, 1990). More recent studies further support the link between DA and motor function: a subset of DA neurons signal postural adjustments with a pause in firing (Dodson et al., 2016), and DA axons in the dorsal striatum signal the onset of movement (Howe and Dombeck, 2016).

Striatal DA has also been implicated in reward-related learning. Single-unit recordings from midbrain DA neurons from awake behaving animals show phasic increases in firing upon the presentation of an unexpected reward (Schultz and Romo, 1990). When the reward is paired with a predictive cue, such as a visual stimulus or auditory tone, the timing of this phasic increase in firing is moved to the presentation of the cue and away from the presentation of the reward (Schultz and Romo, 1990; Mirenowicz and Schultz, 1994; Schultz et al., 1997). The mechanism underlying this shift may involve changes in the synaptic strength of specific excitatory inputs on DA neurons (Stuber et al., 2008). Furthermore, the response to the reward is scaled on reward size (Mirenowicz and Schultz, 1996; Morris et al., 2004; Schultz, 2007) and corresponds with an increase in extracellular DA in the NAc (Phillips et al., 2003; Roitman et al., 2004; Day et al., 2007). Therefore, release of striatal DA plays a central role in many behaviours including movement, motivation, and reward.

1.3.6 Release of other primary neurotransmitters from DA axons

In addition to the synthesis and release of DA, some dopaminergic neurons have the capacity to release glutamate (Chuhma et al., 2004; Stuber et al., 2010; Tecuapetla et al., 2010; Adrover et al., 2014) and/or GABA (Tritsch et al., 2012; Nelson et al., 2014; Kim et al., 2015) from axonal release sites. Release of multiple neurotransmitters or neuropeptides from the same neuron has been shown in other neuronal populations (Seal and Edwards, 2006; Vaaga et al., 2014).

Co-release occurs when multiple neurotransmitters are released by a single neuron in response to an action potential (Vaaga et al., 2014; Tritsch et al., 2016). Vesicle pools may be localised to the same release site but differentially regulated, spatially segregated to different subcellular sites within the axon, or possibly a combination of both (Lee et al., 2010). The term co-transmission refers to release of multiple transmitters from the synapse of a single cell and additionally implies that both neurotransmitters contribute to synaptic transmission by evoking a postsynaptic response in the same postsynaptic cell (Burnstock, 2004). Therefore, co-release does not result in co-transmission, for example, if the postsynaptic cell does not express receptors for both neurotransmitters.

Within the striatum, glutamate co-transmission was evoked in the NAc and olfactory tubercle by optical activation of DA axons (Stuber et al., 2010). The resulting glutamate-mediated excitatory postsynaptic currents (EPSCs) in MSNs were only observed with ventral striatal regions, with no glutamate co-transmission or glutamatergic markers observed in the dorsal striatum (Stuber et al., 2010; Mingote et al., 2015). More recent studies, however, reported monosynaptic EPSCs in MSNs and ChIs in the dorsal striatum with DA axon activation (Tritsch et al., 2012; Chuhma et al., 2018). A subset of midbrain DA neurons, primarily in the

VTA, express the vesicular glutamate transporter type 2 which could explain the regional heterogeneity in glutamate co-release (Kawano et al., 2006; Mendez et al., 2008). VGluT2-positive axonal segments form asymmetric synapses on MSNs spines separate to the symmetric synapses formed by TH-positive DA release sites (Descarries et al., 2008; Zhang et al., 2015). In addition to mediating EPSCs, packaging of glutamate into DA vesicles can promote DA storage, through the effects of VGluT2 on the proton gradient that drives DA accumulation through the vesicular monoamine transporter (VMAT) (Hnasko et al., 2010). Similar effects are also reported for glutamate on vesicular ACh co-storage in striatal ChIs (Gras et al., 2008).

The role of glutamate co-transmission in basal ganglia function is unclear. Mice with conditional deletions of VGluT2 in DA neurons have reduced DA release in NAc, leading to a reduction in cocaine induced hyperlocomotion (Hnasko et al., 2010). Additionally, mice with the conditional heterozygous reduction of the glutamate recycling enzyme glutaminase in DA neurons show normal emotional and motor behaviours and show an unaffected response to acute amphetamine. These mice are less sensitive to amphetamine and potentiated latent inhibition, suggesting that glutamate co-release might be important in attribution of motivational salience (Mingote et al., 2017). In the dorsal medial shell of the NAc, glutamate release from DA axons make strong excitatory connections onto ChIs to drive burst firing (Chuhma et al., 2018).

GABA release from DA neurons has been more recently discovered and is less well-described than glutamate co-transmission. Selective activation of DA neurons has been shown to evoke $GABA_A$ receptor-mediated inhibitory postsynaptic currents (IPSCs) in MSNs, in both CPu and NAc (Tritsch et al., 2012, 2014). The existence of GABA co-release is further

supported by ultrastructural data showing localisation of GABA to VMAT- and TH-positive striatal boutons (Stensrud et al., 2013). GABA is thought to be co-stored and released from DA vesicles as GABAergic IPSCs were dependent on VMAT2 (Tritsch et al., 2012). Synthesis of GABA in canonical GABAergic neurons is typically mediated by glutamate decarboxylase, but only a small number of DA neurons show expression of this enzyme (Tritsch et al., 2014). Instead, GABA co-release in DA neurons is thought to be maintained by a combination of uptake through the plasma membrane GABA transporter (GAT) and synthesis through an alternative pathway, mediated by aldehyde dehydrogenase 1a1 (ALDH1a1) (Tritsch et al., 2014; Kim et al., 2015).

GABA co-release has been shown to have a role in striatal-dependent reward-seeking behaviour. Reduced GABA co-release through conditional reductions in ALDH1a1 expression in DA neurons leads to enhanced alcohol consumption and preference in mice, and GABA co-release is dampened by ethanol concentrations seen in blood alcohol after binge drinking (Kim et al., 2015). Furthermore, conditionally knocking out the Ubiquitin protein ligase E3A (UBE3A) from DA neurons impairs GABA co-release from DA axons in the ventral striatum and enhances reward-seeking behaviour assessed through optical self-stimulation (Berrios et al., 2016). The genetic ablation of ALDH1a1 been reported to substantially increases DA release exclusively in striosomes in mouse dorsal striatum (Sgobio et al., 2017), potentially underlying increased reward-seeking behaviour when GABA co-release is diminished.

1.4 Local striatal modulation of DA release

Control of DA release in the striatum is linked to firing of DA neurons in the level of the soma (Suaud-Chagny et al., 1992; Dreyer et al., 2010). However, local influences in the striatum can affect release by exerting their action directly on axon terminals.

1.4.1 Striatal cholinergic control of DA release

The release of ACh from ChIs exerts powerful control of DA release at the level of the striatum. DA axons express nAChRs that contain the β2 subunit (Jones et al., 2001b) which when activated promotes powerful short-term depression of DA release such that release is largely insensitive to the frequency or duration of presynaptic stimulation (Rice and Cragg, 2004; Zhang and Sulzer, 2004). When these receptors are inhibited, desensitised, or genetically deleted, the amount of released DA becomes closely correlated to stimulation frequency. The activation state of nAChRs *in vivo* remains unclear, as these receptors are readily desensitised by agonists; however, blockade of nAChRs has been shown to enhance DA release in response to events predicted to trigger phasic activity in DA neurons (Collins et al., 2016). This suggests that nAChRs are tonically activated rather than desensitised under physiological conditions.

Furthermore, synchronous activation of ChIs with optogenetic techniques can evoke DA release events independently of midbrain or presynaptic activity (Cachope et al., 2012; Threlfell et al., 2012). When DA release is evoked simultaneously with ChI activation, for example during local electrical stimulation of striatal tissue, DA release is greater than when nAChRs are blocked (Zhou et al., 2001). While this finding was initially interpreted as control of DA release probability by nAChR activation state, these transients are now thought to be a

composite of two release events; an initial event driven by activation of DA terminals, followed by a longer-latency event triggered by synchronous activation of local ChIs (Wang et al., 2014; Shin et al., 2015).

DA release is also regulated by activation of mAChRs. DA neurons in SNc are thought to express M5-type mAChRs (Vilaró et al., 1990; Weiner et al., 1990), which enhance DA release when activated in the striatum (Shin et al., 2015) through a mechanism that may involve changes in Ca^{2+} mobilisation (Foster et al., 2014). mAChRs are also expressed on ChIs and show region-specific expression; in dorsal striatum, M2 and M4 receptors inhibit ACh release, while in NAc this function is exclusively performed by M4 receptors (Threlfell et al., 2010). Activation of mAChRs in striatum can therefore have different roles. Depending on the pattern of activation, mAChRs can either promote DA release or reduce ACh release, therefore limiting DA release while enhancing sensitivity to the frequency of presynaptic activity.

1.4.2 Striatal GABAergic control of DA release

GABA is the primary inhibitory neurotransmitter in the adult mammalian brain. GABA activates both ionotropic $GABA_A$ receptors and metabotropic G-protein coupled $GABA_B$ receptors to mediate inhibition. In the central nervous system, two forms of GABAergic inhibition co-exist to modulate the excitability of neuronal networks: phasic and tonic inhibition (Farrant and Nusser, 2005). Within the striatum, an ambient GABA tone provides tonic inhibition to principal striatal neurons though action at $GABA_A$ and $GABA_B$ receptors.

$GABA_A$ receptors are pentameric ligand-gated ion channels that undergo a conformational change upon agonist binding, increasing membrane permeability to chloride

and bicarbonate ions. In most mature neurons, this leads to a net inward flow of anions resulting in a hyperpolarising postsynaptic response and reduced neuronal activity. $GABA_A$ receptors can facilitate both phasic and tonic inhibition depending on the synaptic or extrasynaptic cellular location of their expression, and the biophysical properties of the $GABA_A$ subunits that make up the receptor.

$GABA_B$ receptors are chloride-independent receptors that mediate inhibition by heterotrimeric G-protein activation. $GABA_B$ receptors regulate neuron excitability through their locations both presynaptically and postsynaptically. Presynaptic $GABA_B$ receptors generally suppress neurotransmitter release by inhibiting calcium channels at the nerve terminal (Ulrich and Bettler, 2007), but second-messenger-mediated effects can also retard release by modulating synaptic vesicle priming (Sakaba and Neher, 2003). Postsynaptic $GABA_B$ receptors exert their effects through activating Kir3-type potassium channels, which hyperpolarise the membrane and shunts excitatory currents (Ulrich and Bettler, 2007). In addition to $GABA_A$ receptors, presynaptic $GABA_B$ receptors can also be under tonic activation by low concentration extrasynaptic GABA to tonically gate probability of neurotransmitter release (Le Feuvre et al., 1997; Kirmse and Kirischuk, 2006; Mapelli et al., 2009; Dvorzhak et al., 2010; Laviv et al., 2010).

Striatal GABA is in a key position to directly modulate DA output. The average arbour of a given rat nigrostriatal DA neuron, which reaches ~3% of striatal volume (Matsuda et al., 2009), encompasses ~70,000 GABAergic neurons (Oorschot, 1996). Furthermore, ultrastructural studies in monkey and rat striatum report $GABA_B$ receptors on structures that resemble DA axons (Charara et al., 1999; Yung et al., 1999). Conversely, there is a little evidence of GABAergic axoaxonic synapses on DA axons (Charara et al., 1999) but it should

be noted that extrasynaptic ambient GABA might spill over onto DA axons. Furthermore, there is evidence that GABA could modulate DA release indirectly through ChIs, which express both $GABA_A$ and $GABA_B$ receptors (Waldvogel et al., 1998; Yung et al., 1999).

There is a variety of previous evidence indicating that striatal $GABA_A$ and $GABA_B$ receptors can modulate DA release, but this interaction has not yet been extensively studied. Striatal administration of pregnanolone, a positive allosteric modulator of the $GABA_A$ receptor, or bicuculline, a $GABA_A$ antagonist, respectively decreased and increased extracellular DA levels in intact rats measured by microdialysis *in vivo* (Smolders et al., 1995). Muscimol, a $GABA_A$ agonist, has been shown to inhibit DA release from striatal synaptosomes prepared from rat striatum (Ronken et al., 1993). A $GABA_A$-mediated enhancement of DA release in acute *ex vivo* striatal guinea pig slices has also been described, this is hypothesised to arise indirectly via inhibition of H_2O_2 release from MSNs during prolonged train stimulations (Avshalumov et al., 2003). Striatal administration of baclofen, a $GABA_B$ receptor agonist, or phaclofen, a $GABA_B$ receptor antagonist, respectively decreased and increased extracellular DA levels in intact rats measured by microdialysis *in vivo* (Smolders et al., 1995). Furthermore, striatal perfusions of baclofen decreased electrically evoked DA release in acute *ex vivo* slices of mouse CPu (Schmitz et al., 2002) and NAc (Pitman et al., 2014).

These findings suggest that an endogenous striatal GABA source might locally modulate DA output though action at GABA receptors on DA axons, however, further evidence is required. Pharmacological agonists for $GABA_A$ and $GABA_B$ receptors might induce a nonphysiological attenuation in DA output, and might not reveal a physiologically relevant role, like antagonists do. Previous studies which use antagonists are conducted using an *in vivo* approach (Smolders et al., 1995), which are confounded by potential effects on long loop

extrasynaptic effects that could regulate striatal DA output via changes in midbrain DA firing. Furthermore, these studies do not rule out indirect actions of GABA receptors to modulate DA release though, for example, acting at ChIs which express both $GABA_A$ and $GABA_B$ receptors (Waldvogel et al., 1998; Yung et al., 1999). ChIs can also mediate effects of other neuromodulators on DA release, including opioids, nitric oxide, glutamate, and insulin (Britt and McGehee, 2008; Hartung et al., 2011; Stouffer et al., 2015; Kosillo et al., 2016). Whether striatal GABA signalling can modulate DA release through direct actions at putative $GABA_A$ and $GABA_B$ receptors on DA axons is tested in **Chapter 3.**

1.4.3 Striatal extrasynaptic GABA tone

Within the striatum, where GABAergic neurons constitute most of the neuronal population (Oorschot, 1996), a sizeable ambient GABA tone provides tonic inhibition of MSNs at $GABA_A$ and $GABA_B$ receptors. A tonic $GABA_A$ receptor-mediated inhibitory conductance has been recorded in MSNs from acute mouse brain slices as depolarising shifts in the baseline currents in response to $GABA_A$ receptor block (Ade et al., 2008; Kirmse et al., 2008, 2009; Janssen et al., 2009; Santhakumar et al., 2010; Cepeda et al., 2013; Tritsch et al., 2014). In adult mice, MSNs express extra- and perisynaptic $GABA_A$ receptors containing α4, α5 and δ subunits (Ade et al., 2008; Santhakumar et al., 2010), which have high affinity for GABA and a low degree of desensitisation. Extrasynaptic $GABA_A$ receptors mediate tonic inhibitory currents that are larger in iMSNs than in dMSNs during development (Ade et al., 2008; Janssen et al., 2009), but larger in dMSNs than in iMSNs in adult mice (Santhakumar et al., 2010). This developmental switch is thought to occur due to changes in subunit composition (Luo et al., 2013). This persistent tonic inhibition by striatal ambient GABA tone acting at $GABA_A$

receptors has also been demonstrated in primate striatum *in vivo* (Darbin and Wichmann, 2008). Tonic activation of presynaptic $GABA_B$ receptors have also been demonstrated in mouse striatal MSNs, in conditions with reduced GABA uptake, assessed as changes in vesicular transmitter release (Kirmse et al., 2009).

Whether this striatal ambient GABA tone arises from action-potential dependent GABA release or is action-potential independent, i.e. due to "spontaneous" GABA release, is still unclear. One study reported that tetrodotoxin (TTX) application abolished the $GABA_A$ receptor-mediated tonic current (Ade et al., 2008). Another study indicted only a minor dependence of this inhibitory current on action-potential dependent GABA release (Wójtowicz et al., 2013). Therefore, striatal ambient GABA tone and tonic inhibition at $GABA_A$ receptors might arise from extrasynaptic spillover of both action-potential dependent and spontaneous GABA release. Given the density of GABAergic neurons within the striatum, even low rates of spontaneous vesicle release from a small fraction of these GABAergic neurons might summate sufficiently to provide a tone at GABA receptors.

The dimension of the ambient GABA tone is determined by the amount of GABA release and spillover into the extrasynaptic environment relative to the rate of GABA uptake by plasma membrane GABA transporters (GATs) (Brickley and Mody, 2012). GATs rapidly remove GABA from the extracellular space after presynaptic release to terminate GABAergic synaptic transmission and limit GABA spillover to neighbouring synapses or extrasynaptic sites (Borden, 1996). Four different isoforms of the GAT have been currently identified, GAT-1, GAT-2, GAT-3, and the betain/GABA transporter type 1.

There are two isoforms of the GAT in striatum: GAT-1 (*Slc6a1*), abundant in axons of GABAergic neurons (Augood et al., 1995; Durkin et al., 1995; Yasumi et al., 1997; Ng et al.,

2000); and GAT-3 (*Slc6a11*), expressed moderately (Yasumi et al., 1997; Ficková et al., 1999; Ng et al., 2000) and seen particularly on astrocytes (Ng et al., 2000; Chai et al., 2017; Yu et al., 2018). In addition, mRNA for GAT-1 and for GAT-3 has been found in midbrain DA neurons and these GATs have been suggested to be located on striatal DA axons to support GABA co-storage and co-release (Tritsch et al., 2014).

Ambient GABA tone onto MSNs in the adult rodent striatum is limited by the activity of GAT-1 and GAT-3: the pharmacological inhibition of striatal GATs increases the $GABA_A$-mediated tonic inhibitory currents recorded in MSNs (Kirmse et al., 2008, 2009; Santhakumar et al., 2010; Wójtowicz et al., 2013; Tritsch et al., 2014). Recent evidence suggests that GATs on striatal astrocytes play a particularly important role, as increased GAT-3 expression on astrocytes results in decreased $GABA_A$-mediated tonic inhibitory currents recorded in MSNs (Yu et al., 2018). This reduction in the tonic GABA level profoundly altered MSN activity and striatal-dependent behaviours.

1.5 Parkinson's disease

PD is the second most common neurodegenerative disease affecting ~6 million individuals globally (Dorsey et al., 2018). The worldwide burden of PD has more than doubled over 26 years, from 2.5 million patients in 1990 to 6.1 million patients in 2016 (Rocca, 2018). PD therefore represents a significant health and economic burden and a more in-depth understanding of the aetiology and progression of PD would be crucial in facilitating the development of novel treatment options.

The disease is most commonly an idiopathic disorder, although rare genetically inherited forms of the disease do exist (Singleton et al., 2003; Chartier-Harlin et al., 2004).

The hallmark of PD, common to both idiopathic and genetic forms, is the selective degeneration of a subpopulation of DA neurons residing in the SNc resulting in reduced DA signalling in the striatum and disrupted basal ganglia function. This degeneration leads to patients suffering from motor symptoms including bradykinesia, rigidity, and resting tremor. In addition, particularly in later disease stages, PD patients present with cognitive and neuropsychiatric impairments (Dubois and Pillon, 1997).

1.5.1 DA neuron degeneration in PD

Degeneration of DA neurons is the central dysfunction in PD. In particular, degeneration of neuromelanin-positive and calbindin-negative ventral tier SNc DA neurons results in dopaminergic denervation of the dorsolateral striatum (Iacopino et al., 1992; Hornykiewicz, 1998; Surmeier and Sulzer, 2013). This striatal DA denervation leads to downstream aberrant synaptic weighting of basal ganglia activity and the manifestation of motor symptoms (Albin et al., 1989; DeLong, 1990; Graybiel et al., 1994). The success of DA replacement therapies in alleviating motor impairments, such as the DA precursor levodopa (L-DOPA), substantiates that dopaminergic deficits are central to the motor phenotype in PD (Smith et al., 2012b).

Furthermore, the extensive nigrostriatal DA axonal arbours could play a significant role in the preferential DA denervation in the dorsal striatum. A substantial metabolic function is required to maintain the resting membrane potential and propagate action potentials across these highly branched, unmyelinated axons. This high energetic demand and metabolic stress is thought to contribute to their preferential degeneration in PD (Bolam and Pissadaki, 2012; Pissadaki and Bolam, 2013). In contrast, DA neurons of the VTA innervating

the ventral striatum are significantly less branched and are spared (Arbuthnott and Wickens, 2007; Bolam and Pissadaki, 2012). Furthermore, the degree of terminal loss in striatum appears to be more pronounced than the magnitude of SNc DA neuron loss (Bernheimer et al., 1973) and an initial loss of nigrostriatal DA axons has been proposed as one of the earliest features of PD (Burke and O'Malley, 2013). Consequently, the striatum is a critical site for targeting the disease.

1.5.2 Impact of parkinsonism on basal ganglia function

As previously described, the classical model of PD function segregates striatal MSNs into two populations based on their projection targets, dMSNs and iMSNs. D_1 receptor-positive dMSNs project directly to the basal ganglia output nuclei GPi/SNr (DeLong, 1990; Gerfen et al., 1990), and activation of this pathway is thought to promote movement by decreasing basal ganglia output and disinhibiting the thalamus. D_2 receptor-positive iMSNs project indirectly to the output nuclei through GPe and STN (DeLong, 1990; Gerfen et al., 1990), and activation of this pathway is thought to suppress movement. Due to the opposing effects of DA on these two MSN populations, the net effect of nigrostriatal dopaminergic signalling is to promote movement by suppressing basal ganglia output from the GPi. In PD, the loss of striatal DA signalling results in excessive indirect-pathway activation and diminished direct-pathway activity. This imbalance is thought to drive GPi-mediated thalamic inhibition, and therefore suppress motor output (DeLong, 1990; McGregor and Nelson, 2019).

1.5.3 α-synuclein involvement in Parkinson's disease

A common feature of PD is the accumulation of filamentous cytoplasmic protein inclusions, known as Lewy bodies, which are principally comprised of α-synuclein (Baba et al., 1998; Spillantini et al., 1998; Marques and Outeiro, 2012). Genetic and genome-wide association studies (GWAS) point to α-synuclein involvement in both sporadic and familial PD. Duplication, triplication, and point mutations of the α-synuclein gene (SNCA) locus have been identified in autosomal dominant PD cases (Singleton et al., 2003; Chartier-Harlin et al., 2004; Bekris et al., 2010), with pathophysiology data from SNCA locus multiplication suggesting gene triplication leads to earlier symptom onset and a more severe disease progression compared to gene duplication (Fuchs et al., 2007). GWAS also support the involvement of α-synuclein in sporadic cases (Satake et al., 2009; Simón-Sánchez et al., 2009; Venda et al., 2010).

The role of α-synuclein is still not fully understood, but it appears to have presynaptic roles and binds to vesicles (Clayton and George, 1998), modulates transcription (Baptista et al., 2003; Yu et al., 2007), and modifies striatal DA storage, synthesis and release in a dose-dependent manner (Senior et al., 2008; Anwar et al., 2011; Janezic et al., 2013). Studies suggest that both wild-type (WT) and mutant oligomeric α-synuclein species show neurotoxic properties and provide the rudimentary structure for fibril formation (Lashuel et al., 2002; Kayed et al., 2003; Feng et al., 2010). Furthermore, in adult rodent dopaminergic neurons, aggregation of α-synuclein into fibrils promotes progressive neurotoxicity *in vivo* (Taschenberger et al., 2012; Paumier et al., 2015). Post-mortem tissue from idiopathic PD patients present with α-synuclein fibrillar tangles and increased α-synuclein burden (Spillantini et al., 1997, 1998). However, it is not clear whether formation of these aggregates follow or precede dysfunction in DA physiology and cell death.

1.5.4 Mouse models of Parkinson's disease

Animal models of PD are commonly employed to elucidate PD pathophysiology. Toxin based models, such as 6-OHDA nigrostriatal lesions, allow the study of the effects of striatal DA depletion. However, these models are very acute and are not representative of the slower, progressive, system-wide phenotype seen in human PD. In contrast, emerging genetic models are more representative of the PD phenotype and allow examination across different time stages of the disorder. Therefore, such models are valuable for elucidating the earliest pathological and physiological processes underlying the final common pathway of DA neuron degeneration.

Animal models which manipulate α-synuclein in rodent models are commonly employed for PD research. Models that use a vector-driven approach to overexpress human WT α-synuclein in striatum or midbrain show progressive DA neuron degeneration and deficits to striatal DA transmission (Lo Bianco et al., 2002; Kirik et al., 2002; Lundblad et al., 2012). Furthermore, in models expressing mutant α-synuclein A53T variant overexpression and A30P variant expression also present with striatal DA deficits (Gispert et al., 2003; Kurz et al., 2010; Platt et al., 2012; Taylor et al., 2014). These models provide a causal link between overexpression/dysfunction of α-synuclein and a parkinsonian-like nigrostriatal DA deficit. However, they employ general promoters to express these α-synuclein variants, and do not recapitulate the native expression profiles of the SNCA gene.

The human α-synuclein overexpressing mouse model of PD (SNCA-OVX), developed at the Oxford Parkinson's Disease Centre, is a highly physiological, slowly progressive mouse model of parkinsonism, that captures a human disease-relevant genetic burden of α-synuclein overexpression (Janezic et al., 2013). This model was generated using a BAC construct carrying

the complete WT human *SNCA* locus, on a mouse α-synuclein gene (*Snca)* knock-out background. This avoids the confounding expression of mouse α-synuclein in a "humanized" genetic model. The SNCA-OVX mouse expresses human WT α-synuclein protein at approximately twice the endogenous levels seen in for endogenous mouse *Snca.* These SNCA-OVX mice show deficits in DA transmission by 3 months of age restricted to the dorsal striatum, but not observed in the ventral striatum. These deficits occur prior to late-stage degeneration of DA neurons, disturbed encoding of behaviour in surviving neurons, and manifestation of a motor phenotype at 18 months of age (Janezic et al., 2013; Dodson et al., 2016).

1.6 Conclusions

Striatal DA signalling has been shown to play an important part in fundamental processes related to action selection and reinforcement learning and is crucial in the normal functioning of the basal ganglia. DA release is powerfully controlled by local striatal factors such as ACh, which can dramatically change the relationship between DA neuron activity and DA release.

The high density of striatal GABAergic projection neurons and interneurons, which are interspersed among DA axons, could impact on DA release. Furthermore, these neurons contribute to an extrasynaptic ambient GABA tone in striatum, which exerts tonic inhibition onto principal striatal neurons. Whether these factors can impact on DA release is not fully understood. Furthermore, it is not understood whether these factors are affected during PD.

Chapter 2 provides an overview of the methods used throughout this thesis. In **Chapter 3**, I tested how manipulating striatal GABA receptors affects DA release. **In Chapter**

4, I described the characterisation of a new transgenic mouse cross which will allow for the genetic targeting of ChIs within a parkinsonian disease state, and the implementation and results from a new immunohistochemical procedure for accessing ChI function and cell number. I will also discuss the implementation of a method for measuring ACh fluxes indirectly by detecting choline within acute striatal slices. Finally, in **Chapter 5** I explored the impact of conditionally knocking out midbrain DA neuron-derived insulin-like growth factor 1 (IGF-1) in striatal DA release.

2. General Methods

In this chapter I will describe the general methods and techniques used throughout this thesis. I will focus on fast-scan cyclic voltammetry (FCV) with carbon-fibre microelectrodes (CFMs) in *ex vivo* mouse striatal slices, the main technique used throughout this thesis. Other techniques were used exclusively within individual chapters, and the details of these methods and techniques are present within their respective chapters.

2.1 Mice as a model organism for investigating DA signalling

The study of neurotransmission depends making use of a range of experimental models, from cultured neurons to human subjects. Studies of cultured cells and simpler organisms offer a greater degree of experimental control, while work on more complex organisms such as mammals may more accurately describe the physiology of intact neuronal circuits. The choice of experimental models is important when attempting to answer an experimental question.

Rodents are a commonly used animal model in the study of neuronal circuits, since they share conserved neuronal properties, circuit organisation, and even some behavioural patterns with humans. Consequently, their use is usually preferred over that of non-mammalian animal models such as nematode worms (*Caenorhabditis elegans*) or fruit flies (*Drosophila melanogaster*), which are more commonly used for the study of genetics and fundamental properties of cells and synapses.

The use of rodents to study neurotransmission in place of more complex mammals is mainly driven by both practical and ethical considerations. Studying the regulation of DA release in human brains would be of the greatest relevance and applicability to medical science, however, the range of experimental techniques that can be performed in humans is limited. Non-invasive approaches such as imaging markers of DA neurotransmission can be used, for example, to compare healthy humans to those suffering from DA-related disorders such as PD. These approaches do not offer much opportunity for specific manipulations of the DA system. Invasive recording techniques and manipulations can be performed in non-human primates, offering a more relevant system to study. However, these animals are considered to have a greater capacity to experience pain and suffering than other animals, and a strong, specific scientific rationale is required for their experimental use in the UK.

Rodents are therefore an appropriate model for the study of striatal DA release. The experiments described in this thesis were performed in acute sections of striatal tissue from the mouse (*Mus musculus*). Mice are preferable to rats and other rodents for several reasons. Mice reach maturity more rapidly than rats, allowing them to be used sooner. This additionally reduces the time and cost required for breeding of transgenic animals. Mice are also commonly used as experimental models in neuroscience, so many genetically-modified strains are readily available. Finally, mice are smaller and have a lower energetic demand. Consequently, they can be housed in larger groups than other rodents, further improving their cost-effectiveness. This is also important to consider for animal welfare, as rodents are highly social animals.

2.1.1 Animals

All procedures were carried out in accordance with UK Home Office-approved project licences (30/3035, P9371BF54; personal licence authority PIL-C) and local guidelines. Adult WT C57Bl/6NCrl (Charles River) were used for most FCV experiments in **Chapter 3**. All transgenic animals used in this thesis are under this background. The C57Bl6 strain is commonly used as a background strain for genetically-modified mice, so using this model allows easier comparison of the new data to the existing literature. The C57Bl/6NCrl strain is derived from the commonly-used C57Bl/6J strain, and is useful in the study of DA neurotransmission as it carries a WT gene for α-synuclein, a protein important in the regulation of DA release (Abeliovich et al., 2000), unlike some C57Bl/6 strains in which a spontaneous deletion of this gene has been observed (Specht and Schoepfer, 2001).

For some experiments in **Chapter 3**, transgenic mice expressing Cre-recombinase under the control of the DA transporter (DAT) promoter were used. In these animals, an internal ribosome entry site-linked Cre-recombinase (IRES-Cre) gene has been inserted downstream of the endogenous DAT gene (*Slc6a3)* (Bäckman et al., 2006). Heterozygous $Slc6a3^{IRES\text{-}Cre}$ mice , used for these experiments, were locally bred from homozygous $Slc6a3^{IRES\text{-}Cre}$ mice on a C57BL/6J background (B6.SJL-$^{Slc6a3tm1.1(cre)Bkmn}$/J; stock no. 006660, Jackson Laboratories).

In Chapter 4, a cross between the SNCA-OVX line (Janezic et al., 2013) with a ChAT-Cre;$Snca^{-/-}$ was employed. Both lines were bred to a mouse α-syn-null ($Snca^{-/-}$) pure C57Bl6 background (Abeliovich et al., 2000) to preclude confounding interactions with endogenous α-syn.

In Chapter 5, a Slc6a3$^{CreERT2/+}$; Igf1$^{flox/flox}$ cross was employed. Selective ablation of IGF-1 from DA neurons is accomplished by expressing Cre under the control of the DAT promoter, which would then delete IGF-1 from DA neurons by Cre-dependent recombination of a floxed *Igf1* gene. The control genotype contains solely the floxed *Igf1* gene. Slc6a3$^{CreERT2/+}$ and Igf1$^{flox/flox}$ mice, generated and characterised in previous studies (Liu et al., 1998; Rieker et al., 2011), were crossed to produce the experimental line in The Francis Crick Institute, London. Igf1$^{flox/flox}$ line was used as control animals for this chapter.

2.2 Studying DA transmission in slice preparations

Several methods can be used to study neuronal circuits within rodents. These range from *in vivo* experiments, in which data are collected from living animals; *ex vivo* preparations, in which tissue is collected and studied outside of the body under approximately physiological conditions; and *in vitro* studies, in which biological cells or molecules are studied outside of their physiological context. Selection of an experimental preparation to answer a question requires a balance between control over experimental variables and the relevance of findings to physiological conditions. The experiments described in this thesis have been conducted in acute coronal sections of mouse dorsal striatum, as this technique is suitable for the study of striatal factors that locally regulate DA release. The advantages of the coronal slice preparation will be described below.

Slices obtained from adult mice preserve the normal connectivity of the striatum and allow the development of the unique axonal arbour of midbrain DA neurons. In contrast, synaptosomal preparations, which may be useful for the study of synaptic machinery present at DA release sites, do not include intact axonal projections. Primary DA neuron cultures can

be prepared from DA neurons located in the midbrain nuclei, however, these cultured neurons lack the diverse neuronal populations and physiological patterns of synaptic connectivity found in the adult striatum. Properties such as axonal geometry and ion channel localisation may also differ in cultured neurons. Furthermore, DA neurons cultured from induced pluripotent stem cells may represent a promising model for the study of DA neuron physiology in the future, but currently do not replicate the structural and physiological properties of mature DA neurons. Slice preparations are ideal within the context of this thesis because it is not currently possible to replicate the unique morphology and physiology of DA neurons *in vitro*.

Slice preparations also allow for a ready administration of drugs and manipulation of the extracellular environment. Drugs used during *in vivo* experiments are typically administered through peripheral routes, such as intraperitoneal or intravenous injections, or into the brain tissue, such as through implanted cannulae. While these techniques can permit drug application across different ranges of spatial specificity, the drug concentration reaching the recording site cannot be consistently controlled to the degree that is possible with bath application in a slice preparation. In this thesis accurate, sustained changes in drug concentrations within the striatum and the ionic composition of the artificial cerebrospinal fluid (aCSF) are required. The degree of experimental control required in experiments described in this thesis would therefore not be readily attainable using an *in vivo* approach.

The measurement of extracellular [DA] in slice preparations is more straightforward than in *in vivo* recordings. The regulation of DA release can be readily studied using FCV in both anaesthetised and freely-moving animals (Millar et al., 1985; Garris et al., 1997). However, data collected in these experiments require complex analysis to extract DA signals,

since these signals are small and are influenced by factors which cannot be easily controlled in the intact brain, such as pH and temperature (Runnels et al., 1999). In anaesthetised animals, the choice of anaesthetic can also be problematic as these can interact with experimental drugs (McFarlane et al., 1995) and alter DA neuron physiology (Marinelli and McCutcheon, 2014). DA signals collected using FCV in slice preparations have a high signal-to-noise ratio, and the extracellular environment can be easily controlled to account for factors such as pH and temperature. Experiments performed in slice preparations offer a simpler interpretation of results and should be the preferred approach when the advantages offered by *in vivo* preparations are not considered crucial.

Finally, there are ethical advantages to the use of slices. Animals used for experiments in this thesis were killed by cervical dislocation, a method that causes immediate death with minimal suffering. Furthermore, several striatal slices can be collected from each animal, allowing multiple experiments to be conducted on tissue from the same animal. This contrasts with *in vivo* experiments, during which animals must typically be anaesthetised for long periods or maintained after invasive surgery.

A limitation of slice preparations is the loss of DA projections from the midbrain to the striatum. Coronal sections preserve the local striatal circuitry and the striatal portion of DA axons but sever these axons from their cell bodies in the midbrain. The absence of intrinsic DA activity means stimulation of DA axons is required to evoke DA release. This could also be considered an advantage, as the properties of DA axons can be studied in the absence of presynaptic activity.

To preserve the mesostriatal pathways parasagittal slices could be obtained, allowing striatal DA release to be evoked by stimulation of the SNc (Ammari et al., 2009). However,

preparation of these slices is associated with a higher failure rate than coronal sections, and only small DA signals could be consistently evoked (Ammari et al., 2009). While a parasagittal preparation was not used in this thesis, it might be useful for future experiments exploring the differences between populations of midbrain DA neurons.

2.2.1 Preparing slices

Mice were killed by cervical dislocation and brains extracted into ice-cold HEPES-based buffer containing in mM: 120 NaCl, 20 $NaHCO_3$, 6.7 HEPES acid, 5 KCl, 3.3 HEPES salt, 2 $CaCl_2$, 2 $MgSO_4$, 1.2 KH_2PO_4, 10 glucose, saturated with 95% O_2/5% CO_2 (carbogen). The calculated osmolarity of this solution was 334.8 mOsm. Acute 300 µm thick coronal striatal slices, containing both CPu and NAc were cut in ice-cold HEPES-based buffer using a vibratome (VT1200S; Leica). Slices were kept at room temperature in carbogenated HEPES-based buffer for at least 1 hour before being transferred to the recording chamber.

2.3 Methods for striatal DA detection

Electrochemical detection techniques use the faradaic current produced by a change in the oxidation state (oxidation or reduction) to quantify the concentration of an electroactive substrate. For voltammetric methods, a subtype of electrochemical detection techniques, the voltage at a working electrode is varied allowing for the detection of the faradaic current at the different applied potentials.

FCV is a voltammetric electrochemical detection technique in which the applied potential at a working electrode is rapidly cycled across a range of potentials that oxidise and reduce the compound of interest. DA has two hydroxyl groups which are readily oxidised and

reduced. For the electrochemical detection of DA, the forward sweep (from a negative to a positive potential) oxidises DA to dopamine-O-quinone at approximately +600 mV. This reaction is reversed by a negative sweep which reduces the quinone derivative back to DA. This cycle of applied potentials is repeated at a frequency of 8 Hz, corresponding to a measurement every 125 ms **(Figure 2.1)**.

FCV applied in neuroscience is commonly coupled with CFMs. Prior to the invention of CFMs in the 1980s (Gonon et al., 1978; Armstrong-James and Millar, 1979), voltammetry for *in situ* DA detection was performed with carbon paste electrodes. These electrodes were approximately 150-300 µm in diameter, and their implantation into brain tissue caused significant damage.

CFMs have a much smaller diameter (7 µm) and incur little tissue damage *in vivo* or *ex vivo*. The size of commonly used CFM tips is several orders of magnitude larger than a synaptic cleft (~10 nm), allowing for the extrasynaptic detection of DA. Striatal DA is thought to act as a volume transmitter (Gonon et al., 2000; Cragg and Rice, 2004), and FCV is therefore compatible to assess the dynamics of this neurotransmitter.

The faradaic current is proportional to the concentration of DA detected by the CFM. Therefore, it is possible to convert the current to DA concentration following calibration of the CFM with a known concentration of DA. However, only transient changes in $[DA]_o$ can be measured using FCV. This is due to a large background signal which must be subtracted from the total signal to obtain the faradaic current attributable to DA oxidation (Hermans et al., 2008). This background signal is produced by the capacitive properties of the electrode and oxidation of functional groups at the electrode surface. Consequently, continuous FCV

recordings are limited to approximately less than 1 minute over which the background current remains relatively stable.

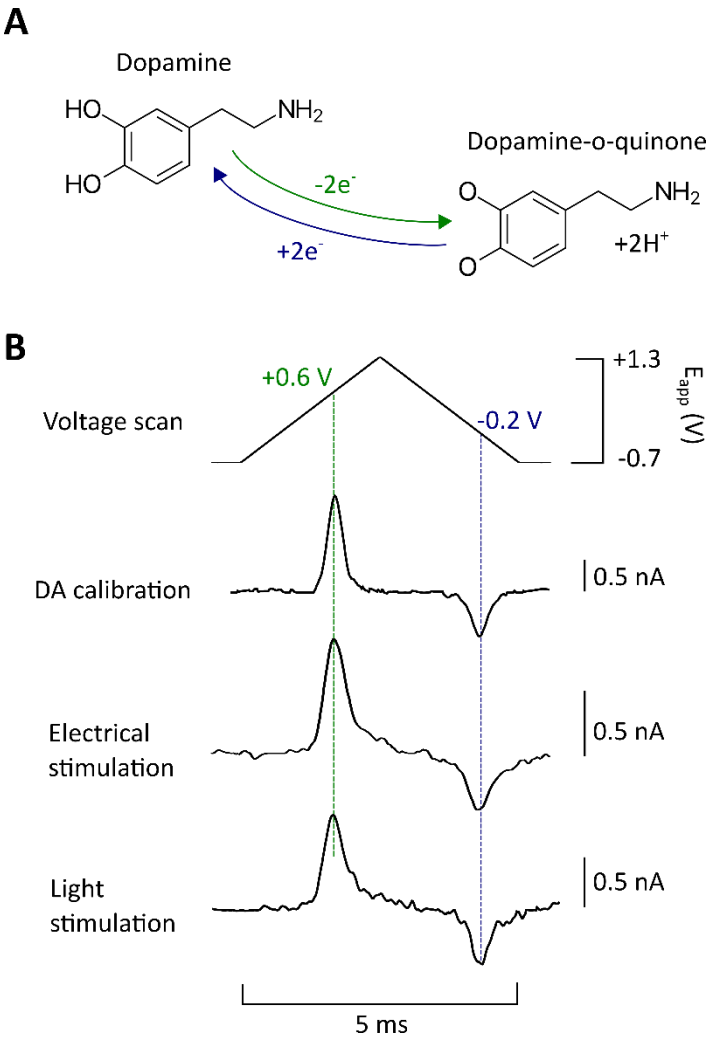

Figure 2.1 - Oxidation of dopamine to dopamine-o-quinone generates faradic current recorded at carbon fibre microelectrodes with fast-scan cyclic voltammetry. ***(A)*** DA is electroactive and can undergo changes to its oxidation state. ***(B)*** During the positive phase of the triangular waveform scan across the carbon fibre microelectrode (from -0.7 V to +1.3 V), DA is oxidised (green) to dopamine-o-quinone and reduced back (blue) to DA during the negative phase of the scan (from +1.3 V to -0.7 V). The resulting faradaic current recorded produces a voltammogram showing typical oxidation peak at +0.6 V and reduction peak at -0.2 V. Scan rate of 800 V/s, 5 ms in duration. Also shown are voltammagrams demonstrating DA signals resulting from calibration with 2 µM DA, and electrically and light evoked DA release from an acute striatal slice.

Several other methods for detecting striatal DA release could be considered. The temporal resolution afforded by FCV allows the detection of rapid DA signalling events, but accurate study of the time course of DA release often requires higher rates of detection. Constant-potential amperometry, a similar technique in which the applied potential is maintained at the oxidation potential for the chemical species of interest, provides a continuous signal and offers much higher temporal resolution. However, as the recording electrode is held at a constant potential, this approach does not allow distinction of currents produced by different oxidised species. Using FCV, certain monoamine neurotransmitters such as 5-hydroxytryptamine (5-HT), as well as other signalling molecules such as hydrogen peroxide, can be distinguished from DA due to their distinct oxidation or reduction potentials. Consequently, FCV offers an appropriate temporal resolution and selectivity for the detection of DA release events.

While FCV offers some chemical selectivity for DA, there may be situations where similar concentrations of different oxidizable species are detected simultaneously. Furthermore, species with similar chemical structures to DA such as noradrenaline can be difficult to electrochemically separate. In this case, microdialysis is typically employed to distinguish between these species. Microdialysis probes are inserted into the tissue and used to collect samples of the extracellular fluid across a semi-permeable membrane, which are then separated using high-performance liquid chromatography coupled to electrochemical detection or an alternative identification method. This technique can distinguish between chemical species, and can measure absolute baseline concentrations of neurotransmitters, which is not possible using FCV.

Modern microdialysis probes can only sample at approximately 1 sample/minute, which does not allow for the sub-second study of individual DA release events. Furthermore, electrically stimulating striatal tissue is thought to evoke greater DA release than other monoamine neurotransmitters, as the resulting FCV signal is enhanced by selective DAT inhibitors, but not by altering the activity of other monoamine transporters (Bull et al. 1990; Cragg 2003). Furthermore, mouse striatal levels of noradrenaline are significantly lower than DA (Toomey et al., 2012). Therefore, in acute striatal slices, the release of other detectable monoamine transmitters that could confound DA detection is limited. FCV is therefore appropriate for the study of DA release in striatal tissue.

Novel methods allowing for spatiotemporally precise measurements of DA have recently emerged: the dLight and $GRAB_{DA}$ imaging methods (Patriarchi et al., 2018; Sun et al., 2018). dLight and $GRAB_{DA}$ are genetically encoded G protein-coupled receptors coupled to a circularly permutated green fluorescent protein. When bound to DA, these sensors exhibit large fluorescence increases, with signals exhibiting subcellular resolution, subsecond kinetics, nanomolar to submicromolar affinities, and excellent molecular specificity. Data indicate that these sensors can resolve a single electrically-evoked DA release event in acute *ex vivo* mouse brain slices and detect endogenous DA release *in vivo* in mice during complex behaviours (Sun et al., 2018). However, these techniques are new and need to be evaluated and compared to signals obtained from FCV before being considered for future experiments.

2.3.1 Fabrication of CFMs for fast-scan cyclic voltammetry

CFMs were produced in-house and each used for a single experiment, as changes in electrode kinetics can occur due to tissue fouling and repeated exposure to DA. Borosilicate capillary tubes (2.0 mm outside diameter, 1.16 mm inside diameter, Harvard Apparatus, UK) were threaded with a single uncoated carbon fibre (7 µm diameter, Goodfellow Cambridge Ltd., UK). Each glass capillary was filled with acetone, to ease insertion and to clean the carbon fibre, which was subsequently removed by blotting with tissue paper. Following acetone removal, the capillary tube was sealed around the carbon fibre using a PE-2 vertical microelectrode puller (Narishige, Japan). A high heat setting was used to ensure a tight seal between the glass microelectrode and the carbon fibre, as this promotes a high signal-to-noise ratio. The resulting seal was visible under 100x magnification, so it can be visually inspected for damage. The carbon fibre was then cut to a length of 50-100 µm from seal to tip, which typically produced a sensitivity within the desired range; shorter electrodes have a reduced sensitivity to DA, while longer electrodes have higher noise levels. A short length of insulated 0.1 mm tinned copper wire was coated with silver conductance paint and inserted into the open end of the capillary tube, in electrical contact with the carbon fibre close to the tip and secured with cyanoacrylate glue.

2.3.2 Methods for fast-scan cyclic voltammetry

Slices were transferred to a recording chamber and secured using silver pins placed on the tissue surrounding the striatum. Slices were continuously superfused with carbogenated aCSF which contained (in mM): 124.3 NaCl, 26 $NaHCO_3$, 3.8 KCl, 2.4 $CaCl_2$, 1.3 $MgSO_4$, 1.23 KH_2PO_4, 10 glucose. The calculated osmolarity of this solution was 331.6 mOsm.

Superfusion was at a rate of 1.8-2 mL/minute, and aCSF was warmed to a temperature of 31-33^{o}C. A CFM was connected to the voltammeter headstage and left to cycle in aCSF for approximately 10 minutes, before being inserted into a region of non-striatal tissue (typically cortex) and left to cycle for a further 30 minutes. These steps allow the electrode to equilibrate to the recording conditions and reduce subsequent baseline drift during the experiment.

The CFM was then inserted at a depth of 100 µm into the recording site. Following CFM insertion, the full current was inspected to determine whether the microelectrode seal remained intact, and full signal gain was set to provide a working range of 5 V. CFMs with a full signal gain in the range 3-10 mV/nA were considered suitable for recording. The full signal gain was monitored throughout the experiment, as CFMs typically become more sensitive during use, which can result in saturation if left uncorrected.

A biphasic triangular voltage waveform from -700 mV to +1300 mV vs an Ag/AgCl reference electrode (World Precision Instruments, USA) at a rate of 800 V/s was applied to the CFM using a Millar voltammeter (Julian Millar, Barts and the London School of Medicine and Dentistry). The extension of the anodic scan limit beyond +1000 mV has been shown to increase sensitivity to DA at the expense of slower electrode kinetics (Hafizi et al., 1990; Heien et al., 2003). The high scan rate used here further increases the sensitivity to DA but increases the charging current due to a greater number of adsorption sites (Bath et al., 2000; Keithley et al., 2011). The waveform was delivered at a frequency of 8 Hz, and between sweeps the electrode is held at 0 mV (i.e. switched out of circuit) to limit adsorption (Heien et al., 2003). Background subtraction was performed on-line by the Millar voltammeter, using a baseline recording of the total current stored before each stimulation was delivered. Background-

subtracted currents were sampled at 50 kHz and digitised using a Digidata 1440A (Molecular Devices, USA).

Data were collected using Axoscope 10.7 (Molecular Devices, USA), and analysed using locally-written scripts in Visual Basic for Applications (Microsoft, USA). The threshold for statistical significance in all analyses $p < 0.05$, adjusted for multiple comparisons where appropriate.

2.4 Stimulation of DA release in slice preparations

The acute coronal striatal sections used in this thesis sever the DA axons from their cell bodies located in the midbrain. Consequently, DA release cannot occur from DA neuron firing and is not suggested to occur from spontaneous axonal activity (Rice et al., 2011). Spontaneous nAChR-evoked DA release has been observed in acute striatal slices, although these events are small in amplitude and occur irregularly (Yorgason et al., 2017). Local DA axon stimulation is therefore required to evoke DA release. Two approaches to stimulation of DA axons have been used in this thesis: electrical and light stimulation.

Electrical stimulation has been used to evoke DA release in studies using both *ex vivo* tissue and intact *in vivo* brains. Within this thesis, local stimulation is used where a stimulating electrode is placed in contact with the slice and current pulses are passed into the tissue. DA release using the slice preparation method detailed in **Section 2** is capable of reliably evoking DA release for several hours. Release is dependent on action potential generation in local axon branches, as it is abolished by inhibition of voltage-gated sodium channels with TTX (Cragg, 2006). TTX-insensitive release, thought to be due to direct depolarisation of release

sites, can occur with very high stimulation intensities (Cragg group, unpublished observations).

While local electrical stimulation is a reliable method to evoke striatal DA release in acute slices, this method is non-specific. Current flow from the stimulating electrode can activate a variety of circuit elements present in a striatal section beyond DA axons, including MSNs, interneurons, and glia. DA release is regulated by GABA (Schmitz et al., 2002; Pitman et al., 2014; Melchior et al., 2015; Lopes et al., 2019; Roberts et al., 2019), glutamate (Avshalumov et al., 2003) and ACh signalling (Exley and Cragg, 2008), as well as by opioids (Schlösser et al., 1995) and the neuropeptide substance P (Brimblecombe and Cragg, 2015), all of which can be released by striatal neurons. These effects should be considered when planning experiments, or interpreting results obtained when using electrical stimulation.

Optogenetic techniques offer much greater selectivity than electrical stimulation. Optogenetics makes use of selective genetic markers to drive expression of light-sensitive proteins, known as opsins, in a specific neuronal population (Deisseroth, 2015). When exposed to light at a wavelength, opsins undergo conformational changes forming ion channels or pumps (Zhang et al., 2011). Depending on the opsin in use, light stimulation can drive depolarisation or hyperpolarisation of target neurons. The selectivity of this approach enables studies of the roles of specific neuronal populations within complex neuronal circuits or behaviours, which are typically infeasible using electrical stimulation.

In this thesis, channelrhodopsin-2 (ChR2), a cation channel developed from the algae *Chlamydomonas reinhardtii*, was used to depolarise neurons (Nagel et al., 2003). Currents mediated by ChR2 have rapid rise times ($\tau \approx 200$ μs) and recover rapidly from desensitisation (Nagel et al., 2003), permitting reliable light-evoked generation of APs in response to train

stimulation up to approximately 20 Hz in DA neuron soma (Tsai et al., 2009). ChR2 has a relatively low single-channel conductance, so in this thesis the H134R variant has been used to reliably evoke DA release, although this comes at the cost of slower channel opening and deactivation kinetics which may limit the frequency at which ChR2-H134R can reliably drive spiking (Nagel et al., 2005).

Selectively targeting opsin expression to target neuronal populations is achieved with high specificity using site-specific recombinases, a general approach for targeting genetic manipulations to specific cells (Branda and Dymecki, 2004). This relies on the specific expression of recombinases in transgenic animals, driven by a cell-type specific genetic promoter.

In the *Slc6a3*$^{IRES\text{-}Cre}$ animals used in **Chapter 3**, Cre recombinase expression was driven by the promoter for the DAT (Bäckman et al., 2006). A viral construct containing an inverted gene for ChR2 fused in-frame with a gene encoding enhanced yellow fluorescent protein (eYFP) was injected intracerebrally into heterozygote *Slc6a3*$^{IRES\text{-}Cre}$ mice. The ChR2-EYFP gene is flanked in the construct by two inverted pairs of short palindromic lox sites, which are recognised and inverted by Cre recombinase, resulting in forward orientation and consequent expression of the ChR2-EYFP gene in DAT-positive neurons (**Figure 2.2**) (Branda and Dymecki, 2004). Other recombinases recognising alternative palindromic sites have also been developed and can be used to define neuronal populations by multiple genetic markers (Fenno et al., 2014). An alternative method for selective targeting uses the Ai32 mouse line, which expresses an inverted gene encoding ChR2-EYFP at the ubiquitous Rosa26 locus (Madisen et al., 2012). In **Chapter 4**, light-activating striatal ChIs is accomplished by crossing the Ai32 line with the ChAT$^{IRES\text{-}Cre}$ mouse line to produce mice that display strong, consistent

expression of Chr2-EYFP in all choline acetyltransferase (ChAT) expressing neurons without the need for viral injections. The Ai32 strategy was not employed to selectively express ChR2 on DA axons, as during pilot experiments these animals were found to show unusually strong depression of DA release (data not shown), raising questions about the developmental effects of ChR2 expression in DA axons.

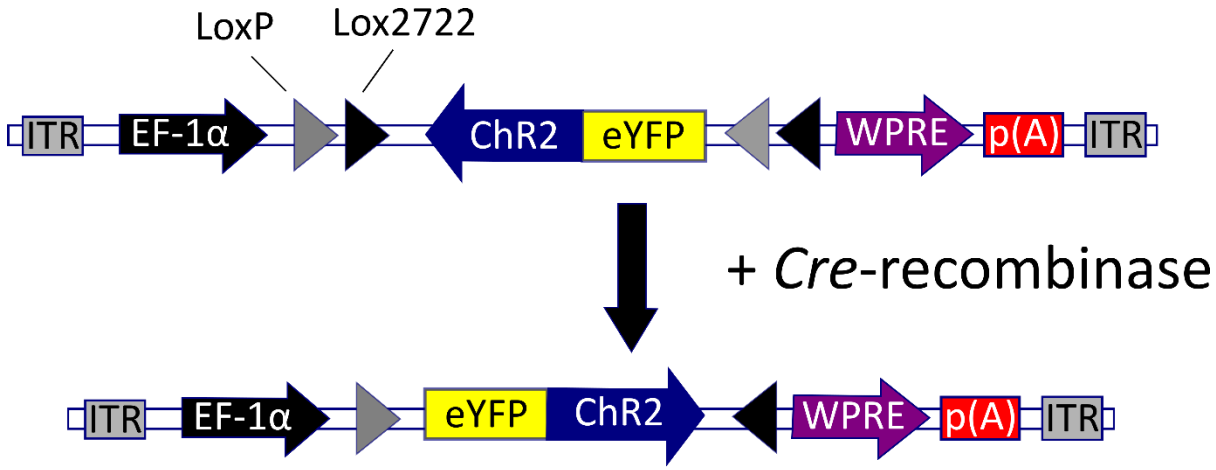

Figure 2.2 - Cre-dependent recombination of virally-delivered ChR2-eYFP construct.

Inverted ChR2-eYFP gene is flanked by two pairs of incompatible inverted lox sites (loxP and lox2722). In the presence of Cre-recombinase, recombination of lox sites results in forward orientation of the ChR2-eYFP gene, such that expression can be driven by the EF-1α promoter. The woodchuck hepatitis virus post-transcriptional regulatory element (WPRE) is included to increase mRNA stability. Adapted from Threlfell et al., 2012.

Expression of ChR2 under the control of a cell-specific promoter allows selective activation of the target, and excludes the effects of modulatory inputs (Melchior et al., 2015). A further advantage of selective activation is that it can be used to selectively identify the source of signalling events, and to observe such events where they would be occluded by converging inputs activated during non-selective stimulation.

Optogenetically driving DA axons has several disadvantages that make it unsuitable as a sole approach to study DA release. The channel kinetics of the currently available opsins make it unclear whether AP generation in DA neurons can follow repetitive stimulation during long trains or at higher frequencies. More recently-developed opsins can drive firing at higher rates (Gunaydin et al., 2010), but do so at the cost of lower single-channel conductance, and as such do not reliably evoke DA release (Cragg group, unpublished observations). Expression of ChR2 may also lead to aberrant short-term depression of neurotransmitter release at hippocampal synapses, although this has not yet been demonstrated at DA release sites (Jackman et al., 2014). In addition, long-term expression of ChR2 has been shown to lead to the development of abnormal morphological features in cortical axons in the rat (Miyashita et al., 2013) However, this effect was more severe following *in utero* electroporation than with the viral transfection method used in this thesis (Miyashita et al., 2013). The transgenic mouse lines used to achieve conditional expression of opsins in specific neuronal populations may display altered physiology that reduces their validity for the study of DA release under normal physiological conditions. For example, the heterozygote *Slc6a3*$^{IRES\text{-}Cre}$ animals used to express ChR2 in DA neurons in this thesis have reduced expression of the DAT compared to WT C57Bl/6J mice (Bäckman et al., 2006). Finally, conditional expression of opsins in DA neurons currently require intracerebral injections in transgenic animals, which is likely to

cause greater suffering and distress to the animal than in experiments where surgery is not required.

2.4.1 Methods for electrical stimulation

A concentric bipolar Pt/Ir electrode with a 25 µm tip diameter (FHC) was placed on the surface of the striatal tissue, approximately 100 µm from site of the recording electrode. In all experiments, individual pulses consisted of a square 0.6 mA current pulse of 200 µs width. Under drug-free conditions in a striatal slice, a single pulse using these parameters evokes near-maximal $[DA]_o$, and as such is considered a perimaximal stimulation (Cragg, 2003). However, in the presence of the nACHR antagonist dihydro-β-erythroidine (DHβE), these stimulation parameters are not perimaximal, but were used to allow ready comparison with previous findings.

Stimulations (single, paired-pulse or trains) were delivered at 2.5 minute intervals, during which time release is reliably recovered. At a given site, single-pulse stimulations were delivered until release was stable (less than 10% variation over 3 consecutive stimulations), after which release was typically stable for up to 10 hours. Data were only included for analysis where release remained stable for the duration of the experiment.

2.4.2 Methods for viral transfection

All surgical procedures were performed according to aseptic technique. Mice were deeply anaesthetized with isoflurane. Prior to surgery, meloxicam (Metacam, 5 mg/kg) was administered intraperitoneally for post-operative analgesia. The scalp was shaved and the animal was placed securely in a stereotaxic frame. The scalp was then cleaned with

chlorhexidine (HiBi scrub) and bupivacaine hydrochloride with epinephrine (Marcaine, 2 mg/kg) was injected subcutaneously into the scalp for local anaesthesia. A craniotomy was made above the injection sites with a hand drill. Injections of 1 µL adeno-associated virus (AAV) serotype 5 construct (pAAV5-double floxed-hChR2(H134R)-EYFP-WPRE-pA) were given bilaterally in the SNc (AP -3.1 mm from Bregma, ML ±1.2 mm from Bregma, DV -4.25 mm from exposed dura matter) using a 2.5 µL 32-gauge Hamilton syringe at 0.2 µL/min with a microinjector. Injection was made at approximately 50 nL/min, followed by a 10-minute delay before retraction of the needle to minimise suction of the vector into the electrode track.

Following wound closure with sterile monofilament suture (Ethicon), animals were allowed to recover in a temperature-controlled cage. Animals were maintained for at least 3-4 weeks following surgery to allow virus expression.

2.4.3 Methods for light stimulation

For all experiments using optical stimulation a 470 nM light-emitting diode (LED) system (OptoLED, Cairn Research) was used to deliver full-field illumination of the field of view, which was a circle of diameter 2.2 mm or 0.55 mm under a 10x or 40x water-immersion objective, respectively (eyepiece field number 22). In all experiments, activation of the light source was driven by a 2 ms TTL pulse. Optical stimulation of DA release in **Chapter 3** was delivered at a perimaximal intensity that was determined at the beginning of each experiment to account for variability in the extent of ChR2 expression.

3. Modulation of nigrostriatal DA release by GABA receptors

3.1 Introduction

In this chapter I will explore the role of GABA receptors in modulating striatal DA release. The striatum is a predominately GABAergic region, and the impact that GABA could play in modulating DA release has not been explored. To assess this, FCV was used in combination with electrical and light-evoked release.

Nigrostriatal DA neurons form dense arborised structures within the striatum, forming approximately 10^5 en passant varicosities and innervating ~3% of striatum in the rat (Matsuda et al., 2009). This dense striatal innervation allows axonal DA output to be modulated by multiple neurotransmitters in a manner independent of ascending midbrain action potentials (Sulzer et al., 2016). ChIs are an example of local striatal modulation of DA release. ChIs only make up 1-2% of striatal neurons, but each neuron forms extensive ramifications, forming on average 500000 varicosities (Bolam et al., 1984; Contant et al., 1996). ChIs play a particularly powerful role in controlling DA release through nAChRs on DA axons (Jones et al., 2001a; Zhou et al., 2001; Rice and Cragg, 2004; Zhang and Sulzer, 2004; Threlfell et al., 2012).

The vast majority of striatal projection neurons and interneurons are GABAergic. The volume of striatum reached by the extensive axonal arbour of a single DA neuron (Matsuda et al., 2009) can be calculated from striatal neuron counts (Oorschot, 1996) to encompass ~70,000 GABAergic neurons (plus additional non-neuronal cells that might provide a source

of GABA). Striatal GABA neurons include the principal MSNs (~95%) as well as interneurons (~2-3%) including FSIs and LTSIs amongst others (Gittis and Kreitzer, 2012).

Furthermore, some more recent findings have revealed that mesostriatal DA neurons can synthesise and co-release GABA (Tritsch et al., 2012, 2014; Kim et al., 2015). ChIs have also been shown to co-release GABA (Lozovaya et al., 2018). These developments have revived the interest in interactions between GABA and DA, and highlight how GABA is in a prime position to locally regulate striatal DA.

Previous studies have suggested a role for striatal $GABA_A$ and $GABA_B$ receptors in modulating DA release. Striatal administration of pregnanolone, a positive allosteric modulator of the $GABA_A$ receptor, or bicuculline, an antagonist, respectively decreased and increased extracellular DA in intact rats measured by microdialysis (Smolders et al., 1995), and muscimol, a $GABA_A$ agonist, inhibited DA release from striatal synaptosomes (Ronken et al., 1993). A $GABA_A$-mediated enhancement of DA release has been reported in guinea-pig striatal slices during prolonged electrical pulse trains, but this is thought to arise indirectly via inhibition of H_2O_2 release from striatal neurons during prolonged stimuli (Avshalumov et al., 2003). Striatal perfusion of $GABA_B$ agonist baclofen, or antagonist phaclofen, respectively decreased and increased extracellular DA in intact rats assessed through *in vivo* microdialysis (Smolders et al., 1995), and baclofen decreased electrically evoked DA release in acute slices of mouse CPu (Schmitz et al., 2002) and NAc (Pitman et al., 2014). Findings in slice preparations are less confounded by potential effects on long loop circuits in vivo that could regulate DA via changes in DA neuron firing, and therefore more directly support a local mechanism of action.

Despite the functional evidence for GABAergic modulation of DA release, the exact mechanism underlying this inhibition is not fully understood. While both $GABA_A$ and $GABA_B$ receptors are densely expressed throughout striatum (Ng and Yung, 2000; Waldvogel et al., 2004) only the $GABA_B$ receptor has been indicated on structures that resemble DA axons: ultrastructural studies report $GABA_B$ receptors in striatal neuropil in monkey and rat (Charara et al., 1999; Yung et al., 1999). Therefore, despite the absence of strong evidence it remains plausible that GABA receptors located on DA axons might directly modulate DA output. There is evidence that GABA could modulate DA release indirectly: ChIs express both $GABA_A$ and $GABA_B$ receptors (Waldvogel et al., 1998; Yung et al., 1999). As mentioned previously, ChIs directly modulate axonal DA release and furthermore can mediate effects of other neuromodulators on DA, including opioids, nitric oxide, glutamate, and insulin (Britt and McGehee, 2008; Hartung et al., 2011; Stouffer et al., 2015; Kosillo et al., 2016).

3.1.1 Hypothesis

Given the prominence of GABA in the striatum, the role of this neurotransmitter in regulating axonal DA release has not been fully explored. In this chapter I tested the hypothesis that GABA impacts on striatal DA release.

3.2 Methods

Experiments described in this chapter were carried out according to the general methods laid out in Chapter 2. Variations and further details are described below.

3.2.1 Animal surgery

Slc6a3$^{IRES\text{-}Cre}$ mice were injected with an adeno-associated virus encoding Cre-dependent ChR2. For experiments with light activation, *Slc6a3*$^{IRES\text{-}Cre}$ mice were bred from homozygotes for DAT-internal ribosome entry site (IRES)-Cre, obtained from Jackson Laboratories (B6.SJL-Slc6a3$^{tm1.1(cre)Bkmn}$/J). P25–P35 *Slc6a3*$^{IRES\text{-}Cre}$ mice were anesthetized with isoflurane, placed in a small animal stereotaxic frame (David Kopf Instruments), and injected with an adeno-associated virus (~10^{12} genome copies per ml; UNC Vector Core Facility, Chapel Hill, NC) encoding Cre-dependent ChR2 (AAV5-EF1α-DIO-hChR2(H134R)-eYFP). A total volume of 1 µl of virus solution was injected bilaterally (500 nl per hemisphere/injection) into SNc (SNc, AP −3.1 mm, ML ±1.2 mm from bregma, DV −4.25 mm from exposed dura mater). Virus solution was injected at an infusion rate of 50 nl/min with a 32 gauge Hamilton syringe and withdrawn 5–10 min after the end of injection. Virus-injected mice were used for experiments >4 weeks after viral injection.

3.2.2 Slice preparation

In FCV experiments where electrically-evoked $[DA]_o$ was recorded, adult 7- to 10-week-old WT male C57BL/6J mice (Charles River) were used. In FCV experiments where light-evoked $[DA]_o$ was recorded through the selective activation of DA axons, adult 8- to 14-week-old male Slc6a3$^{IRES\text{-}Cre}$ mice conditionally expressing ChR2-eYFP in DA axons after AAV

intracranial injections ~3-4 weeks prior were used. Acute *ex vivo* coronal slices containing striatum were prepared for FCV as described in Chapter 2. All experimental procedures involving the use of animals were carried out according to institutional guidelines and conformed to the UK Animals (Scientific Procedures) Act 1986.

3.2.3 Fast-scan cyclic voltammetry

Where light-evoked $[DA]_o$ was recorded, light stimulation was delivered by an LED system (OptoLED; Cairn Research). DA release was evoked with full-field 470 nm blue light and a pulse duration of 2 ms. Experimental stimulation intensity was determined by delivering a light pulse sufficient to drive ~50% maximal $[DA]_o$. During recordings, slices were visualized on an upright microscope (Olympus BX50WI) with fluorescence optics for visualizing eYFP. Mean $[DA]_o$ evoked by a single light pulse in control conditions was 0.90 ± 0.09 µM.

For experiments exploring changes in short-term plasticity (STP), the ionic composition of the aCSF was altered. To change the extracellular concentration of Ca^{2+} ($[Ca^{2+}]$), the $[CaCl_2]$ was altered accordingly. No divalent cation ionic substitution was used to compensate. Substitution of Ca^{2+} with another divalent ion Mg^{2+} was not used as other effects of $[Mg^{2+}]_o$ can confound interpretation. Changes in $[Mg^{2+}]$ have been shown to alter Ca^{2+} currents through VGCCs (Lansman, 1986; Agus et al., 2017), alter G-protein-coupled receptor function, including D2 receptors (van der Westhuizen et al., 2015), change the affinity of calbindin binding to Ca^{2+} (Berggård et al., 2002), trigger complexing of Ca^{2+} by ATP (adenosine triphosphate) (Michailova and McCulloch, 2001), and alter the sensitivity of FCV electrodes to DA (Kume-Kick and Rice, 1998). To change the extracellular concentration of K^+ ($[K^+]_o$), KCl was replaced with NaCl, and KH_2PO_4 was replaced with NaH2PO4. 5 mM $[K^+]_o$ contained (in

mM) 3.77 KCl, 124.3 NaCl and 1.23 KH_2PO_4, 1 mM [K^+] contained 1.00 KCl, 127.1 NaCl and 1.23 NaH_2PO_4, and 7.5 mM [K^+] contained 6.3 KCl, 121.8 NaCl and 1.23 KH_2PO_4. These changes resulted in small decreases/increases of [Na^+], but these were not considered to be significant and likely to interfere with our findings due to the high concentration of NaCl in control aCSF (150.3 mM total). Concentrations of all other ions remained unchanged.

In experiments with changes in [Ca^{2+}], calibrations were performed within both Ca^{2+} conditions to account for altered electrode sensitivity with different divalent ion concentrations.

For experiments with changes in bath temperature, a stable site was initially found at 32°C before increasing the temperature to 37°C. Slices were allowed to acclimatise within the new temperature for ~10 minutes prior to data acquisition.

3.2.4 Drugs

DHβE (1 mM stock in dH_2O), saclofen (100 mM stock in dH_2O), GYKI 53655 hydrochloride (10 mM stock in aqueous acid), α-Methyl-4-carboxyphenylglycine (MCPG, 50 mM stock in dH_2O), and bicuculline (10 mM stock in dimethyl sulfoxide - DMSO) were obtained from Tocris Bioscience. Baclofen (50 mM stock in dH_2O), picrotoxin (100 mM stock in DMSO), and GABA (5 M in dH_2O) were obtained from Sigma-Aldrich. Muscimol (50 mM stock in dH_2O) and CGP 55845 hydrochloride (8 mM stock in DMSO) were obtained from Abcam. DL-2-Amino-5-phosphonovaleric acid (D-APV, 50 mM stock in dH_2O) was obtained from Santa Cruz biotechnology. Stock aliquots of drugs were stored at −20°C.

3.2.5 Experimental design and statistical analysis.

Data are represented as means ± SEM, and n refers to the number of sites sampled. Each experiment was performed at a single recording site in one brain slice. More than 1 site/slice per animal was used, and the number of animals in each dataset was ≥ 3. Data are expressed as extracellular $[DA]_o$ or as $[DA]_o$ normalized to mean peak $[DA]_o$ evoked by single pulses in control conditions. In all cases, $[DA]_o$ displayed typical kinetics to peak and decay, indicative of good slice quality and were obtained from recording sites that maintained sufficiently stable levels of release over time. No data were excluded after acquisition.

For drug wash-on experiments, data acquired immediately before drug application were used as pre-drug control data and were compared with data acquired after drug effects had equilibrated after ∼10–20 min of application. Pre-drug control data was obtained by averaging the 4 stimuli obtained immediately prior to drug wash-on, whereas data for the drug condition was acquired after drug effects had equilibrated (approximately 10-20 minutes after application). For clarity, the data points used for analysis are highlighted with a shaded zone in the wash-on figures (e.g. **Figure 3.1A**). For ratios of $[DA]_o$ evoked by 5p/1p, these were obtained by dividing a 5p-evoked $[DA]_o$ value with an averaged 1p-evoked $[DA]_o$ value in the same condition at that recording site.

A paired-pulse paradigm was used to assess STP. 1p and paired pulse (2p) stimulations with inter-pulse intervals (IPIs) of 10, 40, 100 and 200 ms (corresponding to frequencies of 100, 25, 10 and 5 Hz) were applied at 2.5-minute intervals, with 2p at each IPI applied in pseudorandom order and in triplicate. 2p stimulations were grouped in sets of 3 stimuli and flanked by 1p stimulations (for example: 1p, 2p 40 ms, 2p 10 ms, 2p 200 ms, 1p). In some experiments, only 2p 10ms IPI was used and was alternated with 1p stimuli in triplicate. IPIs

of 40-100 ms, corresponding to frequencies of 10-25 Hz, were chosen because they fall within the range of most commonly observed burst firing frequencies in DA neurons in vivo (Grace and Bunney, 1984a; Hyland et al., 2002). Spike pairs at 10 - 25 ms IPIs, corresponding to 40 – 100 Hz, have been rarely observed during burst firing in DA neurons (Hyland et al., 2002; Cohen et al., 2012) but allow investigation of the mechanisms underlying short-term facilitation and changes in initial release (Rice and Cragg, 2004; Jennings et al., 2015).

Extracellular DA in response to 1p was interpreted as a measure of average release probability across a population of DA release sites (Cragg, 2003). Paired-pulse ratios (PPR) were used as a measure of STP, defined by the ratio P2/P1 where P1 is peak $[DA]_o$ following initial stimulation and P2 is peak $[DA]_o$ attributable to the second stimulation. Since some of the IPIs used in these experiments do not exceed the time between successive FCV sweeps at 8 Hz (i.e. 125 ms), the $[DA]_o$ transients evoked by each stimulation appear summated and cannot be separately resolved. To determine P2, the average of 1p $[DA]_o$ transients measured before and after the triplicates of paired pulse stimulation was subtracted from the summated 2p transient.

Comparisons for statistical significance were assessed by one- or two-way ANOVA, paired t tests (for 5p/1p ratio before and after drug application within each slice), or Mann–Whitney U tests where data were not normally distributed using GraphPad Prism.

3.3 Results

3.3.1 GABA receptor agonists suppress DA release

GABA acts through $GABA_A$ and $GABA_B$ receptors to mediate its effects. Therefore, we tested whether agonists of both these receptors are capable of modulating DA. DA release induced by single electrical pulses was decreased with the application of muscimol (**Figure 3.1B**: Mann-Whitney test: U = 0, p = 0.0022 , n = 6). These effects are blocked by the $GABA_A$ channel blocker picrotoxin, suggesting an effect on $GABA_A$ receptors (**Figure 3.1D**: Mann-Whitney test: U = 0, p = 0.0079, n = 5). Activation of the $GABA_B$ receptor with the agonist baclofen suppressed single pulse evoked DA release (**Figure 3.1G**: Mann-Whitney test: U = 0, p = 0.0286, n = 4), indicating activation of $GABA_B$ receptors suppresses DA release independently of ChIs. This effect is confirmed to be due to $GABA_B$ receptors as co-application of the $GABA_B$ antagonist saclofen prevented the suppression (Figure **3.1I**: Mann-Whitney test: U = 5, p = 0.11, n = 5). These results suggest that GABA receptors locally modulate striatal DA release.

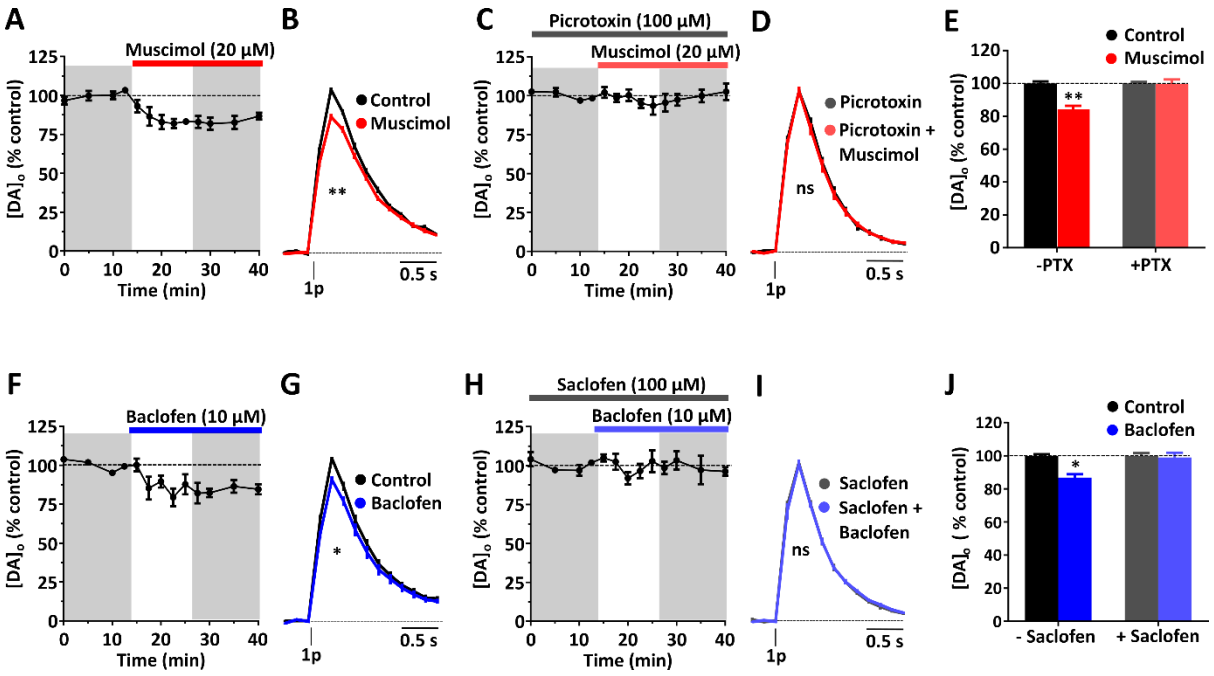

Figure 3.1 - GABA receptor agonists suppress DA release. Shown is the mean peak $[DA]_o$ (± SEM) versus time ***(A, C, F, H)***, the mean $[DA]_o$ (± SEM) versus time ***(B, D, G, I)***, and the mean peak $[DA]_o$ (± SEM) ***(E, J)*** evoked by 1 electrical pulse before and after application of: ***(A, B, E)*** 20 µM muscimol, *n* = 5; ***(C, D, E)*** 20 µM muscimol in the presence of 100 µM picrotoxin, *n* = 5; ***(F, G)*** 10 µM baclofen, *n* = 7 ***(F, G, J)***; or 10 µM baclofen in the presence of 100 µM saclofen, *n* = 5 ***(H, I, J)***. Shaded areas in **A**, **C**, **F**, and **H** indicate points used for transients represented in **B**, **D**, **G**, and **I**, respectively. Data are normalized to peak $[DA]_o$ before drug application. **p* < 0.05, ***p* < 0.01, Mann–Whitney tests.

3.3.2 GABA, $GABA_A$ agonists, and $GABA_B$ agonists inhibit DA release in nAChR block

GABA receptors could locally modulate striatal DA release by directly acting on DA axons, or indirectly by altering the activity of factors that regulate DA release. ChIs express both $GABA_A$ and $GABA_B$ receptors (Waldvogel et al., 1998; Yung et al., 1999), and are a potential input for GABA to regulate DA release. We then assessed whether GABA can modulate striatal DA release in the absence of nAChR activity using the antagonist DHβE (1 μM) to inhibit nAChRs as described previously (Rice and Cragg, 2004; Threlfell et al., 2012). The endogenous agonist GABA was applied to striatal slices in the presence of the nAChR antagonist DHβE. Bath application of GABA (100 μM, 5 mM) concentration-dependently reduced DA release evoked by single electrical pulses by ∼15–50% (**Figure 3.2B: 100 μM GABA**, Mann–Whitney test: U = 6, p = 0.0157, n = 7; **5 mM GABA**, Mann–Whitney test: U = 6, 5 mm, p = 0.0079, n = 5). The effect was significantly different between the two concentrations used (**Figure 3.2A:** two-way ANOVA: Effect of drug concentration: F(1,10) = 48.32, p < 0.0001). These results indicate that GABA is capable of inhibiting DA release independently from any effects on ChI input to nAChRs.

To identify whether both $GABA_A$ and $GABA_B$ receptors can inhibit DA release in nAChR block, we tested the effect of muscimol and baclofen. Activation of $GABA_A$ receptors with muscimol (20 μM) suppressed DA release evoked by single electrical pulses by ∼30% (**Figure 3.2D**: Mann–Whitney test: U = 0, p = 0.0079, n = 5) and this effect was prevented by prior application of $GABA_A$ channel blocker picrotoxin (100 μM), confirming an effect via $GABA_A$ receptors (**Figure 3.2F**: Mann–Whitney test: U = 11, p = 0.85, n = 5). Activation of $GABA_B$ receptors with baclofen (10 μM) also suppressed DA release evoked by single electrical pulses by ∼25% (**Figure 3.2H**: Mann–Whitney test: U = 0, p = 0.0006, n = 7) and this effect was confirmed to be due to $GABA_B$ receptors by prior application of the $GABA_B$ antagonist saclofen

(100 µM), which prevented the effect of baclofen (**Figure 3.2J**: Mann–Whitney test, U = 5, *p* = 0.11, n = 5). These results demonstrate that cholinergic input is not required for the previously described GABAergic effects.

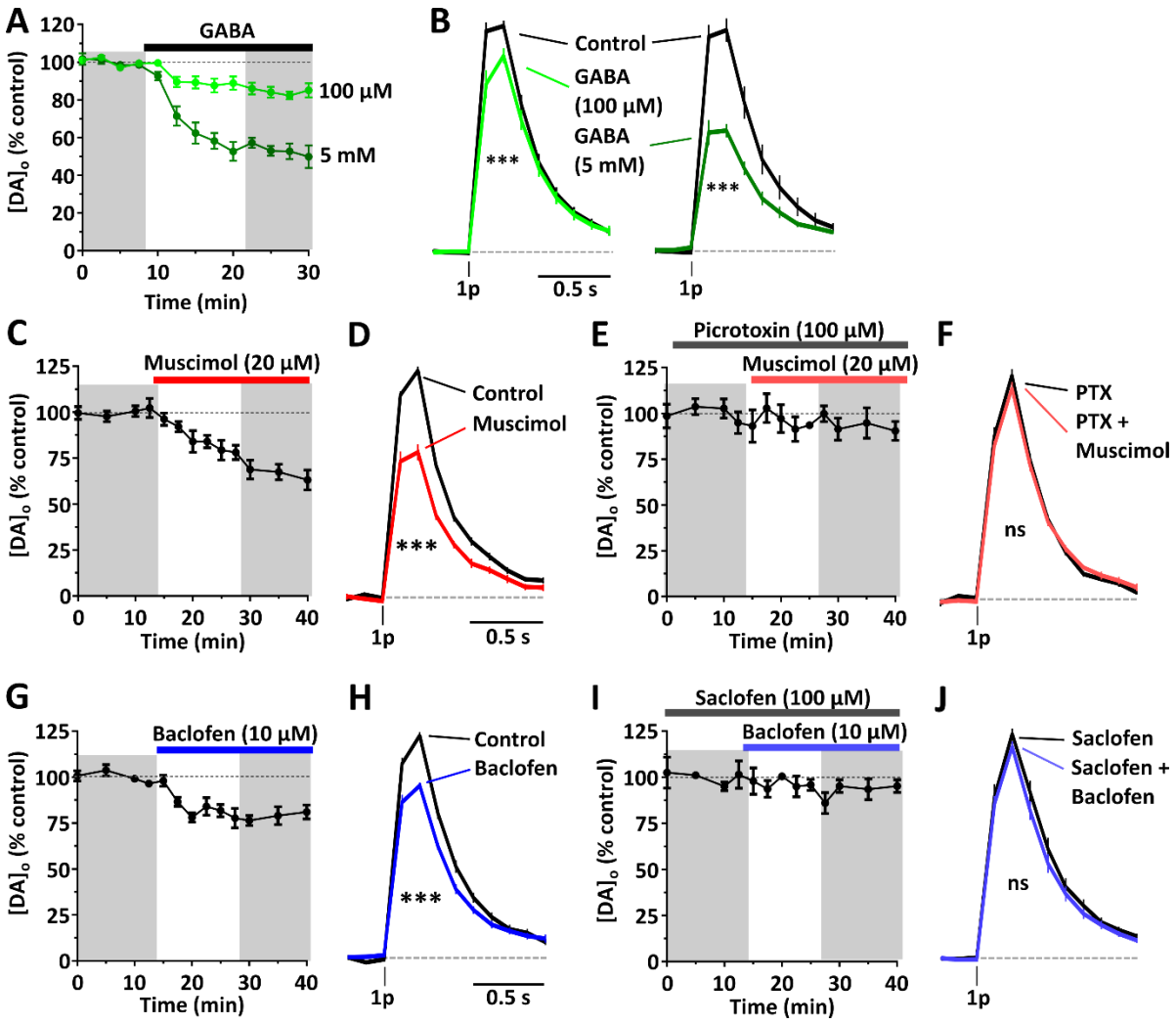

Figure 3.2 – GABA agonist effect is independent of nAChRs. Shown is the mean peak $[DA]_o$ (± SEM) versus time ***(A, C, E, G, I)*** and the mean $[DA]_o$ (± SEM) versus time ***(B, D, F, H, J)*** evoked by 1 electrical pulse before and after application of: 100 µM GABA, *n* = 7, or 5 mm GABA, *n* = 5, ***$p < 0.001$, two-way ANOVA ***(A, B)***; 20 µM muscimol, *n* = 5 ***(C, D)***; 20 µM muscimol in the presence of 100 µM picrotoxin, *n* = 5 ***(E, F)***; 10 µM baclofen, *n* = 7 ***(G, H)***; or 10 µM baclofen in the presence of 100 µM saclofen, *n* = 5 ***(I, J)***. Shaded areas in ***A, C, E, G***, and ***I*** indicate points used for transients represented in ***B, D, F, H***, and ***J***, respectively. The nAChR antagonist DHβE (1 µM) is present throughout. Data are normalized to peak $[DA]_o$ before drug application. *$p < 0.05$, **$p < 0.01$, ***$p < 0.001$, Mann–Whitney tests. Data from panel ***A*** and ***B*** collected by B Roberts and R Siddorn.

3.3.3 GABA receptors inhibit DA release evoked by targeted optogenetic stimulation

To determine whether the inhibition of DA release by GABA receptors depended on the coactivation of some other local neuron type or input during electrical stimulation, we used an optogenetic approach to selectively activate only DA axons. We expressed ChR2-eYFP in DA neurons and axons in *Slc6a3*$^{IRES\text{-}Cre}$ mice using an established viral approach as described previously (Threlfell et al., 2012; Brimblecombe and Cragg, 2015). Either the $GABA_A$ agonist muscimol (**Figure 3.3B**; Mann–Whitney test: U = 0, p = 0.0079, n = 5) or the $GABA_B$ agonist baclofen (**Figure 3.3D** Mann–Whitney test: U = 0, p = 0.029, n = 4), suppressed DA release evoked by single blue light pulses;, indicating that GABA receptor agonists do not require coincident activation of another striatal input to suppress DA release. We also confirmed that, as with electrical stimulation, the effects of muscimol and baclofen were prevented by prior application of antagonists for respectively $GABA_A$ (**Figure 3.3D**, Mann–Whitney test: U = 12, p = 0.36, n = 6) or $GABA_B$ receptors (**Figure 3.3H**, Mann–Whitney test: U = 5, p = 0.127, n = 5).

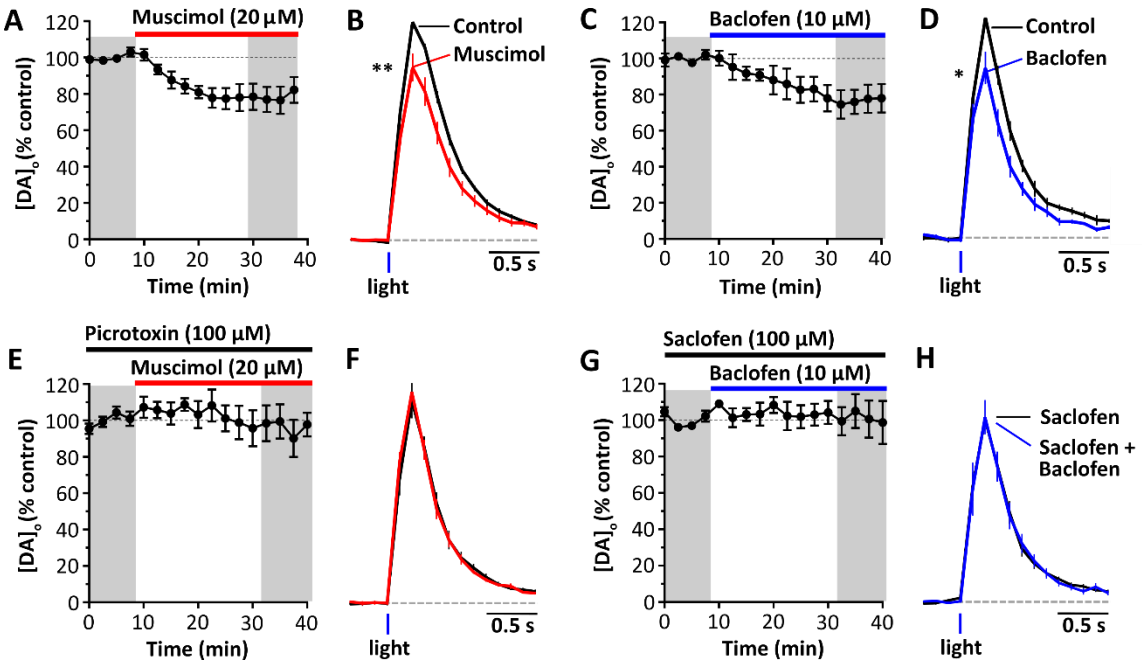

Figure 3.3 - GABA receptors inhibit optogenetically stimulated DA release. Shown is mean peak $[DA]_o$ (± SEM) versus time ***(A,C,E,G)*** and mean $[DA]_o$ (± SEM) versus time ***(B, D, F, H)*** evoked by 1 light pulse before and during application of 20 µM muscimol, *n* = 5 ***(A,B)***; 20 µM muscimol in the presence of 100 µM picrotoxin, *n* = 5 ***(C, D)***; 10 µM baclofen, *n* = 4 ***(E, F)***; or 10 µM baclofen in the presence of 100 µM saclofen, *n* = 6 ***(G, H)***. Shaded areas in ***A, C, E,*** and ***G*** indicate points used for transients represented in ***B, D, F,*** and ***H***, respectively. Data are normalized to mean peak $[DA]_o$ before drug application. **p* < 0.05, ***p* < 0.01, Mann–Whitney tests.

3.3.4 GABA receptors on frequency sensitivity of DA release

We investigated whether GABA receptor activation inhibited DA release during trains of stimuli and across a range of frequencies. Muscimol significantly decreased $[DA]_o$ evoked by 5-pulse trains at all frequencies tested (**Figure 3.4A,B**; two-way ANOVA: drug effect: $F(1,48) = 67.55$; $p = 0.0025$, frequency effect: $F(3,48) = 259.6$, $p < 0.0001$, n = 7) and, furthermore, there was a significant interaction between stimulation frequency and drug effect (**Figure 3.4B**; two-way ANOVA: interaction – drug vs frequency effect: $F(3,48) = 5.485$, $p = 0.0025$, n = 7), which was borne out by an increase in the 5p/1p ratio examined at 100 Hz (**Figure 3.4C**; paired t test: $t(7) = 3.46$, $p = 0.014$, n = 7). In other words, activation of $GABA_A$ receptors can marginally promote the contrast in DA signals released by different firing patterns or rate.

Baclofen significantly decreased evoked $[DA]_o$ (**Figure 3.4E**; two-way ANOVA: drug effect: $F(1,48) = 6.271$, $p = 0.016$; frequency effect: $F(3,48) = 144.5$, $p < 0.0001$, n = 7). We did not detect a significant interaction between stimulation frequency and drug effect (**Figure 3.4E**: two-way ANOVA: interaction – drug vs frequency: $F(3,48) = 0.040$, $p = 0.99$, n = 7); however, the 5p/1p ratio for $[DA]_o$ evoked at 100 Hz was slightly increased with baclofen (**Figure 3.4F**: paired t test: $t(6) = 3.272$, $p = 0.017$, n = 7), suggesting that $GABA_B$ receptors only marginally change the contrast in DA signals released by different activity.

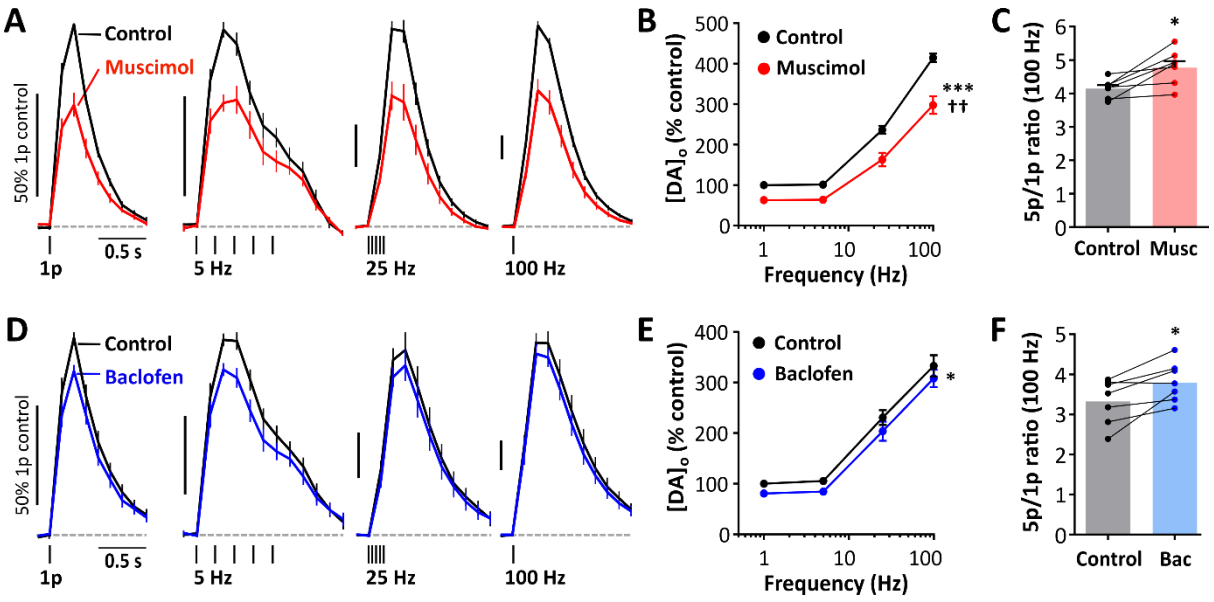

Figure 3.4 - $GABA_A$ and $GABA_B$ receptor agonists modify DA release during pulse trains. The nAChR antagonist DHβE (1 µM) is present throughout. Shown is mean $[DA]_o$ (± SEM) versus time **(*A*,*D*)** and mean peak $[DA]_o$ (± SEM) versus stimulation frequency **(*B*,*E*)** for 1- or 5-pulse trains in control conditions (black); 20 µM muscimol, $n = 7$ **(*A*,*B*)** (red); or 10 µM baclofen, $n = 7$ **(*D*,*E*)** (blue); two-way ANOVA, effect of drug $^*p < 0.05$, $^{***}p < 0.001$, drug × frequency interaction $^{††}p < 0.01$. Data are normalized to peak $[DA]_o$ before drug application. **(*C*, *F*)** Ratio of peak $[DA]_o$ released by 5p versus 1p (100 Hz) in control conditions, muscimol **(*C*)**, or baclofen **(*F*)**. $^*p < 0.05$, paired *t* tests versus control.

3.3.5 GABA operates a tonic inhibition on DA release

Some striatal GABA neurons are tonically active and it has been reported that there is an ambient GABA tone in striatum (Ade et al., 2008; Kirmse et al., 2008, 2009; Santhakumar et al., 2010; Cepeda et al., 2013). We therefore tested whether there was tonic inhibition of DA release by exploring the effects of GABA receptor antagonists on DA release evoked either optogenetically or electrically.

We found that coapplication of $GABA_A$ and $GABA_B$ antagonists bicuculline (10 µM) and CGP 55845 (4 µM), respectively, significantly enhanced $[DA]_o$ evoked by single light pulses in *Slc6a3*$^{IRES\text{-}Cre}$ ChR2-expressing mice by ∼20% (**Figure 3.5A**; Mann–Whitney test: U = 0, p = 0.0079, n = 5), indicating a tonic inhibition of DA release by endogenous striatal GABA in the absence of other stimuli. This tonic inhibition is present and enhanced with electrical stimulation (**Figure 3.5B**; Transients - Mann–Whitney test: U = 0, p = 0.0286, n = 4), with a non-significant trend for a decrease in the 5p/1p ratio (**Figure 3.5B**; 5p1p ratio - paired t-test: t(4) = 2.295, p = 0.0834, n = 5). The GABAergic tonic inhibition does not require glutamatergic input, and similar effects are seen with the presence of the glutamate receptor blockers D-APV (50 µM), GYKI (10 µM) and MCPG (200 µM) (**Figure 3.5C**; Transients - Mann–Whitney test: U = 0, p = 0.0286, n = 4; 5p/1p ratio - paired t-test: t(4) = 3.217, p = 0.0324, n = 4). An ambient GABA level could be an artefact of the low temperatures used in slice FCV. The tonic GABA inhibition in the lab has been demonstrated to be governed by the GABA transporter (GAT) (Roberts et al., 2019), The activity of GAT, like other transporter proteins is temperature dependent (Binda et al., 2002; Mitchell and Silver, 2018). During our experiments, slices are kept at 32°C, which is significantly lower than the average blood temperature of an adult male C57BL6/J mouse (Talan, 1984). Increasing bath temperature to 37-38°C reduced peak $[DA]_o$. The effect of GABA antagonists in 37-38°C was similar than in control conditions at 32°C

(**Figure 3.5D**; two-way ANOVA: effect of temperature $F(1,84) = 0.040$, $p = 0.093$, $n = 4$) suggesting that the tonic GABA inhibition is still present at more physiological temperatures.

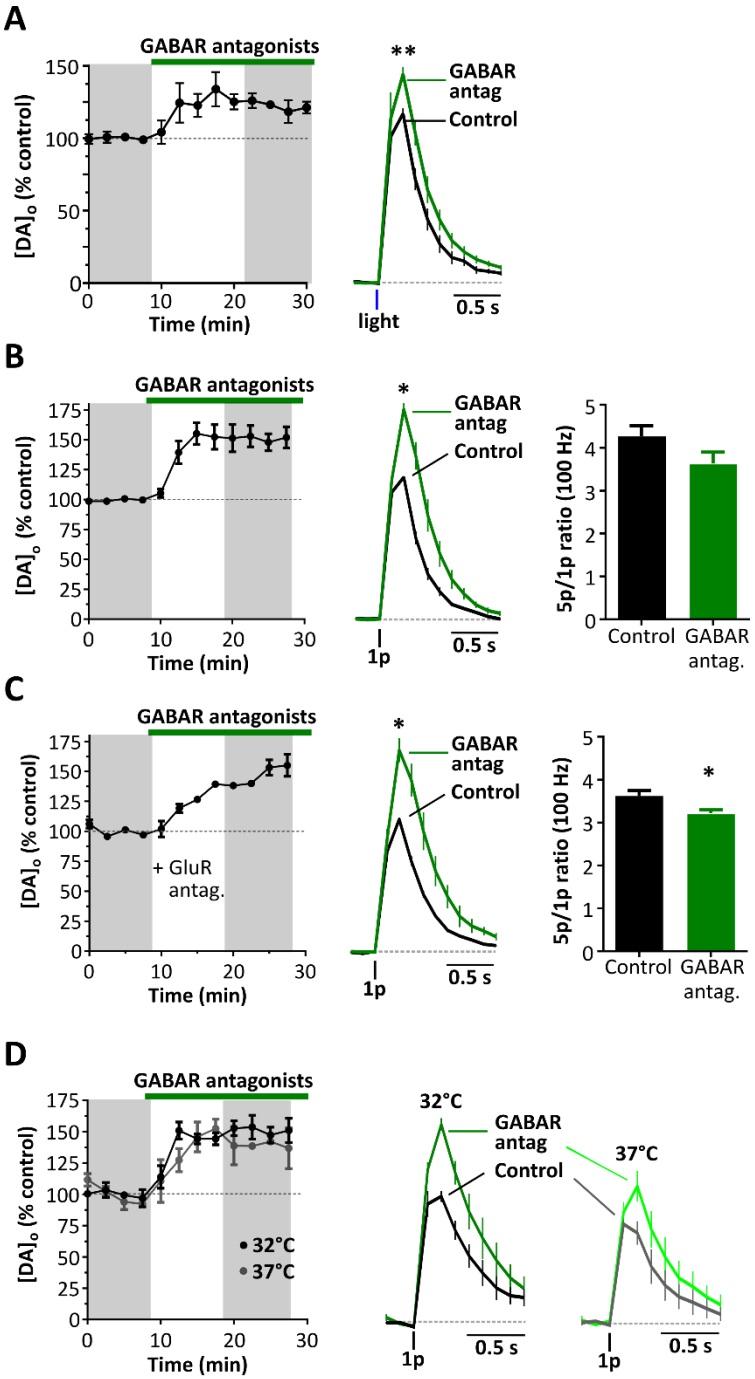

Figure 3.5 - GABA receptor antagonists reveal an ambient striatal tone inhibiting DA release.

The nAChR antagonist DHβE (1 µM) is present throughout. ***(A)*** Mean peak $[DA]_o$ (± SEM) versus time and mean $[DA]_o$ (± SEM) versus time evoked by 1 light pulse before and in the presence of 4 µM CGP 55845 and 10 µM bicuculline (GABAR antagonists), n = 5. ***(B,C)*** Mean peak $[DA]_o$ (± SEM) versus time and mean $[DA]_o$ (± SEM) versus time evoked by 1 electrical

pulse before and in the presence of 4 µM CGP 55845 and 10 µM bicuculline, in the absence ***(B)*** or presence ***(C)*** of glutamate receptor blockers D-APV (50 µM), GYKI (10 µM) and MCPG (200 µM). n = 4. ***(D)*** Mean peak $[DA]_o$ (± SEM) versus time and mean $[DA]_o$ (± SEM) versus time evoked by 1 electrical pulse before and in the presence of 4 µM CGP 55845 and 10 µM bicuculline, at 32 or 37°C. n = 4. Shaded areas in ***A, B, C,*** and ***D*** indicate points used for the respective transients. *p < 0.5, **p < 0.01, Mann–Whitney test. Data from panel ***A*** collected by B Roberts and R Siddorn.

3.3.6 Tonic inhibition is predominately mediated through $GABA_B$ receptors

We investigated which receptors could mediate inhibition of DA release by endogenous GABA using electrical stimulation. $GABA_A$ antagonist bicuculline appeared to slightly elevate, but did not significantly increase, evoked $[DA]_o$ (**Figure 3.6A,B**; two-way ANOVA: effect of drug: $F(1,44) = 1.58$, $p = 0.215$; effect of frequency: $F(3,44) = 128.4$, $p < 0.0001$, n = 5) or interact with stimulation frequency (**Figure 3.6E**: two-way ANOVA: interaction - drug vs frequency: $F(3,44) = 0.115$, $p = 0.95$, n = 8) or the 5p/1p ratio (**Figure 3.6F**: paired t test: $t(7) = 1.217$, $p = 0.263$, n = 8). The $GABA_B$ antagonist saclofen significantly increased evoked $[DA]_o$ (**Figure 3.6C,D**; two-way ANOVA: effect of drug, $F(1,24) = 4.87$, $p = 0.0371$; effects of frequency, $F(3,24) = 57.8$, $p < 0.0001$, n = 4). There was no significant interaction with drug application or stimulation frequency (**Figure 3.6G**: two-way ANOVA: interaction drug x frequency: $F(3,24) = 0.205$, $p = 0.89$, n = 4) or 5p/1p ratio (**Figure 3.6H**, paired t test: $t(3) = 1.49$, $p = 0.233$, n = 4).

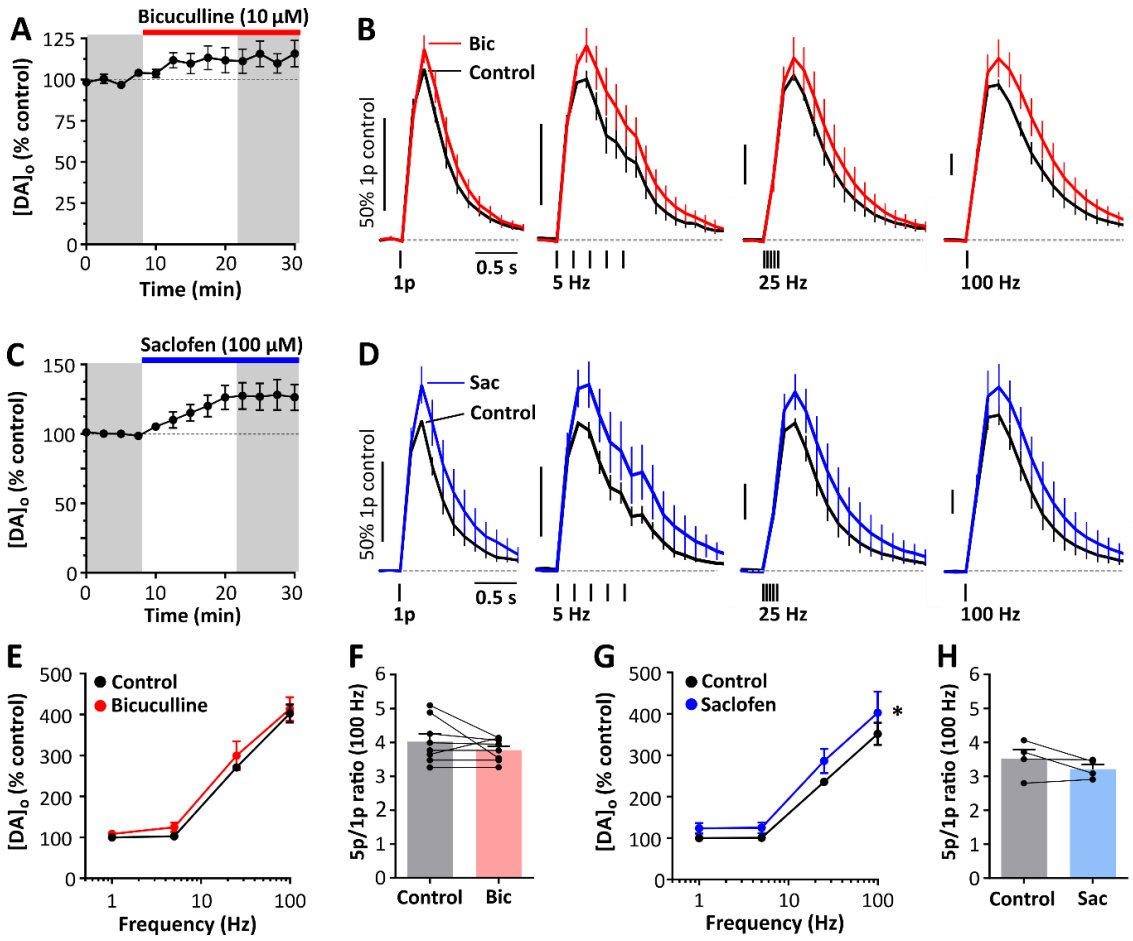

Figure 3.6 - Tonic inhibition is predominately mediated through $GABA_B$ receptors. The nAChR antagonist DHβE (1 µM) is present throughout. ***(A, C)*** Mean peak $[DA]_o$ evoked by 1 electrical pulse with the application of 10 µM bicuculline, n = 5 ***(A)*** or 100 µM saclofen, n = 4 ***(C)***, all in the presence of 1 µM DHβE. ***(B, D)*** Mean $[DA]_o$ (± SEM) versus time in control conditions (black), 10 µM bicuculline, n = 5 ***(B)*** (red), or 100 µM saclofen, n = 4 (***D***) (blue). ***(E, G)*** Mean peak $[DA]_o$ (± SEM) versus stimulation frequency in control conditions (black), with bicuculline ***(E)***, or with saclofen ***(G)***. Data are normalized to peak 1p-evoked $[DA]_o$ before drug application; two-way ANOVA, effect of drug $*p < 0.05$. ***(F, H)*** Ratio of peak $[DA]_o$ released by 5p versus 1p (100 Hz) in control conditions, bicuculline ***(F)***, or with saclofen ***(H)***. Shaded areas in ***A*** and ***C,*** indicate points averaged to obtain 1p transients represented in ***B*** and ***D,*** respectively.

3.3.7 Potassium-mediated changes in STP require ambient GABA tone

Local striatal factors, such as ACh, are capable of powerfully modulating STP. During nAChR inhibition, DA axons show an underlying pattern of STP of short-term facilitation at short stimulation IPIs and short-term depression at longer IPIs (Condon et al., 2018). The patterns of STP are only weakly dependent on the initial release probability (assessed by changing $[Ca^{2+}]_o$), but strongly governed by factors that change axonal excitability (assessed by changing $[K^+]_o$). GABA receptor effects on DA release are expected to be mediated via axonal conductances that include K^+ channels, and also Cl^- channels. Therefore, we aimed to test whether ambient GABA tone on DA axons was required for the control of STP by mechanisms described previously.

We assessed whether changing $[Ca^{2+}]_o$, as a proxy for changing release probability, would be different than previously reported. Under GABA receptor inhibition, decreasing the $[Ca^{2+}]_o$ did not significantly alter the pattern of STP, but significantly reduced 1p-evoked $[DA]_o$ (**Figure 3.7A**: two-way ANOVA: effect of reducing $[Ca^{2+}]_o$, $F(1,32) = 14.95$, $p = 0.0005$, n = 5). These effects are similar to what has been previously demonstrated without GABA receptor inhibition (Condon et al., 2018), and suggests inhibiting ambient GABA tone does not alter the effects from changing factors that modify initial release.

As mentioned previously, altering $[K^+]_o$ powerfully changes the pattern of STP without changing initial release. We were able to replicate those results, reducing $[K^+_o]$ shifts the STP curve to a more facilitated state (**Figure 3.7B**: two-way ANOVA: effect of reducing $[K^+]_o$, $F(1,32) = 14.95$, $p = 0.0005$, n = 5), and increasing $[K^+]_o$ shifts the curve to a more depressed state (**Figure 3.7D:** two-way ANOVA: effect of increasing $[K^+]_o$, $F(1,48) = 28.37$, $p < 0.0001$, n = 7).

Under GABA receptor antagonism, reducing or increasing $[K^+]_o$ no longer significantly modifies the pattern of PPR (**Figure 3.7C**: two-way ANOVA: effect of reducing $[K^+]_o$, $F(1,24) = 1.1$, $p = 0.3047$, n = 5; **Figure 3.7E**: two-way ANOVA: effect of increasing $[K^+]_o$, $F(1,40) = 3.097$, $p = 0.0866$, n = 6). This suggests that there is a requirement for the ambient GABA tone for the effects seen with changing $[K^+]_o$.

To assess the contributions of each GABA receptor, the effects of each individual GABA receptor antagonist on PPR were assessed when $[K^+]_o$ was alternated between 5 mM and 7.5 mM. Both the $GABA_A$ antagonist bicuculline (20 µM) and the $GABA_B$ antagonist CGP55845 (4 µM) significantly altered PPR (**Figure 3.7F**, two-way ANOVA: effect of bicuculline: $F(3,21) = 27.74$, $p < 0.0001$, n = 8**; Figure 3.7G**, two-way ANOVA: effect of CGP55845: $F(3,21) = 15.13$, $p < 0.0001$, n = 8). Following a significant effect of drug application as assessed with the previous analyses, post-hoc tests revealed that bicuculline did not significantly alter the PPR in each $[K^+]_o$ condition, but in the presence or absence of bicuculline altering $[K^+]_o$ significantly changes the PPR (**Figure 3.7F**: control 5 mM vs bicuculline 5 mM, $p > 0.05$; control 7.5 mM vs bicuculline 7.5 mM, $p > 0.05$; bicuculline 5 mM vs bicuculline 7.5 mM, $p \leq 0.0001$; control 5 mM vs control 7.5 mM, $p \leq 0.001$, n = 8, Tukey's multiple comparisons test). Post-hoc tests revealed that CGP 55845 similarly did not significantly alter the PPR within the same $[K^+]_o$ condition, but application of CGP 55845 prevents a significant change in PPR when altering $[K^+]_o$ (**Figure 3.7G**: control 5 mM vs CGP 5 mM, $p > 0.05$; control 7.5 mM vs CGP 7.5 mM, $p > 0.05$; control 5 mM vs control 7.5 mM, $p \leq 0.0001$; CGP 5 mM vs CGP 7.5 mM, $p \leq 0.001$, n = 8, Tukey's multiple comparisons test).

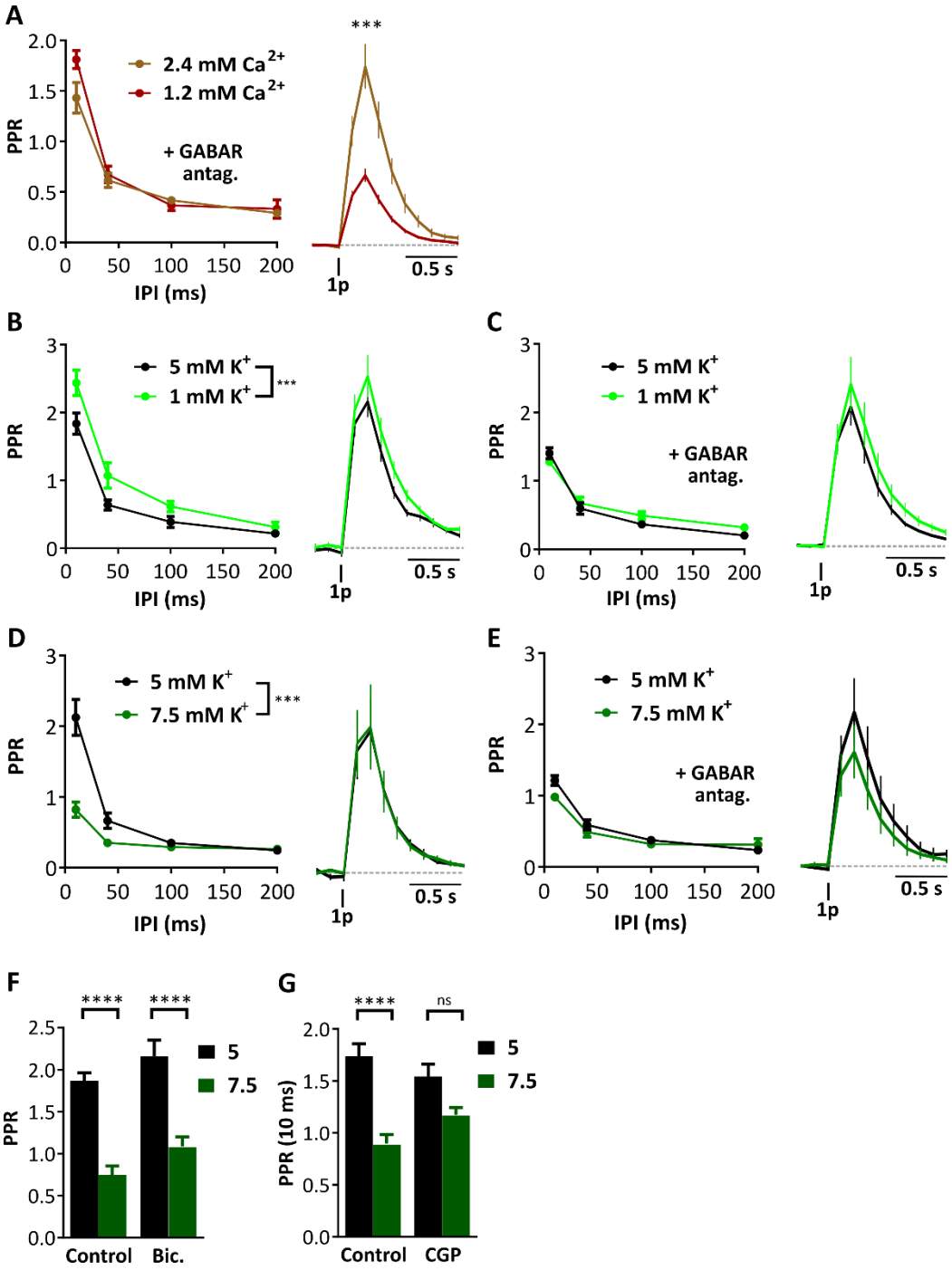

Figure 3.7 - K^+-mediated changes in STP require ambient GABA tone. The nAChR antagonist DHβE (1 µM) is present throughout. ***(A, B, C, D, E)*** Mean PPR and mean peak $[DA]_o$ (± SEM) versus time for 2.4 and 1.2 mM Ca^{2+} in GABA receptor inhibition (n = 5), ***(A)***; 5 mM and 1 mM K^+ in absence (n = 5) ***(B)***, and presence (n = 5) ***(C)*** of GABA receptor antagonism (20 µM bicuculline + 4 µM CGP55845); and 5 mM and 7.5 mM K^+ in absence (n = 7) ***(D)***, and

presence (n = 6) ***(E)*** of GABA receptor antagonism. two-way ANOVA, effect of changing $[K^+]_o$***$p \leq 0.001$ ***(F, G)*** Mean PPR for a 10 ms IPI for 5 mM and 7.5 mM in control or 10 µM bicuculline (n = 8) ***(F)***, and control or 4 µM CGP 55845 (n = 8) ***(G)*** **** $p \leq 0.0001$, Tukey's multiple comparisons test.

3.4 Discussion

In summary, we show that GABA, acting through $GABA_A$ and $GABA_B$ receptors in dorsal striatum inhibit DA release and that these actions are not mediated via regulation of striatal ACh acting at nAChRs. By eliminating ChIs as a site of action for GABA in modulating DA release, a direct action on DA axons becomes more likely as a direct site for GABA action on DA transmission. We additionally show that GABA receptor antagonists increase DA release evoked by single optogenetic or electrical stimuli, revealing that there is a tonic inhibition of DA release by endogenous striatal GABA arising from a tonically active source or ambient level. This ambient GABA tone mediates effects independently of glutamatergic signalling and is temperature insensitive. Furthermore, GABA receptor activation or antagonism slightly modified the frequency sensitivity of DA release during short stimulus trains, but in addition played a critical role in determining whether manipulation of axonal excitability by other means (varying extracellular $[K^+]_o$) modified STP.

3.4.1 GABA influence on DA output does not require striatal ACh

We found that both $GABA_A$ and $GABA_B$ receptor ligands can inhibit DA release whether evoked electrically in the presence of nAChR antagonist or optogenetically by targeted activation of ChR2-expressing DA axons in DAT-Cre mice. Light-activated DA release is not under tonic control by striatal nAChRs in these stimulation conditions (Threlfell et al., 2012; Melchior et al., 2015), consequently, these GABA receptor effects are unlikely to require GABA receptors on ChIs. These findings are consistent with a slice FCV study in NAc indicating that $GABA_B$-mediated control of DA is independent of ACh input (Pitman et al., 2014). Muscarinic M5 receptors on DA axons have been suggested in some studies to regulate DA

release (Bendor et al., 2010; Shin et al., 2015), but we found that electrically evoked DA release in the presence of DHβE and optogenetically evoked DA release were not attenuated by mAChR antagonists (Threlfell et al., 2010, 2012), so these effects of GABA and GABA receptors are unlikely to be mediated by alternative actions of ACh at M5 mAChRs on DA axons. These data do not preclude a potential effect of GABA impacting on DA through ChIs: ChIs receive local and extrastriatal GABA inputs which are capable of modulating ChI excitability, and this could in turn modulate DA release (reviewed in Lim et al., 2014). However, similar effects are seen for GABA receptor activation in and out of nAChR block, so within our experimental paradigm it is unlikely that major effects are mediated through that axis. It is possible that the contribution of ChIs may be more impactful in an *in vivo* context.

Activation of GABA receptors had limited effects on the frequency sensitivity of evoked DA release. Activation of $GABA_A$ receptors, but not $GABA_B$ receptors, interacted in a statistically significant manner with frequency and number of stimulus pulses to slightly promote the ratio of $[DA]_o$ evoked by high-frequency trains over single pulse release, but the effect size was modest. Therefore, GABA receptor activation primarily limits the overall amplitude of DA output with only a minor additional enhancement in the frequency filtering. This contrasts with ACh, which profoundly changes the frequency sensitivity of evoked DA release, changing the relationship between activity and DA output (Rice and Cragg, 2004; Zhang and Sulzer, 2004).

3.4.2 Direct versus indirect actions of GABA receptors

Despite ChIs being unlikely to be the major site of action, the site of GABA receptor localization remains undefined. DA neurons in substantia nigra express $GABA_A$ and $GABA_B$

receptors and these are certainly functional in somatodendritic compartments (Bowery et al., 1987; Nicholson et al., 1992; Boyes and Bolam, 2003; Brazhnik et al., 2008). In a mouse *in vivo* electrophysiological study, GABAergic projections to midbrain DA neurons were shown to be capable of inhibiting DA neuron activity through a $GABA_A$/$GABA_B$ mediated inhibitory response (Brazhnik et al., 2008). Furthermore, local perfusion of GABA receptor antagonists increases the spontaneous firing rate of substancia nigra DA neurons (Paladini and Tepper, 1999; Brazhnik et al., 2008).

However, their trafficking and localization to DA axons has not yet been demonstrated. Some studies have suggested the expression of $GABA_B$ receptors to DA axons: an immunohistochemistry experiment in monkey brain tissue detected $GABA_B$ receptors in striatal neuropil in *en passant* symmetric synapses that display the ultrastructural features of dopaminergic terminals (Charara et al., 1999). On the other hand, $GABA_A$ receptors have not yet been shown on DA axons. It can be difficult to verify the ultrastructural location of membrane bound receptors using classic immunocytochemical methods, which depend on appropriate fixation methods and conditions for antibody penetration. Consequently, the absence of evidence for expression does not preclude their existence on DA axons.

Key candidates for alternative sites of action can however be eliminated. We have excluded actions of GABA receptors on ChIs acting through downstream nAChRs. GABAergic interneurons are unlikely as intermediaries: a GABAergic effect that inhibits a GABAergic intermediary circuit would be expected to increase DA release, which is the opposite of what was seen with the data presented here. An indirect effect via a glutamatergic intermediary could be plausible. DA terminals appear to lack ionotropic glutamate receptors (Bernard and Bolam, 1998; Chen et al., 1998), but an indirect AMPAR-mediated effect has been identified,

where AMPAR activation leads to H_2O_2 generation, which inhibits DA release through ATP-sensitive K^+ channels on DA axons (Avshalumov and Rice, 2003; Avshalumov et al., 2003, 2008; Bao et al., 2009; Patel et al., 2011). However, large electrical stimulus trains were required to evoke H_2O_2 mediated inhibition (10Hz, 3s), whereas the GABAergic effects we see are present in single optogenetic pulses and electrical stimulations, and short burst trains of stimulation. A metabotropic glutamate receptor subtype (mGluR1) has been detected by immuno-EM on striatal DA axons, and mGluR1 activation can inhibit DA release (Paquet and Smith, 2003; Zhang and Sulzer, 2003). These receptors are unlikely to be the main site of action for GABA, our data show that the GABA antagonist effect is unchanged when applied with glutamate receptor antagonists.

Responses to GABA have been described for axons of several other neurons (Kullmann et al., 2005; Trigo et al., 2008; Bucher and Goaillard, 2011). For example, in other CNS neurons, $GABA_A$ receptors can reduce axonal spike amplitude and propagation and promote spike failures (Zhang and Jackson, 1995; Ruiz et al., 2003; Verdier et al., 2003) whereas $GABA_B$ receptors inhibit voltage-gated Ca^{2+} channels (Sun and Chiu, 1999). Similar mechanisms could account for GABAergic inhibition of DA release from DA axonal arbors.

3.4.3 Tonic inhibition of dopamine release

We found that GABA receptor antagonists can enhance DA release evoked by a short single electric or optogenetic stimulation of ChR2-expressing DA axons in *Slc6a3*$^{IRES\text{-}Cre}$ mice, suggesting that DA release is under tonic inhibition by GABA acting on GABA receptors. Light activation is genetically targeted to DA axons and should not activate GABA release from other striatal neurons. Furthermore, the stimulus is sufficiently short (2 ms) that evoked DA

release should not be under the control of any GABA that might be coreleased by this stimulus. Mesostriatal DA neurons can synthesize, store, and corelease GABA (Tritsch et al., 2014; Kim et al., 2015), which can evoke inhibitory currents in postsynaptic medium spiny neurons, but it is unlikely that any GABA coreleased with DA could simultaneously gate the concurrent release of DA evoked by the same single 2 ms stimulus. Therefore, it is more likely that DA release is under tonic inhibition by a pre-existing striatal GABA tone. It is interesting to note that the effect of GABA receptor antagonism differs between optogenetic stimulation and electrical stimulation within our experimental paradigm. Electrical stimulation is non-specific, and globally activates the striatal region it is positioned in, potentially recruiting source of GABA that is inactive during optogenetic stimulation.

A tonic inhibition is consistent with previous reports that there is an ambient GABA tone in striatum detected as a $GABA_A$ receptor-mediated current in postsynaptic neurons (Ade et al., 2008; Kirmse et al., 2008, 2009; Santhakumar et al., 2010; Cepeda et al., 2013). Our findings indicate that tonic inhibition of DA release can readily be detected, at least for $GABA_B$ receptors.

There is precedent for tonic GABA levels within the striatum. At least one type of GABAergic interneuron, the LTSI, is capable of autonomous firing in striatal slices (Beatty et al., 2012). Furthermore, ~95% of striatal neurons are GABAergic, so even low levels of GABA release per neuron could potentially summate for significant impact, regardless of neuronal activity. No GABAergic axoaxonic synapses have been identified on DA axons, but GABA can spillover for extrasynaptic actions in many neurons (Farrant and Nusser, 2005) and might act on DA axons through extrasynaptic effects. The volume of striatum reached by the extensive axonal arbor of a single DA neuron (Matsuda et al., 2009) can be calculated from striatal

neuron counts (Oorschot, 1996) to encompass ~70,000 GABAergic neurons (plus additional non-neuronal cells that might provide a source of GABA). This large number of potential GABA sources might readily spillover and/or otherwise summate to provide an ambient GABA tone that can act at GABA receptors to limit DA output.

No direct evidence for a tonic GABA inhibition on DA terminals is present *in vivo*, and it could be possible that the effects of GABA receptor antagonists are an artefact from our experimental paradigm. This tonic GABA inhibition has been recently demonstrated to be governed by the GABA transporter (GAT) (Roberts et al., 2019). The GAT has a high temperature coefficient (Q_{10}), defined as the change in rate of GABA uptake as a consequence of increasing the temperature by 10°C (Binda et al., 2002; Mitchell and Silver, 2018). During our experiments, slices are kept at 32°C, whereas the average blood temperature of a male C57BL/6J mouse is approximately 38°C (Talan, 1984). However, we have shown that increasing the temperature acute striatal slices are in does not prevent the effects of GABA receptor antagonists, suggesting that the higher temperatures found in vivo would not necessarily impede an ambient GABA tone. Striatal GABA might therefore be in a position to influence striatal output, not only though direct actions on output neurons, local interneurons, and input networks, but also by governing DA transmission.

3.4.4 A role for ambient GABA in axonal excitability and STP

A recent publication from our group described the mechanisms underlying STP of striatal DA release (Condon et al., 2018). As mentioned previously, the dense striatal arbours formed from DA neurons allow DA release to be powerfully controlled by local presynaptic mechanisms that regulate STP. For example, under nAChR block DA axons show frequency-

sensitive release, with a wide spectrum of facilitation and depression depending on the delivered stimulus (Rice and Cragg, 2004; Zhang and Sulzer, 2004). This is a marked shift from when nAChR are active, promoting STD and a frequency insensitive mode of release.

It has been demonstrated that STP in CPu DA axons is largely controlled by mechanisms that modulate K^+-dependent process such as axonal membrane excitability and repolarisation (assessed by changing $[K^+]_o$), and largely independent of changes to initial release or release probability (assessed by changing $[Ca^{2+}]_o$). The role that GABA receptors, and the ambient GABA tone may play on DA axon STP had not been previously considered. GABA receptors regulate K^+ and Cl^- dependent conductances and could therefore impact on axonal excitability. The ability of these receptors to modulate DA release suggest a tonic activation of these receptors could contribute to some of the patterns of STP described previously.

While GABA receptor antagonists do not seem to alter the effect of changing Ca^{2+} on PPR or 1p-evoked release, inhibiting $GABA_A$ and $GABA_B$ receptors prevents the changes to PPR induced by changing $[K^+]_o$. These effects appear to predominately be due to $GABA_B$ receptors, but co-application of $GABA_A$ and $GABA_B$ antagonists is required to prevent significant changes of changing $[K^+]_o$. Varying the concentration of extracellular $[K^+]_o$ alters a number of mechanisms which underlie axonal membrane potential and repolarisation. At the level of DA axons, changing $[K^+]_o$ modifies the Nernstian driving force for K^+ currents, altering the rate of repolarisation at DA axons and therefore the degree of Na^+ channel inactivation, but also alters the rate of K^+ channel inactivation.

It is not fully understood why a GABA receptor activity is required for these effects. There are explanations that could describe how GABA receptors could impact on K^+-mediated STP.

Activity in GABA receptors via an ambient GABA source as critical component for this modulation could suggest mechanisms outside the DA axons play a role in these effects. Changing $[K^+]_o$ could alter the amount of GABA evoked by electrical stimulation, by modulating the excitability of a source of GABA. In this scenario, increasing $[K^+]_o$ could cause more GABA to be released by the initial pulse, which reduces the amount of DA release on the second pulse, decreasing the overall PPR. Alternatively, changing $[K^+]_o$ could modify the dimension of the ambient GABA tone. Increasing $[K^+]_o$ could increase the excitability of a tonically active GABAergic interneuron, or cause an increase in the spontaneous release of GABA. However, no significant changes are seen at the level of 1p-evoked release, which would be expected with a change in tonic GABAergic inhibition.

GABA receptors mediate different ionic conductances, and the GABA-dependent K^+ mediated change in STP could require an enhanced K^+ conductance to occur. The data presented in **Figure 3.7F,G** support a more prominent role for $GABA_B$ receptors in mediating the effects of an ambient GABA tone on DA neurons. $GABA_B$ receptors couple to GIRKs (Sodickson and Bean, 1996), which are a likely candidate for the effector channel for the K^+ dependent $GABA_B$ effects seen here.

Changes in $[K^+]_o$ that influence membrane potential/repolarisation are likely to alter axonal conduction failure (Brody and Yue, 2000; He et al., 2002), and influence the fidelity and extent of action potential propagation through the DA axonal arbor. As the more prominent effects of changing $[K^+]_o$ occur during shorter IPIs, where the second pulse is more

likely to be influenced by the initial pulse and rates of repolarisation, it is possible that different $[K^+]_o$ could differentially affect re-release at the second pulse through this mechanism. When $GABA_B$ receptors are inhibited these effects no longer occur due to a reduction of K^+ conductance on axons.

The effect of $GABA_A$ receptors on PPR is not significant, but coapplication of both receptor antagonists is required to fully prevent modification of STP by varying extracellular $[K^+]_o$. This suggests $GABA_A$ receptors play a role in this mechanism, and previous studies have offered a precedent for this to occur. $GABA_A$ receptors on axons have been described to modulate spike propagation: $GABA_A$ receptor-mediated currents in hippocampal mossy fibers inhibit spike propagation (Ruiz et al., 2003), and in spinal dorsal column tracts from young rats with incomplete myelination there is a $GABA_A$ mediated slowing of conduction (Sakatani et al., 1991). In many axons, however, $GABA_A$ mediates depolarising responses, such as in peripheral sensory axons (Bhisitkul et al., 1987). This excitatory response is hypothesised to be due to the expression of different chloride transporters that enrich the intra-axonal environment with Cl^- (Rocha-González et al., 2008). How in our paradigm altering Cl^- conductances through $GABA_A$ receptors on DA axons could impact on a K^+-mediated mechanism is not understood, but it is likely that altering Cl^- conductance would impact effects mediated by another ion.

The presence of a GABA tone on DA neurons appears to create an additional layer of modulation acting on DA release. Local factors that mediate a change in K^+ conductance can more powerfully alter STP of DA release, dependent on the activation or inactivation of GABA receptors. This could allow for a more tuned, locally integrative signal that further modifies ascending midbrain signals, and alters their final DA output.

In conclusion, we show here not only that $GABA_A$ and $GABA_B$ receptors can gate DA output, but that there is a tonic inhibition by endogenous GABA through an apparent ambient GABA tone. In addition to directly regulating striatal output, striatal GABA tone might therefore also govern striatal integration via dampening DA output. We exclude ChIs acting through nAChRs on DA axons as intermediaries for GABA regulation of DA, thereby adding support to the hypothesis that GABA is acting directly on DA axons. We further explore a role for tonic GABA in manipulating STP of DA release and demonstrate how K^+-mediated changes in STP require activity on GABA receptors.

4. Interrogating striatal cholinergic circuits in parkinsonism

4.1 Introduction

In this chapter, I have described the setting up of a number of approaches to further our understanding of the striatal ACh/DA axis. I have discussed the characterisation of a new mouse cross which will allow for the genetic targeting of ChIs within a parkinsonian disease state. I haved also described the implementation of a new immunohistochemical procedure for accessing ChI cell count/function, and a method for detecting ACh within striatal slices.

4.1.1 Cholinergic interneurons in PD

Despite being only ~1% of striatal neurons, projections from ChIs innervate a large striatal area forming large arbors that are similar in size to DA axons (Contant et al., 1996; Descarries and Mechawar, 2000). Early observations from PD showed that antimuscarinic drugs could be used to ameliorate PD symptoms, suggesting a hypodopaminergic and hypercholinergic disorder. Classically, this led to an suggestion ACh and DA act in opposition (Barbeau, 1962). However, within the striatum, it is now understood that these two neurotransmitter systems have more complex interactions. As opposed to an antagonistic relationship, ACh and DA systems have complementary firing patterns: when DA neurons burst, ChIs can show a coincident pause flanked by brief bursts (Aosaki et al., 1994; Apicella, 2002; Morris et al., 2004). Moreover, striatal ACh via nAChRs powerfully drives DA transmission. DA axons in striatum express multiple types of β2-subunit-containing nAChRs (Exley and Cragg, 2008; Exley et al., 2012). ACh acting through nAChR could operate through

different mechanisms. Pauses in ACh activation of nAChRs reduces DA release probability which, through relieving short-term depression, allows for a frequency sensitivity of release (Rice and Cragg, 2004; Zhang and Sulzer, 2004). Furthermore, synchronous optogenetic activation of a small population of ChIs can directly drive DA release (Threlfell et al., 2012). These observations suggest that pauses in ChIs might promote DA release due to activity from DA neurons, but that synchronized activity in ChIs could additionally provide a major drive of DA release.

Several lines of evidence suggest that ChIs may be altered in PD. Cholinergic compounds are capable of modulating parkinsonian motor symptoms. AChE inhibitors and mAChR agonists are capable of inducing jaw tremors similar to tremors seen in the hands and jaw of PD patients (Mayorga, 1997; Salamone et al., 1998, 2013; Koganemaru et al., 2014). Jaw tremors in rodents are positively correlated with striatal ACh levels and neuronal activity (Koganemaru et al., 2014). AChE inhibitors have also been shown to worsen tremor in PD patients, suggesting that tremor could be a correlate for elevated striatal ACh (Duvoisin, 1967; Ott and Lannon, 1992).

Studies attempting to assess changes in cholinergic markers in PD have not been conclusive. Several studies in PD patients show less expression of ChAT, (Rinne et al., 1973, 1991; Reisine et al., 1977; Bugiani et al., 1980; Mesulam et al., 1984; Nordberg et al., 1985), while others show none, or even higher expression of markers such as ChAT or the vesicular ACh transporter (McGeer and McGeer, 1971; Ruberg et al., 1982; Gangarossa et al., 2016). The variability of these results could be due to assessing different states of disease progression, or differential treatment effects from various PD therapeutic strategies. These

results are suggestive, however, that changes in cholinergic cell number or innervation could occur within parkinsonism.

Most of the mechanistic data regarding ChI changes in PD are from acute toxin models of PD, such as reserpine, 6-OHDA or MPTP administration. These have also suggested functional changes to ChIs. Loss of striatal DA in these models has been shown to lead to aberrant regulation of ChI excitability via downregulation of muscarinic M4 autoreceptor function (Ding et al., 2006) and the disruption of a barium-sensitive component of a slow afterhyperpolarization current (sAHP) (Sanchez et al., 2011). Loss of M4 autoreceptor function, a $G_{i/o}$ linked metabotropic receptor, could lead to elevated striatal ACh release, moreover, disruption of the sAHP allowed ChIs to fire continuously and at higher rates during sustained excitation. A more recent study has suggested that, in a model of DA deficiency responsive to L-DOPA, there is a reduction in ACh availability and the transcription of hyperpolarization-activated cation (HCN) channels that encode the spike timing of ChIs, leading to decreased firing of ChIs (McKinley et al., 2019). Therefore, the published data suggests that loss of striatal DA leads to altered function of ChIs. These findings allow us to revisit the role ChIs play PD, opening up the striatal ACh axis as a target for treating PD symptoms. However, while toxin models are informative, the acute nature of these models are not representative of the slower, progressive, system-wide phenotype seen in human patients. Consequently, it is not yet known whether there is a functional change in ChIs in a more progressive, system-wide phenotype.

The Oxford Parkinson's Disease Centre (OPDC), has generated α-synuclein-based transgenic mouse models of PD that express the human wildtype *SNCA* transgene from the complete genomic locus in bacterial artificial chromosome (BAC) genomic DNA inserts

(Janezic et al., 2013). The *SNCA* BAC transgenes were crossed onto the mouse null (*Snca*$^{-/-}$) background to avoid the confounding expression of mouse α-synuclein in a "humanized" genetic model. This model carries multiple copies of a single site-integrated BAC resulting in overexpression of α-synuclein (*SNCA*-OVX) generating α-synuclein levels twice those seen for endogenous mouse *Snca*, therefore representing a model of PD caused by α-synuclein overexpression linking both familial and sporadic PD. These animals show a 30% reduction in DA transmission detected by FCV in dorsal but not ventral striatum, and ensuing age-dependent changes that include loss of DA neurons in the SNc, reduction of firing rate of SNc DA neurons, and a motor deficit phenotype, together indicating that *SNCA*-OVX is a valuable new animal model of PD. With such a key phenotype, it is essential that we exploit this genotype to probe the disease state further (Janezic et al., 2013).

To that end, we have crossed the *SNCA*-OVX line with a *Snca*$^{-/-}$;ChAT-Cre line. This would allow for the selective expression of Cre recombinase under the *Chat* promoter, encoding ChAT, which within the striatum is selectively expressed in ChIs. This cross will permit the selective genetic manipulation of ChAT+ve neurons within a Parkinsonian context, opening up the options to potentially opto- or chemogenetically modulate these neurons, or to record calcium transients by expressing a fluorescent reporter protein.

The data presented in this chapter aims to verify that this new cross has similar DA release deficits to those seen in the original SNCA-OVX line. Further voltammetry and immunohistochemical experiments using the SNCA-OVX;ChAT-Cre line will aim to assess whether there is evidence of altered ChIs in the parkinsonian state.

4.1.2 Ribosomal protein S6: a marker for cell activity

We have also implemented a new immunohistochemical protocol to assess ChI cell numbers and activity by assessing fluctuations in phosphorylation levels of the ribosomal protein S6 (S6rp). S6rp is an integrant of the ribosomal complex localized interfacing between the 40S and 60S ribosomal subunits (Nygård and Nilsson, 1990). While the mechanisms have not been fully understood, S6rp has been implicated in the stimulation and/or inhibition of certain types of mRNA translation, in the regulation of cell size and in cell proliferation in different cell systems (Ruvinsky et al., 2005; Ruvinsky and Meyuhas, 2006). Additionally, S6rp is phosphorylated by ribosomal protein S6 kinases (S6K1 and 2). These kinases act as effectors downstream of the mammalian target of rapamycin complex 1 pathway (mTORC1 pathway) (Flotow and Thomas, 1992; Ruvinsky et al., 2005). This phosphorylation occurs in a train of evolutionary conserved c-terminal serine residues between Ser235 and Ser247, and has been shown to be functionally relevant for glucose homeostasis regulation and cell size (Ruvinsky and Meyuhas, 2006). In the brain, strong regulation of S6rp phosphorylation has been described in the two populations of MSNs after different dopaminergic pharmacological manipulations (Santini et al., 2009; Valjent et al., 2011; Gangarossa et al., 2013), and has been used to capture translating ribosomes from activated neurons in response to a variety of stimuli (Knight et al., 2012).

A publication by the Bertran-Gonzalez group reported a strong and sustained phosphorylation of different c-terminal serine residues of S6rp specifically occurring in striatal ChIs in basal conditions (Bertran-Gonzalez et al., 2012). This S6rp phosphorylation signal was markedly decreased when neuronal firing was pharmacologically inhibited and increased by pharmacological stimulation of neuronal firing in a rapamycin-dependent manner. These findings suggest a link between neuronal activity and S6rp phosphorylation occurring in

striatal ChIs, potentially indicating an immunofluorescent means of estimating activity in this striatal population. Having a measure of ChI activity and cell numbers would allow for a read-out to assess whether this population is more active between genotypes and would allow us to interrogate whether increased neuronal activity or number underlie a potential hypercholinergic state.

4.1.3 Electrochemical detection of choline

Despite being a crucial neurotransmitter in both the CNS and the periphery, cholinergic transmission in most tissues remains incompletely understood. This is in large part due to ACh being electrochemically inactive, and rapidly metabolised by acetylcholinesterase (AChE). This has restricted the available approaches to detect ACh. Rapid *in situ* determination of fluctuating extracellular levels of ACh and choline (Ch) is important for the characterization of cholinergic transmission in normal and pathological physiology.

Several techniques for the analytical measurement of ACh exist, and many have significant caveats. The majority of data regarding ACh levels in the brain have been mainly obtained using *in vivo* brain microdialysis. However, *in vivo* microdialysis offers poor spatial and temporal resolution, as it is broadly sampling the extracellular environment with a resolution of minutes. Other approaches include postsynaptic patch clamp, which is useful for monitoring post-synaptic effects of ligand-gated ion channels such as nAChRs. However, limited by the number of cells that can be recorded simultaneously and by the rapid and prominent desensitisation of ACh currents. Direct amperometry recordings of ACh have also been used, however and the need to use multiple complex enzymes to break down ACh complicate the interpretation of obtained signals. Finally, fluorescent sensors have also been

developed, however these have until recently shown low sensitivity to ACh, and generally require an invasive approach for their expression.

An alternative approach would be to target its precursor and metabolite, choline (Ch); ACh is synthesised in nerve terminals from acetyl coenzyme A and Ch by the enzyme ChAT, while rapid inactivation of ACh by acetylcholine esterase (AChE) produces Ch. *In vivo*, the rapid fluxes of Ch produced by this process have been validated as a marker of cholinergic (ACh) activity in brain tissue (Burmeister et al., 2003; Parikh et al., 2007).

To attempt to assess choline levels in slice, we employed a Pt-based polymer enzyme composite sensor (Baker et al., 2015, 2017). The electrode incorporates the enzyme choline oxidase (ChOx), which breaks down Ch and releases H_2O_2. H_2O_2 is then oxidised by the Pt wire (held at +0.7 V).

This electrode has been used and verified *in vivo*, but it would be of interest to detect choline within acute striatal slices. Assessing Ch levels *ex vivo* allows for easier mechanistic manipulations and could potentially be used to draw parallels with slice voltammetry recordings.

4.1.4 Hypothesis

This chapter has three global aims:

1- To assess whether the SNCA-OVX;Snca$^{-/-}$;ChAT-Cre line is an appropriate mouse line to assess the ACh/DA axis;

2- To assess changes in ChI cell count/activity in SNCA-OVX;Snca$^{-/-}$;ChAT-Cre mice;

3- To implement detection of Ch.

4.2 Materials and methods

4.2.1 Fast scan cyclic voltammetry

For multisite experiments: on each recording day, a pair of experimental animals consisting of one *SNCA*-OVX;ChAT-Cre animal (*SNCA*-OVX; *Snca*$^{-/-}$; ChAT-Cre) and one control *Snca*$^{-/-}$; ChAT-Cre animal at 3-4 m.o., were humanely killed by cervical dislocation and decapitated, and the brain slices obtained as outlined in Chapter 2. A total of 8 experimental animals were used, 4 from each genotype. Data was acquired from at least two slices per experimental animal. In each slice, $[DA]_o$ was monitored in 3 dorsal striatal sites (dorsomedial, dorso-mid, and dorsolateral) and 3 ventral striatal sites (ventromedial CPu, NAc core, and NAc shell). Recording sites are represented in **Figure 4.1B**. Each site was sampled once per slice. Stimuli delivered to each site were single pulses and 4 pulses at 100 Hz at 2.5 min intervals. The order of preparation and sampling of each genotype was randomised, as was the order of sampling from each site. Data are represented as means ± SEM, and n refers to the number of sites sampled.

For wash-on experiments, data acquired immediately before drug application were used as predrug control data and were compared with data acquired after drug effects had equilibrated after ~10–20 min of application. Ratios for $[DA]_o$ evoked by 4p/1p were obtained by dividing each 4p-evoked $[DA]_o$ value with an average 1p-evoked $[DA]_o$ value in the same condition at that recording site. Data are represented as means ± SEM, and n refers to the number of sites sampled.

Comparisons for statistical significance were assessed by one- or two-way ANOVA, paired and unpaired t tests, or Mann–Whitney U tests where data were not normally distributed using GraphPad Prism.

4.2.2 Immunohistochemistry

4 pairs of control and *SNCA*-OVX animals (3-4 m.o.) were sacrificed by transcardial perfusion. Briefly put, animals were injected with 0.1 mL pentobarbitol (200 mg/ml, Animalcare), and flushed with 10 mL ice-cold 4% PFA. The brain was extracted and held at 4% PFA for 24 hours at 3°C. Following this, brains were sliced at 40 µm and processed for staining immediately after slicing. A 1 in 8 striatal series was randomly selected. Slices were washed in phosphate-buffered saline with sodium fluoride (PBS-NaF) (0.1mM NaF), incubated in PBS-NaF +3% H_2O_2 + 10% methanol (vol/vol) for 5 minutes, and then washed again with PBS-NaF. The slices were then incubated for 20 minutes in 0.2% Triton in PBS-NaF + 10% donkey serum and washed again in PBS-NaF. Slices were incubated overnight at 4°C in PBS-NaF (0.2% Triton + 3% DS) and 1:300 rabbit anti-phosphorylated ribosomal protein S6 (Cell Signalling Technology, 2215S), 1:200 goat anti-ChAT (Millipore, AB144P). Following a wash, slices were incubated for 60 min in 1:1000 Alexa Fluor 568 donkey anti-goat, 1:400 donkey anti-rabbit Alexa-488-coupled secondary diluted in PBS-NaF + 3% DS. Slices were again washed, dried and mounted on slides with Vectashield Antifade Mounting Media (Vector Laboratories). Images were acquired with an Olympus FV1000 Laser Scanning Microscope. Comparisons for statistical significance were assessed by two-way ANOVA, unpaired t tests, or Kolmogorov-Smirnov tests using GraphPad Prism.

Images were processed by a custom made ImageJ macro (Schindelin et al., 2012). Briefly put, a Gaussian blur was applied to the image obtained from the ChAT channel and was thresholded to obtain an appropriate mask identifying cells that are ChAT+ve and excluding particulates too small to be ChIs. Regions of interest (ROIs) were automatically obtained from this image and transferred to the S6rp channel and mean fluorescent intensity values were then obtained for each ROI. When subtracting background fluorescence, the average striatal fluorescence in either channel was calculated without the ChAT+ve ROIs and subtracted from the S6rp values obtained from the ROIs. Comparisons for statistical significance were assessed by two-way ANOVA, unpaired t tests, or Kolmogorov-Smirnov tests using GraphPad Prism.

4.2.3 Choline detection

The choline probes used in this chapter were manufactured by the John Lowry group, University of Maynooth, Ireland according to the following protocol. 5T Teflon®-coated Pt/Ir (90%/10%) disc electrodes or cylinder electrodes (125-µm bare diameter, 175-µm coated diameter, Advent Research Materials, Suffolk, UK) of approximately 6 cm in length were utilised in this study. 3 mm of Teflon® insulation was stripped from the wire and soldered onto a gold clip (Fine Science Tools GmbH, Heidelberg, Germany) to facilitate an electrical connection to the potentiostat while the opposite end of the wire was freshly cut to form an active surface disc for the biosensor. All cylinder electrodes had an additional 1.0 ± 0.1 mm of Teflon stripped away. Poly(o-phenylendiamine) (PPD) was electrochemically grown onto the active surface and stored at 4 °C for a minimum of 3 h before biosensor constituent addition. The active surface of each electrode was coated with biosensor constituents using a dip

absorption method. Briefly, electrodes were dipped for 0.5 s into monomeric immobilisers MMA or Styrene, followed by incorporation of Nafion® (5%) or cellulose acetate (2%) and then consecutively dipped into ChOx (50 or 500 U/ml), BSA (0.1–1%), glutaraldehyde (0.1–1%) and PEI (1–2%) for a total of 10 layers. 5 min drying incubations were conducted between each layer (**Figure 4.8A**). Sensors were prepared in batches of four, typically taking three days to manufacture.

A platinum wire served as the reference electrode, and both the working and reference electrodes were threaded through a tapered capillary fibre to aid in mounting in our *ex vivo* manipulators **(Figure 4.8B)**. Due to the working electrode's sensitivity to DA, in later experiments a number of probes were manufactured incorporating a null sensor **(Figure 4.8C)**. The null sensor was also manufactured in the John Lowry group and were almost identical to the working electrode in active surface composition but did not include ChOx in the manufacturing process. The null sensor was also threaded through the capillary tube, in an attempt to obtain recordings from a site close to the working electrode. However, no data was obtained from these probes due to the difficulty in correctly embedding two sensors in the tissue.

Constant potential amperometry at +0.7 V was performed in all electrochemical experiments using the custom designed low-noise potentiostat (Biostat IV, ACM Instruments, Cumbria, UK). Data acquisition was performed PowerLab interface system (ADInstruments Ltd, Oxford, UK) and LabChart® for Windows (Version 6, ADInstruments Ltd).

Slices were obtained from ChAT-Cre;Ai32 animals (B6.Cg-*Gt(ROSA)26Sor*$^{tm32(CAG-COP4*H134R/EYFP)Hze}$/J, The Jackson Laboratory), and were prepared as previously described in **Chapter 2**. These animals constitutively express ChR2 in ChIs, allowing for selective light-

activation of these interneurons and consequent release of ACh. Prior to inserting the electrodes into the striatum, a 10 µM choline chloride (ChCl), and a 2 µM DA solution were washed on to the electrode to assess its sensitivity to both compounds. Following the embedding of the probes into striatal tissue, a 30 minute acclimatisation period was allowed prior to recording.

Stimuli were optically or electrically evoked every 2.5 minutes. All recordings were done in 1 µM DHβE to prevent ACh-evoked DA release. Ch signals were light/electrically evoked with 10/20 pulse trains at 25Hz. Light stimulation was delivered by an LED system (OptoLED; Cairn Research). ACh release was evoked with full-field 470 nm blue light and a pulse duration of 2 ms. Electrical stimulation intensity was set to 0.6 mA, with a duration of 200 µs.

4.2.4 Drugs

DHβE (1 mM stock in dH_2O), TTX (1 mM stock in dH_2O), and bicuculline (10 mM stock in DMSO) were obtained from Tocris Bioscience. CGP 55845 hydrochloride (8 mM stock in DMSO) was obtained from Abcam. Stock aliquots of drugs were stored at −20 °C, and were diluted with aCSF to final concentration immediately before use.

4.3 Results

4.3.1 Characterising DA release in SNCA-OVX;ChAT-Cre

We crossed the SNCA-OVX mouse model with a $Snca^{-/-}$;ChAT-Cre line, generating a new cross that expresses Cre recombinase in striatal ChIs within the SNCA-OVX context. Expression of Cre recombinase under the ChAT promoter could alter the phenotype of this model. To verify that expression of Cre recombinase in ChIs does not alter the DA release deficits described in original publication describing the SNCA-OVX line (Janezic et al., 2013), we measured DA release within the dorsal and ventral striatum. Similarly to reported observations in *SNCA*-OVX mice without ChAT-Cre, *SNCA*-OVX;ChAT-Cre animals show a 30% reduction in DA release in the dorsal striatum compared to the $Snca^{-/-}$;ChAT-Cre controls, with no significant changes in the ventral striatum (**Figure 4.1A**: unpaired t test: dorsal striatum - $t(44) = 2.313$, $p = 0.0254$, n = 23; ventral striatum - $t(46) = 0.754$, $p = 0.94$, n = 24).

Dividing the data into the different subregions of the striatum showed trends for a decreased $[DA]_o$ in the dorsal regions of the striatum, particularly in the most dorsolateral recording sites, but no subregion showed a significant difference (**Figure 4.1B**: unpaired t-tests: dorsomedial striatum: $t(14) = 1.009$, $p = 0.3301$, n = 8; dorso-mid striatum: $t(14) = 0.6961$, $p = 0.4977$, n = 8; dorsolateral striatum: $t(12) = 2.089$, $p = 0.0587$, n = 7; ventromedial striatum: $t(14) = 0.074$, $p = 0.9418$, n = 8; NAc core: $t(14) = 0.44$, $p = 0.6665$, n = 8; NAc shell: $t(14) = 0.4782$, $p = 0.6399$, n = 8). These results suggest that inclusion of Cre recombinase under the ChAT promoter does not alter the overall DA release deficits seen in the original *SNCA*-OVX animals.

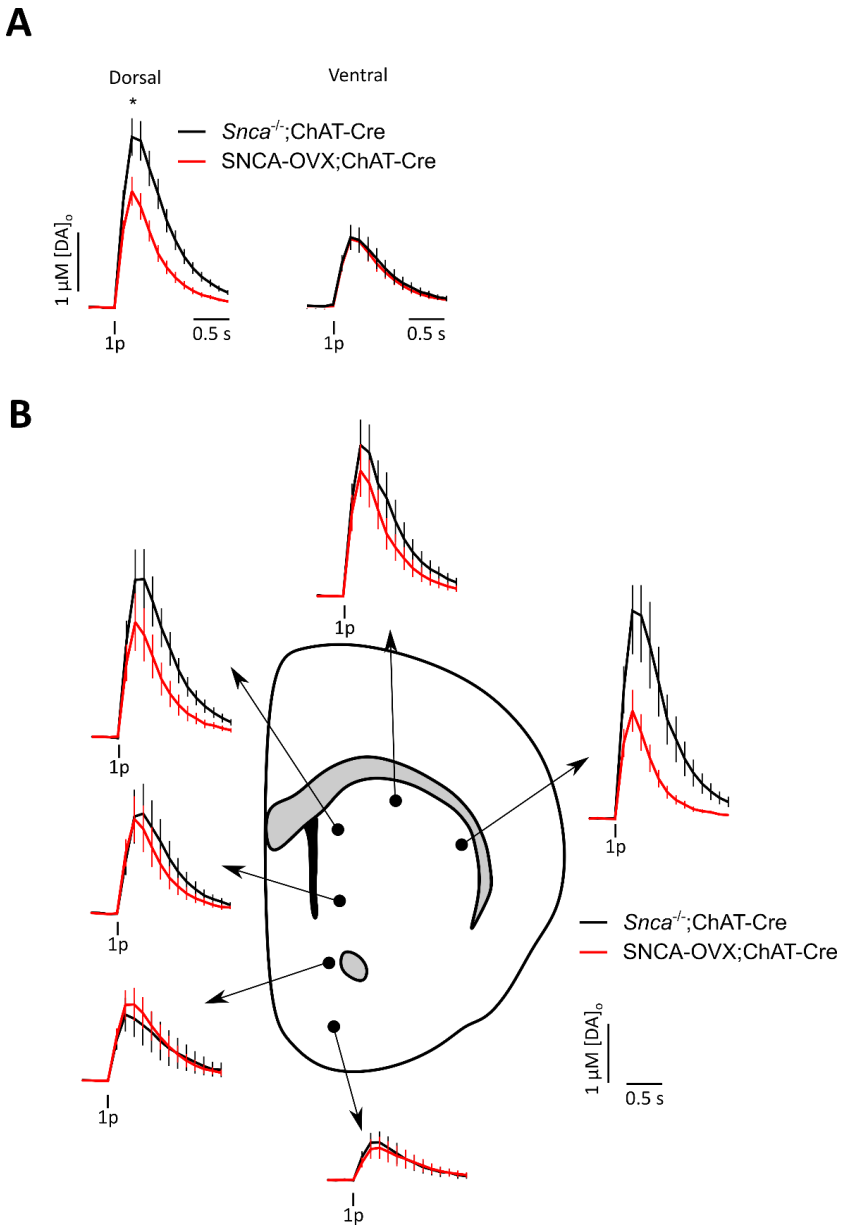

Figure 4.1- SNCA-OVX;ChAT-Cre mice show a dorsal-striatum specific DA deficit. ***(A)*** Mean peak $[DA]_o$ (± SEM) evoked by 1 electrical pulse between *Snca*$^{-/-}$;ChAT-Cre and *SNCA*-OVX;ChAT-Cre mice in dorsal (n = 23) and ventral (n = 24). ***(B)*** Mean peak $[DA]_o$ (± SEM) evoked by 1 electrical pulse between Snca-/-;ChAT-Cre and *SNCA*-OVX;ChAT-Cre mice in the 3 dorsal striatal sites (dorsomedial – n = 8, dorso-mid – n = 8, and dorsolateral – n = 7) and 3 ventral striatal sites (ventromedial CPu – n = 8, NAc core – n = 8, and NAc shell – n = 8) recorded. *p < 0.05, unpaired t-test.

We then explored the effects of nAChR inhibition of DA axons by comparing *SNCA*-OVX;ChAT-Cre and Snca$^{-/-}$;ChAT-Cre animals. 1 µM DHβE suppresses 1p-evoked DA release in both dorsal (**Figure 4.2A**) and ventral striatum (**Figure 4.2B**) in both *SNCA*-OVX;ChAT-Cre and Snca$^{-/-}$;ChAT-Cre genotypes. This suppression was not significantly different between *SNCA*-OVX;ChAT-Cre and Snca$^{-/-}$;ChAT-Cre animals (**Figure 4.2A**: Mann-Whitney tests: dorsal striatum: U = 5, p = 0.4857, n = 8; **Figure 4.2B**: ventral striatum: U = 7, p = 0.5556, n = 10). Likewise, the profiles of 4p/1p ratios are not significantly different between these genotypes in drug-free conditions (**Figure 4.2C**: two-way ANOVA: genotype effect: F(1,42) = 0.5599, p = 0.4585, n = 8; **Figure 4.2D**: two-way ANOVA: genotype effect: F(1,53) = 3.179, p = 0.0803, n = 10). However, with the application of 1 µM DHβE there was significant effects between each genotype for 4p/1p ratios (**Figure 4.2E**: two-way ANOVA: genotype effect: F(1,53) = 3.179, p = 0.0129, n = 10; **Figure 4.2F**: two way ANOVA: ventral striatum: genotype effect: F(1,53) = 4.474, p = 0.0391, n = 10).

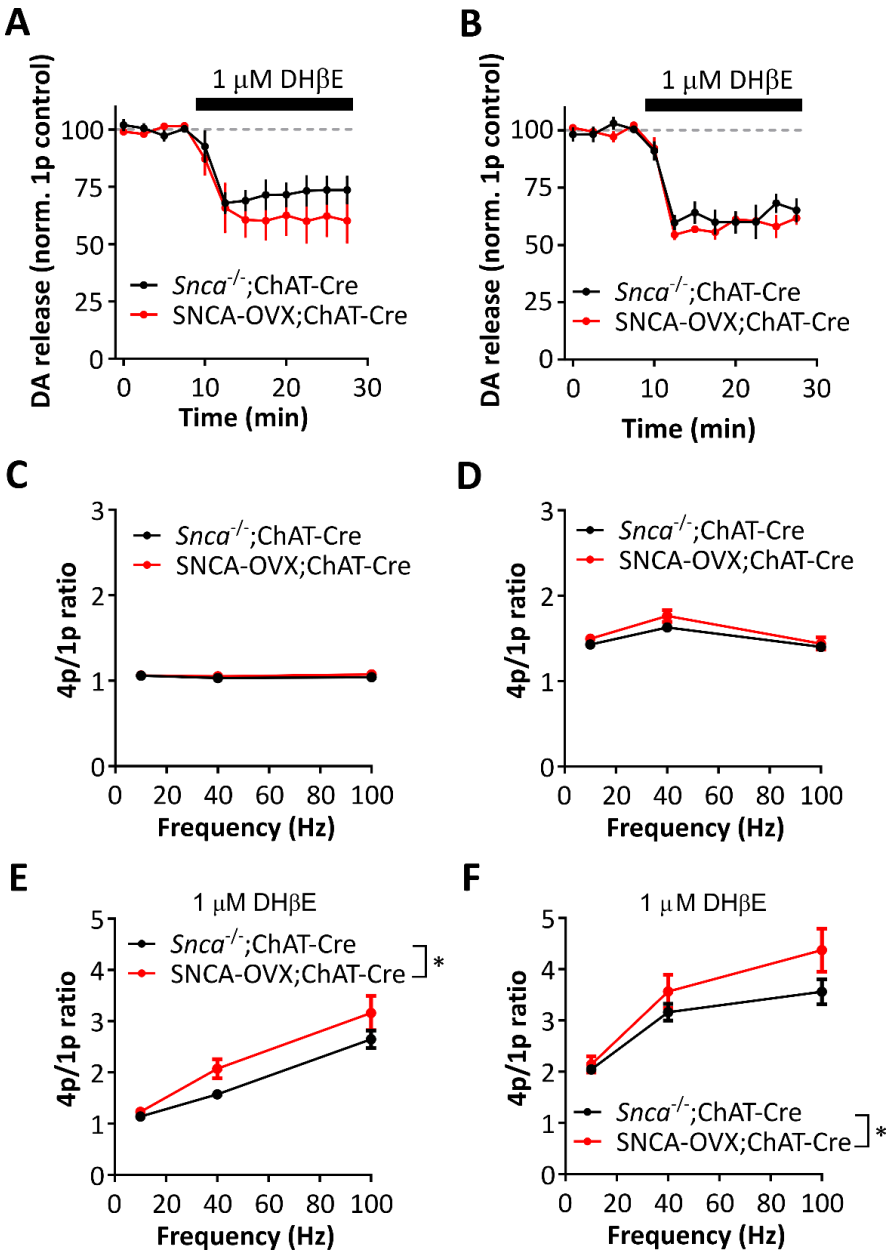

Figure 4.2- nAChR block differentially effects 4p/1p ratios between *Snca*$^{-/-}$;ChAT-Cre and *SNCA*-OVX;ChAT-Cre mice. Shown are the mean peak $[DA]_o$ (± SEM) versus time between *Snca*$^{-/-}$;ChAT-Cre and *SNCA*-OVX;ChAT-Cre mice in dorsal (n = 8) **(A)** and ventral striatum (n = 10) **(B)**. Data are normalized to peak $[DA]_o$ before drug application. Shown are the 4p/1p ratios for 10, 40, and 100Hz in drug-free conditions in dorsal (n = 8) ***(C)*** and ventral (n = 10) ***(D)*** striatum, and in 1 μM DHβE in dorsal (n = 10) ***(E)*** and ventral (n = 10) ***(F)*** striatum. *$p < 0.05$, two-way ANOVA, effect of genotype.

We then explored the effect of GABA receptor antagonism on DA release and compared the effect between the *SNCA*-OVX;ChAT-Cre and Snca$^{-/-}$;ChAT-Cre genotypes. As previously described in Chapter 3 blocking GABA receptors enhances 1p-evoked DA release. Data from our group has also demonstrated that there is a greater GABA antagonist effect in the dorsal striatum of *SNCA*-OVX animals (Roberts et al., 2019). To confirm that this enhanced GABA receptor effect is not altered by expression of Cre recombinase, we repeated this experiment with the *SNCA*-OVX;ChAT-Cre and Snca$^{-/-}$;ChAT-Cre animals. Application of GABA receptor antagonists (bicuculline - 10 µM, CGP 55845 - 4 µM) enhanced 1p-evoked DA release in both dorsal (**Figure 4.3A**) and ventral striatum (**Figure 4.3B**) in both *SNCA*-OVX;ChAT-Cre and Snca$^{-/-}$;ChAT-Cre mice. A significantly greater increase of $[DA]_o$ evoked by the GABA receptor antagonists occurs selectively in the dorsal striatum of *SNCA*-OVX;ChAT-Cre in comparison to the Snca$^{-/-}$;ChAT-Cre (**Figure 4.3A**: Mann-Whitney test: dorsal striatum: U = 7, p = 0.0286, n = 6; **Figure 4.3B**: Mann-Whitney test: ventral striatum: U = 10, p = 0.6667, n = 7). Application of GABA receptor antagonists did not differentially alter the 4p/1p ratio between genotypes in the dorsal striatum (**Figure 4.3C**: dorsal striatum: two-way ANOVA: genotype effect: F(1,54) = 0.8701, p = 0.0237, n = 8) or the ventral striatum (**Figure 4.3D**: ventral striatum, two-way ANOVA: genotype effect: F(1,39) = 0.8701, p = 0.3567, n = 11).

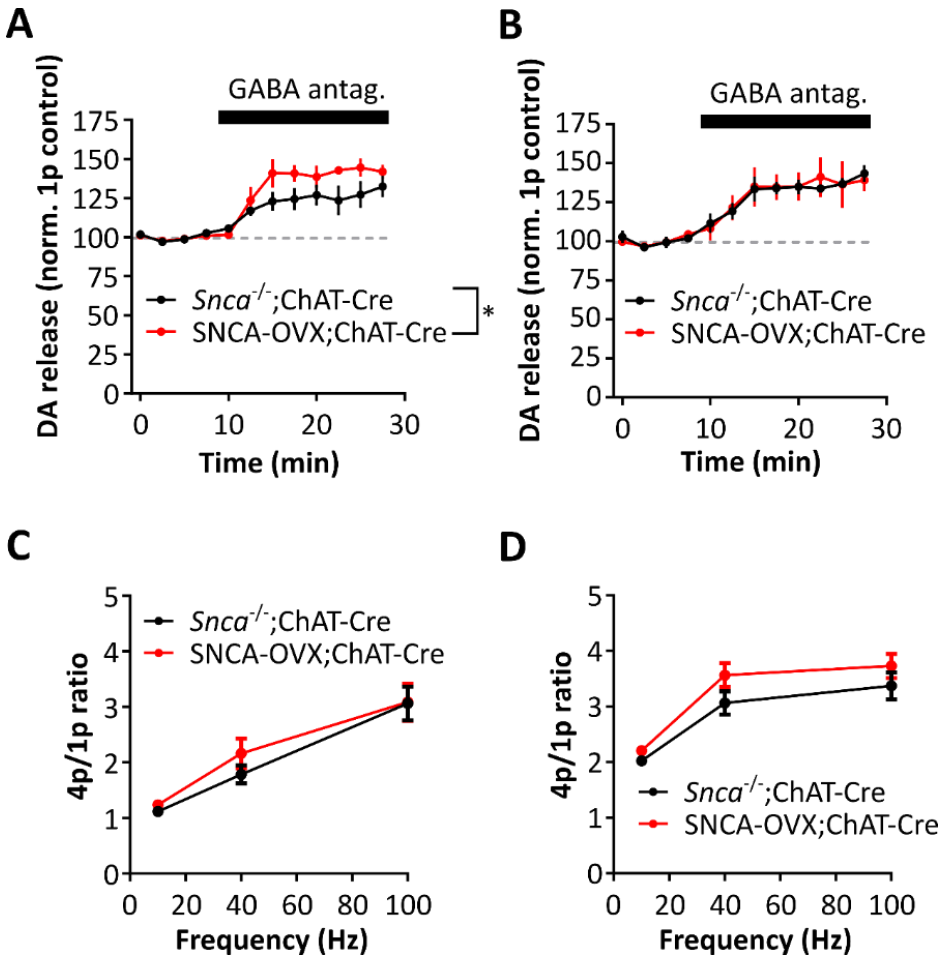

Figure 4.3- Effect of GABA receptor antagonism is enhanced in the dorsal striatum of *SNCA*-OVX;ChAT-Cre. 1 µM DHβE is present throughout. Shown are the mean peak $[DA]_o$ (± SEM) versus time between *Snca*$^{-/-}$;ChAT-Cre and *SNCA*-OVX;ChAT-Cre mice in dorsal (n = 6) ***(A)*** and ventral striatum (n = 7) ***(B)*** with application of 10 µM bicuculline and 4 µM CGP 55845. Data are normalized to peak $[DA]_o$ before drug application. Shown are the 4p/1p ratios for 10, 40, and 100Hz in dorsal (n = 8) ***(C)*** and ventral (n = 11) ***(D)*** striatum. *$p < 0.05$, Mann-Whitney test.

4.3.2 ChI count and activity in SNCA-OVX;ChAT-Cre

To assess whether ChI numbers and/or activity are different between control and SNCA-OVX animals, we co-stained fixed striatal slices for ChAT (to identify ChIs), and S6rp (to assess cell activity). Representative slices used for analysis are demonstrated in **Figure 4.4**. This figure also demonstrates the dorsal/ventral division selected for analysis. Three slices were obtained from a 1 in 8 series and were chosen to be representative of the AP axis in which previous voltammetry experiments in this chapter were performed (approximately 1.5, 1.8, and 2.1 mm from bregma). By considering cell counts per region and animal as individual datapoints, there is a significantly higher number of ChAT+ve neurons between SNCA-OVX;ChAT-Cre and *Snca*$^{-/-}$;ChAT-Cre animals (**Figure 4.5A**: two-way ANOVA: genotype effect: $F(1,44) = 4.072$, $p = 0.0497$; region effect: $F(1, 44) = 7.644$, $p = 0.0083$, n = 12). By sub-dividing the datapoints into the AP coordinate they occupy, the significant effect is lost (**Figure 4.5B**: two-way ANOVA: genotype effect: $F(1, 42) = 3.476$, $p = 0.0693$; AP axis effect: $F(2, 42) = 0.8569$, $p = 0.4318$, n = 8). A similar non-significant trend can be seen when considering dorsal and ventral regions for single animals as individual datapoints (**Figure 4.5C**: two-way ANOVA genotype effect: $F (1, 12) = 1.903$, $p = 0.1929$). By considering total cell counts per animal as a datapoint, there is a trend for a higher number of ChAT+ve neurons in the SNCA-OVX;ChAT-Cre animals, but counts were not significantly different between SNCA-OVX;ChAT-Cre and *Snca*$^{-/-}$;ChAT-Cre (**Figure 4.5D**: unpaired t-test: $t(6) = 1.801$, $p = 0.1218$, n = 4).

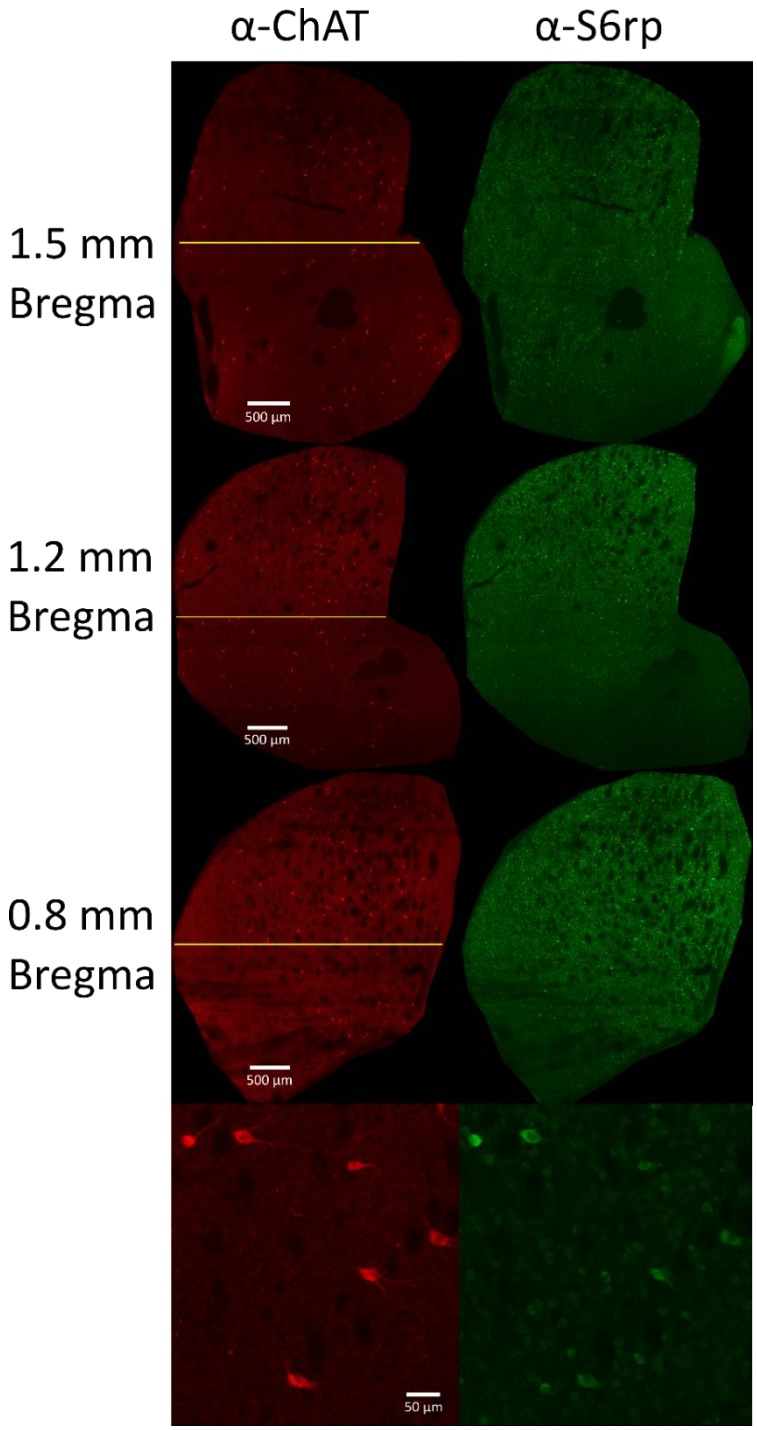

Figure 4.4- ChAT/S6rp co-stain. Representative images from slices used to obtain data, and the approximate coordinates they were obtained from. Yellow line indicates dorsal/ventral striatal division. Anti-ChAT stain is in red on the left, and the complementary anti-S6rp stain in green on the right. Bottom panels: individual co-stained ChAT+ve interneurons.

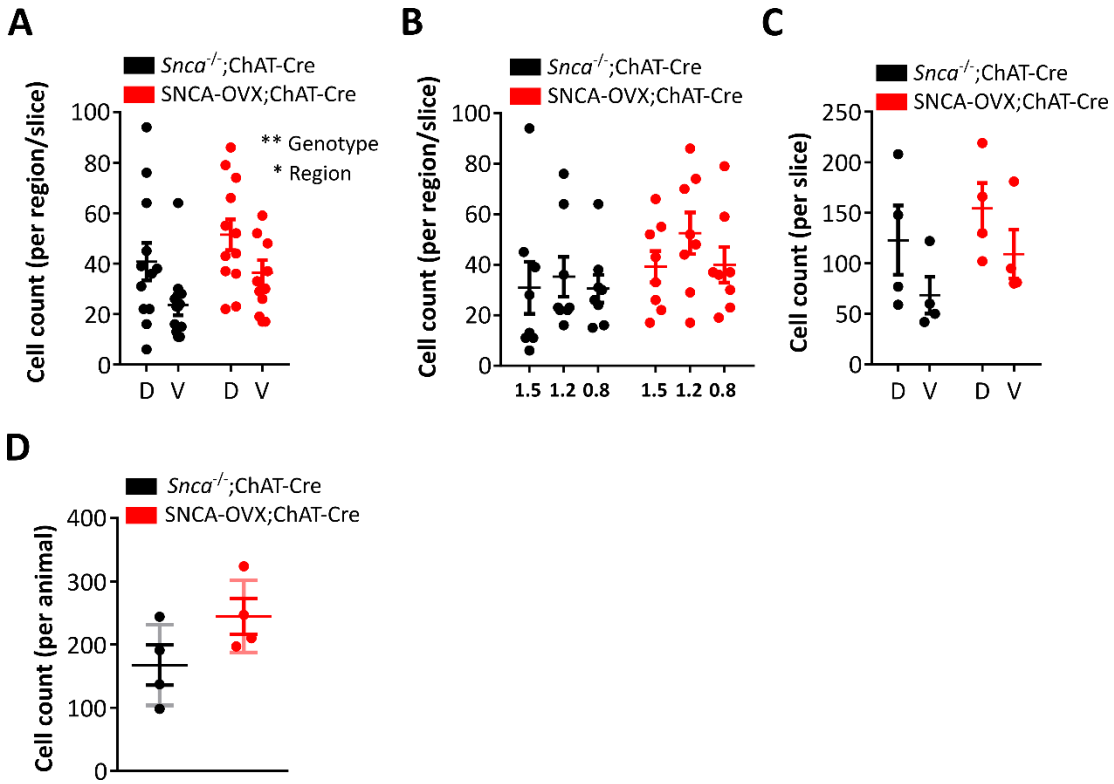

Figure 4.5- Modest increase in striatal ChAT+ve cells in SNCA-OVX;ChAT-Cre mice. ***(A)*** Average cell count from SNCA-OVX;ChAT-Cre and *Snca*$^{-/-}$;ChAT-Cre mice. Each data point is a cell count from a dorsal (D) or ventral (V) striatal subregion, from an individual slice. The solid line indicates the mean, and the solid error bars the SEM, n = 12. ***(B)*** Average cell count for AP coordinates. Each data point is a cell count from a dorsal or ventral striatal subregion, from an individual slice. The solid line indicates the mean, and the solid error bars the SEM, n = 8. ***(C)*** Average cell counts for dorsal (D) and ventral (V) striatum between SNCA-OVX;ChAT-Cre and *Snca*$^{-/-}$;ChAT-Cre mice. Each data point is an average cell count from dorsal or ventral striatal subregions from one animal. n = 4 ***(D)*** Average cell counts per animal from SNCA-OVX;ChAT-Cre and *Snca*$^{-/-}$;ChAT-Cre mice. The solid line indicates the mean, the solid error bars the SEM, and the shaded error bars the SD, n = 4. *$p < 0.05$, **$p < 0.01$, two-way ANOVA.

To assess the activity of the ChIs between the SNCA-OVX;ChAT-Cre and *Snca*$^{-/-}$;ChAT-Cre animals, a marker for phosphorylated S6rp was used. A significant difference was found between the SNCA-OVX;ChAT-Cre and *Snca*$^{-/-}$;ChAT-Cre genotypes, where there are reduced phosphorylated s6RP signals in ChIs in the SNCA-OVX;ChAT-Cre animals (**Figure 4.6A**: unpaired t-test: $t(1834) = 9.921$, $p < 0.0001$). To account for changes in background fluorescence between slices, the values obtained per ChI were normalised to the average background ChAT fluorescence levels within the striatum (**Figure 4.6B**), and to background striatal fluorescence level from the S6rp channel (**Figure 4.6C**). In both circumstances, a significantly smaller S6rp is still seen in the SNCA-OVX;ChAT-Cre over the *Snca*$^{-/-}$;ChAT-Cre animal (**Figure 4.6B**: unpaired t-test: $t(1834) = 9.866$, $p < 0.0001$; **Figure 4.6C**: unpaired t-test: $t(1834) = 7.406$, $p < 0.0001$).

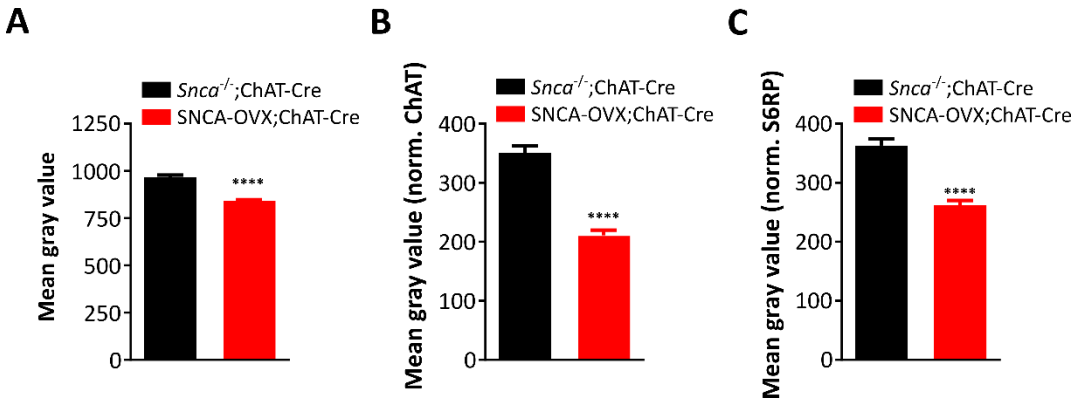

Figure 4.6- Significantly lower S6rp signal in ChAT+ve neurons in SNCA-OVX;ChAT-Cre mice.

(A) Average mean gray value from SNCA-OVX;ChAT-Cre and *Snca*$^{-/-}$;ChAT-Cre mice, error bars represent the SEM. ***(B,C)*** Average mean gray value minus average background ChAT signal ***(B)*** or S6rp signal ***(C)***. **** $p < 0.0001$, unpaired t-test.

Subdividing the fluorescence values into their AP coordinates demonstrated that there is, in addition to a significant effect of genotype, a significant effect across AP coordinates, and an interaction between both genotype and AP coordinate position is also significant (**Figure 4.7A**: two-way ANOVA: genotype effect: $F(1, 1834) = 96.4$, $p < 0.0001$; AP axis effect: $F(2, 1834) = 11.9$, $p < 0.0001$; interaction: $F(2, 1834) = 13.73$, $p < 0.0001$). Furthermore, dividing values into their presence in the dorsal or ventral tiers of the striatum shows a significant effect of striatal subregion with no significant interaction between these variables (**Figure 4.7B**: two-way ANOVA: genotype effect: $F(1, 1634) = 59.64$, $p < 0.0001$; striatal subregion effect: $F(1, 1634) = 92.30$, $p < 0.0001$; interaction: $F(1, 1634) = 0.4451$, $p = 0.5048$).

We also assessed whether S6rp fluorescence levels were differently distributed between *SNCA*-OVX;ChAT-Cre and *Snca*$^{-/-}$;ChAT-Cre animals. To that end, a frequency distribution was plotted to visualise the distribution of the *SNCA*-OVX;ChAT-Cre (**Figure 4.7C**) and *Snca*$^{-/-}$;ChAT-Cre animals (**Figure 4.7D**). Normalising the numbers of ChIs to total amount, and overlaying the distributions for *SNCA*-OVX;ChAT-Cre and *Snca*$^{-/-}$;ChAT-Cre animals shows that the ChIs of *SNCA*-OVX;ChAT-Cre animals are globally less active, and have a more restricted pattern of activity **(Figure 4.7E:** *Snca*$^{-/-}$;ChAT-Cre – interquartile range: 441.42; *SNCA*-OVX;ChAT-Cre: interquartile range: 275.52). Cumulative frequency distributions were plotted for both frequencies and were significantly different between both genotypes (**Figure 4.7F**: $D = 0.2924$, $p < 0.0001$, Kolmogorov-Smirnov test). The change in distribution occurs in both dorsal (**Figure 4.7G**) and ventral striatal (**Figure 4.7H**) tiers.

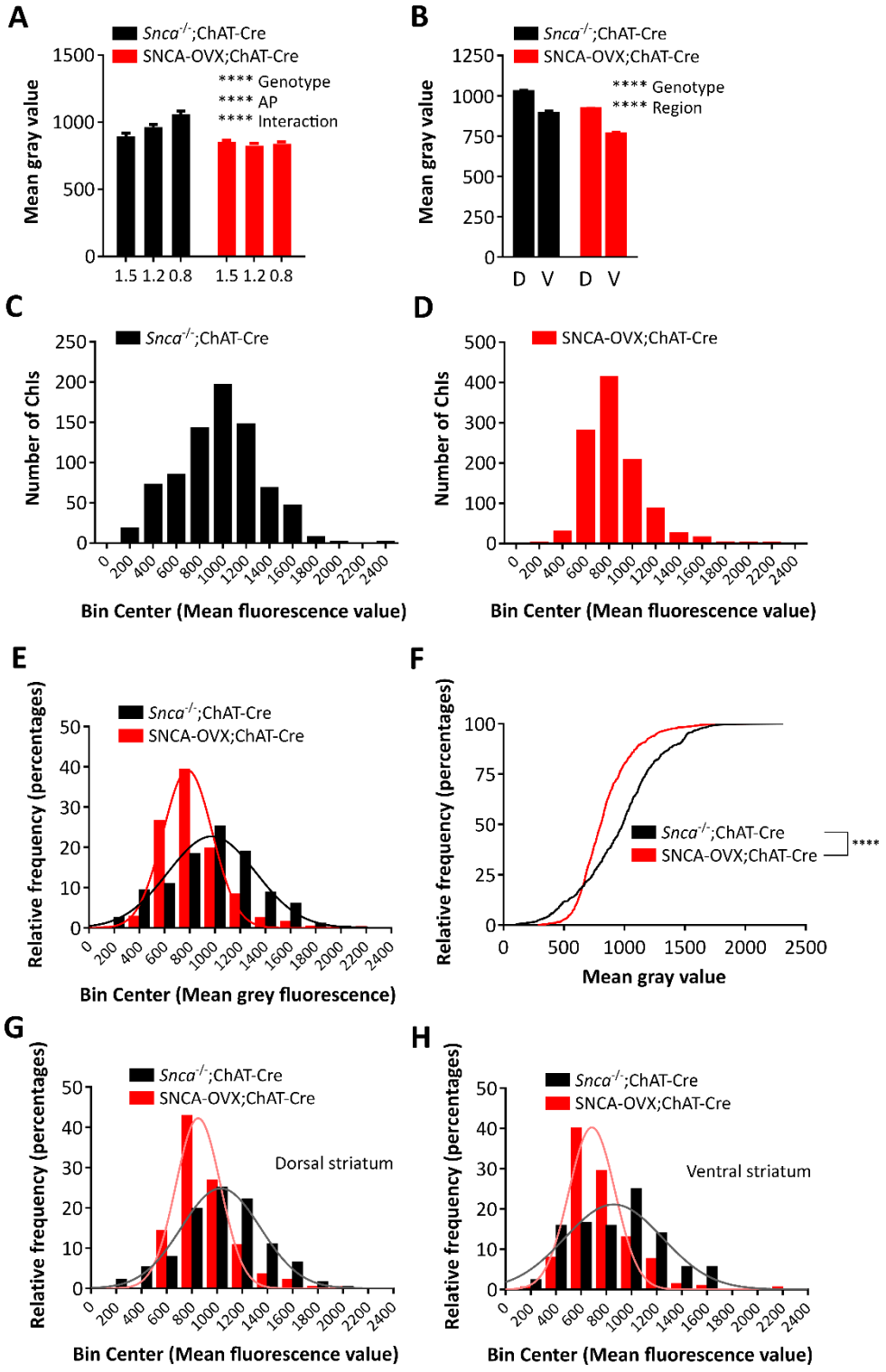

Figure 4.7- S6rp signal is differently distributed in ChAT+ve neurons in SNCA-OVX;ChAT-Cre mice. ***(A)*** Average mean gray value for analysed slice across AP coordinates between SNCA-OVX;ChAT-Cre and *Snca*$^{-/-}$;ChAT-Cre mice. **** $p < 0.0001$, two-way ANOVA. ***(B)*** Average

mean gray value for dorsal (D) and ventral (V) striatum between SNCA-OVX;ChAT-Cre and *Snca*$^{-/-}$;ChAT-Cre mice. **** $p < 0.0001$, two-way ANOVA. ***(C,D)*** Frequency distributions of S6rp signal for dorsal ***(C)*** and ventral ***(D)*** striatum for SNCA-OVX;ChAT-Cre and *Snca*$^{-/-}$;ChAT-Cre mice. ***(E)*** Overlayed frequency distributions of S6rp signal for SNCA-OVX;ChAT-Cre and *Snca*$^{-/-}$;ChAT-Cre mice, expressed as percentage of total values for each genotype. ***(F)*** Cumulative distributions for SNCA-OVX;ChAT-Cre and *Snca*$^{-/-}$;ChAT-Cre mice. **** $p < 0.0001$, Kolmogorov-Smirnov test. ***(G,H)*** Cumulative distributions for SNCA-OVX;ChAT-Cre and *Snca*$^{-/-}$;ChAT-Cre mice in the dorsal ***(G)*** and ventral ***(H)*** striatum.

4.3.3 Electrochemical detection of choline

To attempt to assess choline fluxes in striatal slices, we employed a Pt-based polymer enzyme composite sensor that incorporates the enzyme ChOx, which breaks down choline and releases H_2O_2. H_2O_2 is an electrochemically active species and is oxidised by the Pt wire held at +0.7 V **(Figure 4.8)**. These probes were used on slices from ChAT-Cre;Ai32 animals. This genotype was used to selectively optogenetically activate ChIs and evoke ACh release.

Before initiating experiments, the choline probes were calibrated with 10 µM choline chloride (ChCl) (**Figure 4.9A**), and 2 µM DA (**Figure 4.9B**). As electrically and light-evoking ACh release would also cause the release of DA, and the probes were highly sensitive to both Ch and DA, this is an important consideration to take into account for subsequent experiments. As both electrical and optical stimulation of ChIs evoke DA release through nAChRs (Threlfell et al., 2012), all further choline detection experiments were done in 1 µM DHβE to avoid ChI-induced DA release. An attempt to incorporate a null sensor (as described in Section **4.2.3**) that would cancel out the DA-dependent signal was made, however, the size of both probes made it difficult to insert the electrode into tissue and no data was obtained from this set up.

Following calibration with both DA and choline, the probe was inserted into the tissue. Due to the size of the probes it was not possibly to fully imbed the electrode in a manner similar to FCV carbon fibre microelectrodes, instead the choline sensors only slightly penetrated the striatal slice. This potentially impacted on the ability to detect signals, as the majority of the probes' active surface was not in contact with tissue.

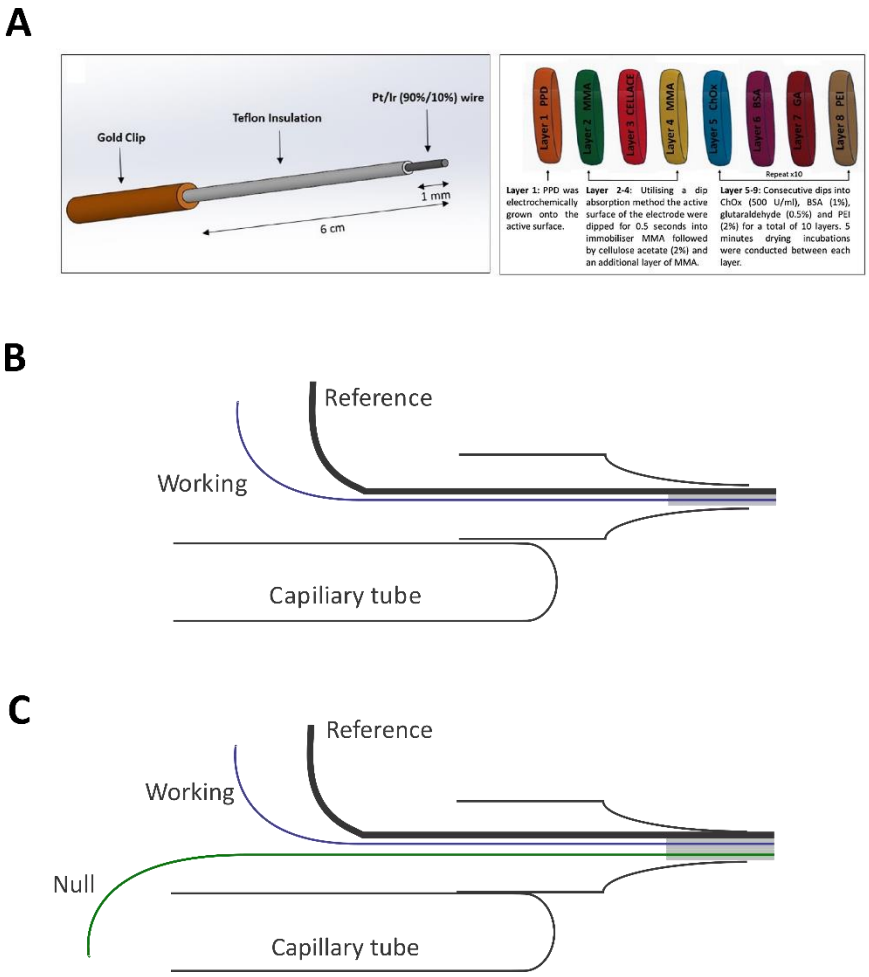

Figure 4.8- A microelectrochemical biosensor for the real-time detection of choline. ***(A)*** Schematic of an electrode (left), with the dip coat layers (right). Adapted from Keeley, et al. (2017). ***(B)*** Electrode configuration for use in our *ex vivo* set up. Working and reference electrodes were threaded through a tapered capillary tube and attached to a second capillary tube for mounting to a manipulator. ***(C)*** Electrode configuration where a null sensor was incorporated (null sensor in green).

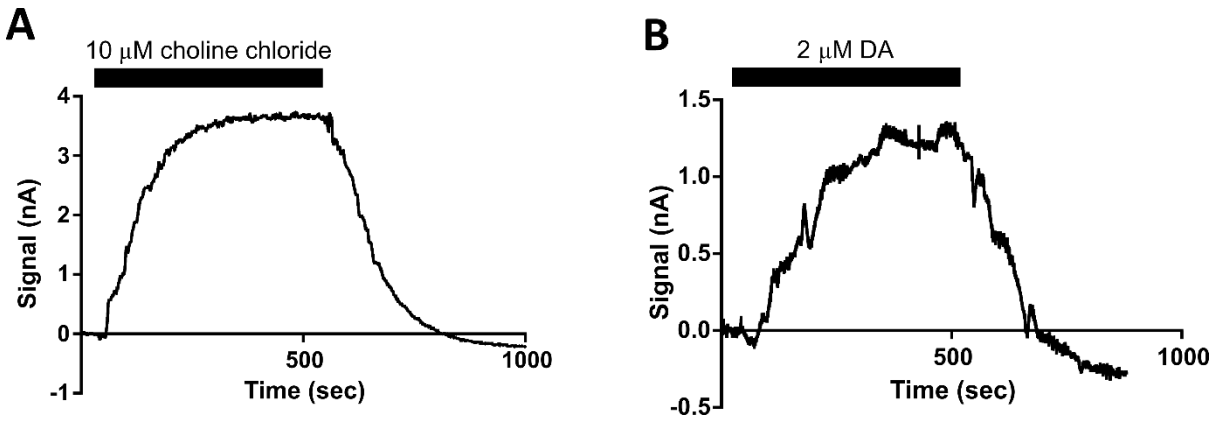

Figure 4.9- Choline biosensor calibration with Ch and DA. Calibration of the choline biosensors with 10 μM choline chloride ***(A)*** or 2 μM DA ***(B)***.

Following insertion of the probe, attempts to stimulate and record choline were made. During most recordings, stimulating the tissue optically or electrically did not always evoke detectable choline. Traces in **Figure 4.10A** and **Figure 4.10B** are representative traces from two experiments, with **Figure 4.10A** demonstrating electrical stimulation, and **Figure 4.10B** demonstrating light stimulation. Detectable release events were infrequent, and this is likely to be due to the size of the probes complicating insertion into the tissue and causing damage to the slice.

Figures 4.10C and **4.10E** show putative choline transients evoked by electrical 10/20 pulse trains at 25Hz, and **Figures 4.10D** and **4.10F** show transients evoked by light stimulations at with the same stimulation parameters, respectively. In most circumstances it was not possible to evoke choline signals. However, we were able to occasionally evoke choline release with 10/20p stimulus trains at 25 Hz. The transients were long-lasting in comparison to FCV DA recordings (approximately 60s), with a rise and fall from peak of similar durations (20-30 seconds).

In both cases, there is an artefact derived from stimulation. In the case of electrical stimulation, it is likely that this is due to an electrical stimulus event coinciding with the recording. The artefact caused by the light stimulus appears to indicate that the electrode is photosensitive. It is not action potential dependent, as the artefact is still present when 1 µM TTX is applied, while the transient is no longer present (**Figure 4.10G**). Subtracting the light artefact after TTX application from the signal in **Figure 4.10F** results in a transient signal demonstrated in **Figure 4.10H**.

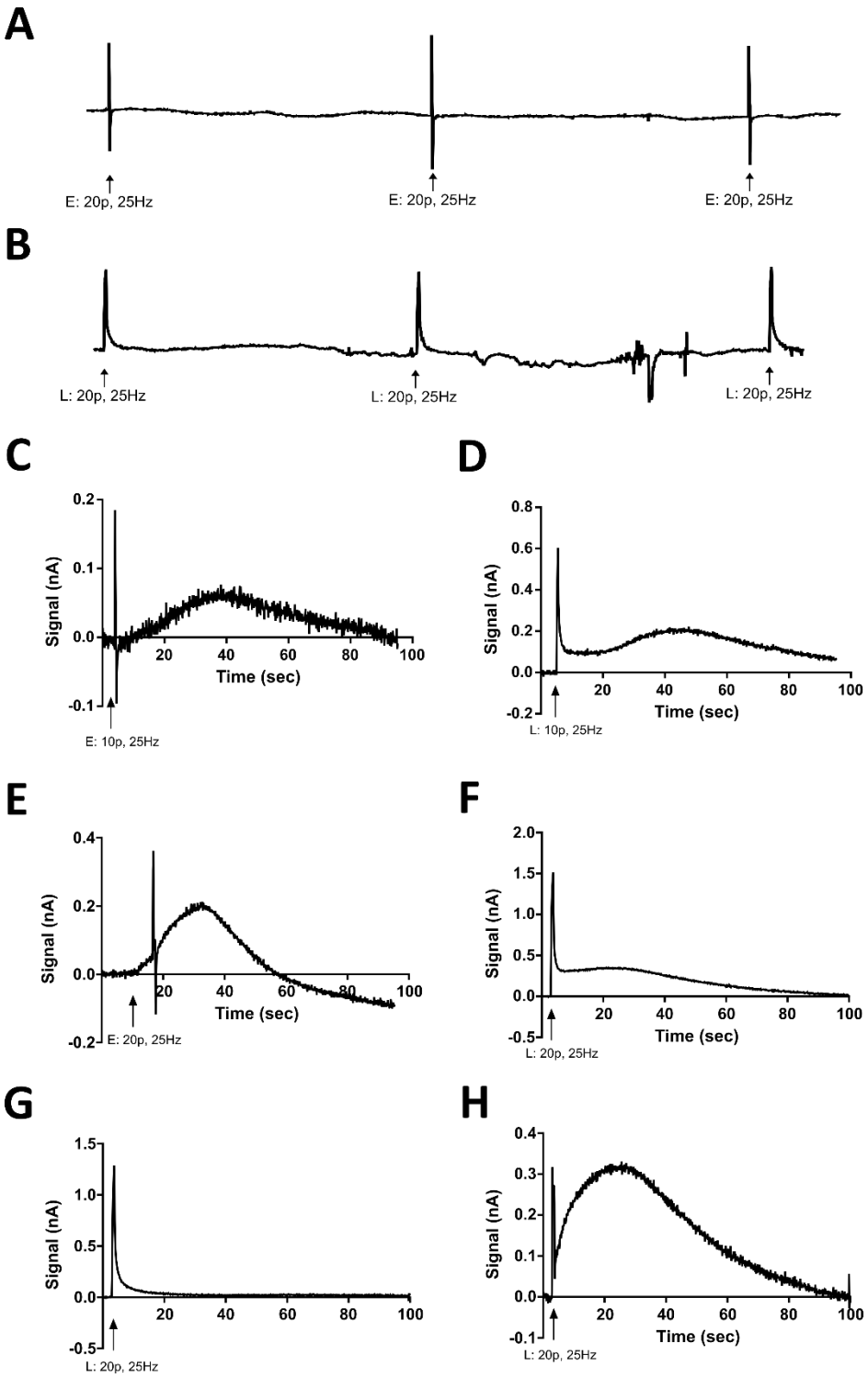

Figure 4.10- Experimental traces and putative Ch transients. ***(A,B)*** Representative experimental Ch transients with light stimulation (20p, 25Hz – ***A***) and electrical stimulation (20p, 25Hz – ***B***). ***(C,D,E,F)*** Putative Ch transients evoked by electrical 10p, 25Hz ***(C)***, light 10p, 25Hz ***(D)***, electrical 20p, 25Hz ***(E)***, and light 20p, 25Hz ***(F)***. ***(G)*** Resulting signal following light

20p 25Hz after application of 1 µM TTX. ***(H)*** Result of subtracting transient (G) from transient (F).

4.4 Discussion

In summary, we show that *SNCA*-OVX;ChAT-Cre animals show normal DA deficits, and could prove a valuable tool in exploring the DA/ACh axis in PD. We also implemented a new immunohistochemical technique for assessing changes in ChI number and activity. *SNCA*-OVX;ChAT-Cre animals show higher ChI numbers, but reduced S6rp signal in comparison to controls. Finally, we attempted to implement a method for the electrochemical detection of choline.

4.4.1 The SNCA-OVX;ChAT-Cre line

We aimed to cross the ChAT-Cre line with the SNCA-OVX mouse model for PD. Selective expression of Cre recombinase in ChIs within a PD model would allow for targeted manipulations within the disease context, within both *ex vivo* and *in vivo* paradigms. However, expression of Cre recombinase has been shown to alter neuronal function (Bäckman et al., 2006; Chen et al., 2018). In particular, ChAT-Cre animals have been shown to have altered behaviour and nicotine-dependent behaviours (Chen et al., 2018). Therefore, it is important to assess whether the DA release phenotype seen in these animals is like that seen in the normal SNCA-OVX animals.

The results presented in this chapter indicate the expression of Cre recombinase does not significantly alter the release deficits seen in SNCA-OVX animals. The dorsal-specific release phenotype is still present with the expression of Cre recombinase in ChIs, and the increased effect of GABA receptor blockers in the SNCA-OVX is present in the dorsal striatum in these mice. There was, however, a significant change in the effect of 1 μM DHβE in the dorsal striatum of the SNCA-OVX;ChAT-Cre animals, potentially suggesting an altered nAChR

control of DA release in these animals. It is worth considering that, while this mouse line does not have any unexpected release phenotypes, the mice used in these experiments were 3-4 months old and expression of Cre recombinase could affect release at older ages.

4.4.2 ChI number and function in Parkinson's disease

We implemented an immunohistochemical technique to identify ChIs and measure their global activity. To accomplish this, a combined staining protocol for ChAT (to identify ChIs) and S6rp (to assess cell activity) was employed.

There appear to be a higher number of ChIs in the striatum of *SNCA*-OVX;ChAT-Cre animals. This suggests that the striatum in the PD context could be hypercholinergic, in a manner consistent with the classical view described in the introduction. The higher ChI count is only significant when subdividing the dataset so that each datapoint is a cell count per a dorsal or ventral region for a single slice. This increases the number of data points in the analysis from 4 counts per genotype (1 cell count value per animal) to 24 counts per genotype (6 cell counts per animal). Furthermore, it is only present when organising the data into dorsal and ventral tiers and assessing for significance with a two-way ANOVA. This significance is lost when reorganising the data points into their positions in the AP axis. Furthermore, when each data point represents a total cell count per animal, or a total dorsal/ventral cell count per animal, this significance is lost. While overall trends for increase can be seen in all cases, the non-significant effect suggests the lack of power could explain the lack of effect.

Our data also indicates there is a significantly lower ChI S6rp fluorescence between *SNCA*-OVX;ChAT-Cre and *Snca*$^{-/-}$;ChAT-Cre animals. This difference in S6rp signal is consistent when normalising the data to background fluorescence levels of S6rp or ChAT, indicating that

ChIs are globally less active within the parkinsonian context. Furthermore, the distribution of fluorescent values were different, in that in addition to the *SNCA*-OVX;ChAT-Cre animals having lower average fluorescence levels, they additionally have a tighter distribution deviating less from the mean.

One confounding factor in the immunohistochemical data obtained is that many striatal neurons were shown to express S6rp. These signals in some cases overlapped with the ROI identified for ChIs, potentially distorting the actual value. One potential way to account for this is by acclimatising the animals to handling prior to transcardial perfusion. Anecdotal evidence suggests that S6rp signals in non-cholinergic neurons can be drastically reduced by a week of habituation to the procedure, or by more rapidly anesthetising the animal prior to the injection of pentobarbitol. Despite this, ChIs continue to be the more heavily stained neurons, this is hypothesised to be due to their tonic firing properties in vivo (Bertran-Gonzalez et al., 2012).

In conclusion, *SNCA*-OVX;ChAT-Cre animals show higher ChI cell numbers, which is consistent with reports of a stronger cholinergic axis in PD. However, *SNCA*-OVX;ChAT-Cre ChIs reduced S6rp fluorescence, indicating they are less active.

4.4.3 Choline detection

The aim of this section was to initially obtain, and then identify and verify choline signals within acute striatal slices. As mentioned previously, these probes are sensitive to choline, so the initial step was to verify their selectivity to the compound of interest. The probe was sensitive to choline, but additionally was found to be sensitive to concentrations of DA seen within the slice. This was not unexpected as the probe was being held at +0.7 V, a

potential capable of oxidising DA. Slice choline recordings were therefore done under nAChR block to prevent evoked DA release mediated by ACh.

Signals were sporadically seen but had the potential of deriving from choline. These signals could be prevented with TTX, suggesting that it is an action-potential mediated signal. Further verification steps would have been useful. A choline signal derived from ACh breakdown should be modified by mAChR receptor ligands, as ChIs express M1 autoreceptors (Hersch et al., 1994). Using an AChE blocker should inhibit the signal by blocking the breakdown of ACh into choline, and blocking the choline transporter could potentially modify the signal.

Release of putative choline transients were seen when providing a long stimulus train of 10-20 pulses at 25 Hz. Longer electrical stimulation trains delivered to the striatum has been shown to release H_2O_2 (Avshalumov and Rice, 2003; Avshalumov et al., 2008), and it is possible that the stimulation protocols directly evoked H_2O_2. However, H_2O_2 release requires AMPA receptor activation on MSNs, and should not be evoked by light-stimulated release which directly acts on ChIs.

A number of issues made data acquisition difficult. The probes were quite large, and it was difficult to imbed within the striatal slice. Consequently, the probes could only be pressed into the slice and were not enveloped by the tissue leaving only a small portion of the probe exposed to striatal tissue. The probe damaged the tissue it was in contact with, which could play a role in the viability of the release sites, leading to few recorded release events. In addition, the probes are highly sensitive to DA. However, light stimulation, which under nAChR block only evokes ACh, caused similar choline fluxes to electrical stimulation.

Nevertheless, the probes' lack of selectivity to choline potentially limits experiments to optically-evoked release under nAChR block.

The putative choline signals were slower than FCV DA transients. This could cause issues when attempting to correlate the DA signals obtained with FCV to the choline signals. Multiple steps are required for the signal to be detected by the probe, and this could alter the kinetics of the transient: AChE breaks down ACh, and choline must cross the polymer layers before it is acted on by ChOx prior to the H_2O_2 signal.

Furthermore, the high sensitivity to DA would be important if combining FCV with Ch detection, as a combined DA/choline signal would be detected by the probe and could confound the recordings. To counteract this issue a null sensor, which did not include ChOx, was incorporated into our set up for later recording attempts. The null sensor, due to its similarity to the working electrode, should detect all signals that are not due to the oxidation of choline. This signal would then be subtracted from the working electrode signal resulting in a recording derived entirely from the oxidation of choline. However, as the probe itself was too large to fully imbed within the striatal slice, it was difficult to imbed a second sensor nearby, and no further progress was made using the null sensor.

Due to the development of genetically encoded markers (discussed in **Chapter 6**), the sensitivity of the probes to DA, and the difficulties in adapting these *in vivo* probes to our *ex vivo* paradigm, the implementation of choline detection was not pursued further.

5. The role of IGF-1 in striatal dopamine release

5.1 Introduction

In this chapter I explore the impact of conditionally knocking out midbrain DA neuron-derived insulin-like growth factor 1 (IGF-1) on striatal DA release. Peripheral hormones such as IGF-1 have been demonstrated to modulate neuronal function and development. However, the impact of IGF-1 on midbrain DA neurons is not fully understood. Midbrain DA neurons appear to synthesise IGF-1, and studies suggest these neurons may be sensitive to IGF-1. We used FCV on acute striatal slices from conditional IGF-1 knock out animals to test whether IGF-1 knockout results in presynaptic changes to DA storage and release.

5.1.1 IGF-1

Insulin-like growth factor 1 (IGF-1) is a 70 amino-acid long hormone secreted by most tissues, albeit predominately from the liver. IGF-1 has a variety of anabolic and growth related roles, dependent on factors such as developmental stage, length of action, and target tissue. In general, IGF-1 has been shown to play an important role in the development and normal functioning of the CNS. Several mutations in the gene encoding IGF-1 (*Igf1*) have been shown to induce microcephaly and mental retardation (Woods et al., 1996). IGF-1 and brain-specific *IGF1* receptor (IGF-1R) knockout mice show reduced brain size (Beck et al., 1995; Kappeler et al., 2008). In adult rodents, IGF-1 plays a role in promoting production of neurons and in regulating neuronal plasticity (Fernandez and Torres-Alemán, 2012).

Release of IGF-1 is controlled by growth hormone (GH) released from somatotroph cells in the pituitary gland. Somatotroph cells are in turn controlled by the stimulatory growth hormone-releasing hormone (GHRH), and somatostatin (SST), both released by hypothalamic cells in response to a number of neuronal, metabolic and hormonal stimuli (Puche and Castilla-Cortázar, 2012).

5.1.2 Neuronally released IGF-1

As mentioned previously, IGF-1 can be synthesised and released by a variety of cell types including neurons. However, the role of neuronally-derived IGF-1 is not fully understood. Olfactory bulb neurons have been shown to secrete IGF-1 by activity-dependent exocytosis from somatic and dendritic sites (Cao et al., 2011). Release of IGF-1 from these neurons has been demonstrated to be crucial in modulating plasticity: preventing IGF-1 release from mitral cells, or conditional deletion of IGF-1R from the olfactory bulb prevented glomerulus-specific long-term potentiation (LTP) of synaptic strength and inhibited memory formation after a social learning test (Liu et al., 2017). Following light deprivation, exposing mice to a period of light leads to an upregulation of IGF-1 in visual cortex vasoactive intestinal peptide (VIP) interneurons. Further electrophysiological studies in acute cortical slices suggest that IGF-1 release from VIP interneurons act postsynaptically and indicate that the experience-dependent enhancement of *Igf1* expression leads to an increase in the number and strength of inhibitory synapses on VIP interneurons. (Mardinly et al., 2016)

5.1.3 Midbrain dopamine neurons and IGF-1

Igf1 transcripts have been found in midbrain DA neurons, with microarray (Chung et al., 2005) and single-cell RT-qPCR (Poulin et al., 2014). The activity of midbrain DA neurons has been shown to be under the control of various neuropeptides such as orexin and dynorphin secreted from afferent neurons (Baimel et al., 2017), and peripheral hormones such as insulin and ghrelin (Labouèbe et al., 2013; Shi et al., 2013). There is potential for midbrain DA neurons to be sensitive to IGF-1: exogenous application of IGF-1 is neuroprotective in cultured DA neurons following MPTP treatment in vitro (Chung et al., 2005) and 6-OHDA treatment in vivo (Ayadi et al., 2016). However, despite the apparent potential for DA neurons to synthesise IGF-1, and the previously described neuromodulatory function of this hormone, there is little information on the role of midbrain DA-derived IGF-1. Given studies from other brain regions indicate a powerful role for IGF-1 in modulating neuronal activity, understanding how it could impact on DA neurons is crucial.

5.1.4 Dopamine neuron-derived IGF-1 controls dopamine neuron firing, skill learning and exploration

The work presented in this chapter forms part of a collaborative study done with Siew-Lan Ang in the Frances Crick Institute (Pristerà et al., 2019). I will now describe the main findings of the work conducted by Dr Ang's group. My own work will be described in the Results section in this chapter. (**Section 5.3**).

Through in situ hybridisation and immunofluorescence on brain section, *Igf1* transcripts and immunoreactivity were found homogenously throughout the midbrain. In midbrain DA neurons, identified through tyrosine hydroxylase (TH) immunoreactivity, IGF-1 immunoreactivity was localised somatically, with no apparent expression on dendrites on the

SNr or on striatal TH-positive axons. IGF-1R was also detectable in approximately 60% of TH-positive neurons in the SNc and VTA. These results suggest midbrain DA neurons are capable of synthesising and are sensitive to IGF-1.

It was then hypothesised that IGF-1 requires neuronal activity to be released, in a manner similar to other neuropeptides. (Merighi et al., 2011; van den Pol, 2012). DA neurons derived from primary cultures of E16 ventral midbrains were assessed for IGF-1 expression following various pharmacological treatments. Blocking D2R with sulpiride increased the firing frequency of the DA neurons. Following a 1h treatment with sulpiride there was a significant reduction of intracellular IGF-1 immunolabeling, indicating IGF-1 is released with increased neuronal activity. Co-treatment of TTX, to block action potentials, and EXO1, to block exocytosis, prevented the sulpiride action. Likewise, increasing K^+ concentration to increase neuronal excitability also reduced intracellular IGF-1 immunolabeling. Together, this data suggests that IGF-1 release is an activity-dependent event that requires exocytosis.

As midbrain DA neurons were confirmed to express IGF-1R, it was then tested whether IGF-1 can modulate the activity of these neurons. Acute brain slices containing the ventral midbrain were loaded with FFN102, a fluorescent neurotransmitter used to measure DA dynamics. Changes in the rate of FFN102 release were then assessed with the application of IGF-1 specific ligands. Exogenous treatment with the IGF-1 agonist des(1-3)IGF-1 slowed release of FFN102, indicating that engagement of the IGF-1R pathway by the IGF-1 agonist slows somatic release of DA. On the other hand, the IGF-1R antagonist AG1024 mediated a small increase in FFN102 release, indicating that blocking IGF-1R signalling can accelerate DA release. These data show that recruitment of the IGF-1 pathway in the ventral midbrain inhibits DA release from DA neuron cell bodies.

Conditional knock out of IGF-1 (*Igf1* cKO) from DA neurons resulted in a reduced engagement of IGF-1R pathway in DA neurons, suggesting IGF-1 acts in an autocrine/paracrine manner in vivo. *Igf1* cKO animals also have reduced phosphorylated TH, indicating a reduced ability to synthesise DA. This correlates with high-performance liquid chromatography (HPLC) data which shows that *Igf1* cKO animals have deficits in striatal DA levels.

Midbrain DA neurons from *Igf1* cKO animals show differences in membrane properties from their controls. *Igf1* cKO DA neurons have increased membrane resistance, and a reduction in the frequency of spontaneous action potentials. These effects can be rescued with IGF-1 treatment, indicating that absence of DA-derived IGF-1 reduces the excitability of these neurons.

The performance of *Igf1* cKO animals in a number of DA-dependent behaviours was then assessed. These animals showed a reduction in spontaneous locomotion, and reduced performance on the accelerating rotarod test. In addition, *Igf1* cKO animals showed reduced novelty-driven locomotor behaviour in an open field test, with no changes in anxiety-like behaviour (light-dark box test), depression-like states (forced swim assay), anhedonia (sucrose preference test) or novel object recognition.

5.1.5 Hypothesis

Given the profound effects of midbrain DA neuron-derived IGF-1 on somatic DA neuron function and a hypodopaminergic phenotype, it remained to be seen whether there is a consequence of knocking out IGF-1 on DA release at the striatal level. In this chapter I

aimed to test the hypothesis that knocking out IGF-1 from DA neurons can modulate striatal DA.

5.2 Methods

Experiments described in this chapter were carried out according to the general methods laid out in Chapter 2. Variations and further details are described below.

5.2.1 Tamoxifen treatment

Slc6a3$^{CreERT2/+}$ and *Igf1*$^{flox/flox}$ mice were crossed to produce Slc6a3$^{CreERT2/+}$; *Igf1*$^{flox/flox}$ mice. Cre-mediated recombination of *Igf1* alleles in DAT expressing neurons was achieved by intraperitoneal injections of tamoxifen at 8 to 12 wk of age. Tamoxifen (Sigma) was reconstituted in 10% ethanol/90% corn oil (Sigma) at a concentration of 10 mg/mL and kept refrigerated and protected from light. All mice were injected with 1 mg of tamoxifen twice a day, for five consecutive days. Slc6a3$^{CreERT2/+}$; *Igf1*$^{flox/flox}$ mice that were tamoxifen-injected are referred to as *Igf1* cKO, while mice harbouring only the floxed allele (*Igf1*$^{flox/flox}$) were used as controls. Mice were analysed 2 to 4 wk after tamoxifen injections.

5.2.2 Stimulation and experimental design

On each recording day, a pair of 3-month old male mice consisting of one control (*Igf1*$^{flox/flox}$) and one *Igf1* cKO, 10-12 days post-tamoxifen, were sacrificed by cervical dislocation, and coronal slices were cut as described in Chapter 2.

In each slice, $[DA]_o$ was monitored in 3 dorsal striatal sites (dorsomedial, dorso-mid, and dorsolateral) and 3 ventral striatal sites (ventromedial caudate-putamen, NAc core, and NAc shell). Stimuli were single pulses and 4 pulses at 100 Hz at 2.5 min intervals. Recordings in each genotype were matched each recording day for days post-tamoxifen and striatal sub-region. The order of preparation and sampling of each genotype was randomised. Electrodes were calibrated in 2 µM DA in experimental media following experiments. Data reported are obtained in 6 animals per genotype. All data were expressed as means ± SEM where n is the recordings. Area-under-curve was calculated for each transient by subdividing transients into trapezoids, calculating the area of each trapezoid and summating the total number. Decay analysis of falling phases of transients were by performed by obtaining concentration matched decay phases of several 1p transients (matched to 1.5 µM $[DA]_o$ ± 0.05 µM). Only timepoints at least 250 ms away from the peak were considered for this analysis to guarantee that the release event is not a confounding factor, and only timepoints purely affected by uptake/diffusion are considered. One phase exponential decay fits were calculated for each genotype, and rate constant (k) values were compared between both conditions. Comparisons for differences in means were assessed by unpaired Student t-tests using GraphPad Prism 6.0 (GraphPad Software, San Diego, CA, USA).

5.2.3 HPLC with electrochemical detection

DA content was assessed following FCV recordings in dorsal and ventral striatum. Following FCV recordings, tissue punches from the dorsal (2 mm diameter) and ventral striatum (1.2 mm diameter) from two brain slices per animal were taken and stored at -80°C in 200 µl 0.1 M $HClO_4$. On the day of analysis, samples were thawed, homogenized and

centrifuged at 16,000 g for 15 min at 4°C. The supernatant was analysed for DA content using HPLC with electrochemical detection. Analytes were separated using a 4.6 x 250 mm Microsorb C18 reverse-phase column (Agilent) and detected using a Decade II SDS electrochemical detector with a Glassy carbon working electrode (Antec Leyden) set at +0.7 V with respect to a Ag/AgCl reference electrode. The mobile phase consisted of 13% methanol (v/v), 0.12 M NaH_2PO_4, 0.5-2.0 mM OSA, 0.8 mM EDTA, pH (3.5-4.6), and the flow rate was fixed at 1 ml/min. Analyte measurements were normalised to tissue punch volume (pmol/mm^3). Data reported were obtained in 6 animals per genotype. All data are expressed as means ± SEM, n is the number of animals. Comparisons for differences in means were assessed by unpaired Student t-tests using GraphPad Prism 6.0 (GraphPad Software, San Diego, CA, USA).

5.3 Results

5.3.1 Striatal dopamine release is not altered in Igf1 cKO animals

Mean peak $[DA]_o$ evoked by either single pulses (**Figure 5.1B** Dorsal striatum control vs *Igf1* cKO: unpaired t-test: t(142) = 0.1872, *p* = 0.8517, n = 72; Ventral striatum control vs *Igf1* cKO: unpaired t-test: t(142) = 0.1703, *p* = 0.8650, n = 72) or trains of pulses (**Figure 5.1D** Dorsal striatum control vs *Igf1* cKO: unpaired t-test: t(70) = 0.2684, *p* = 0.8517, n = 36; Ventral striatum control vs *Igf1* cKO: unpaired t-test: t(70) = 0.1703, *p* = 0.8650, n = 36) were not significantly different between *Igf1* cKO vs control animals in either dorsal or ventral striatum. The ratio of 4p to 1p release was also not changed in both genotypes (**Figure 5.1E** Dorsal striatum control vs *Igf1* cKO: unpaired t-test: t(70) = 0.6565, *p* = 0.5136, n = 36; Ventral

striatum control vs *Igf1* cKO: unpaired t-test: t(70) = 0.5203, p = 0.6045, n = 36). These results suggest that the ability to release DA in the striatum is not compromised in *Igf1* cKO mice.

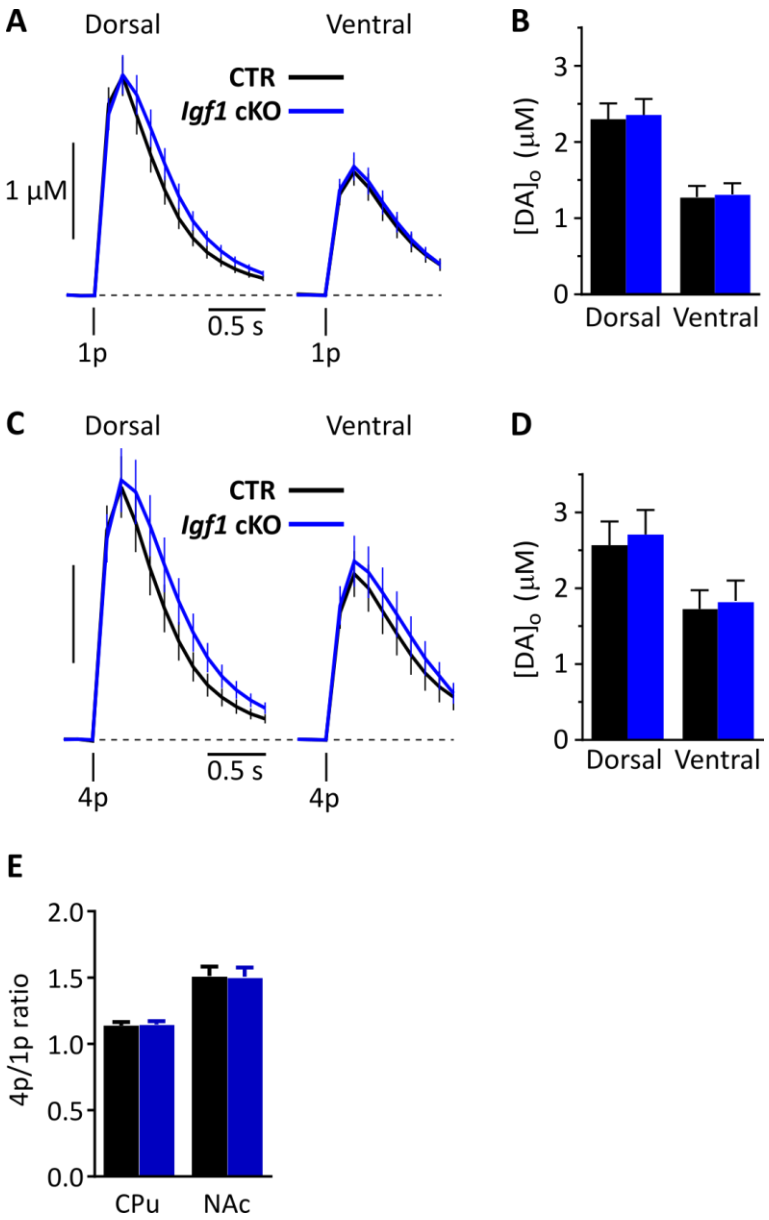

Figure 5.1 - Evoked striatal dopamine release per stimulus is unchanged in *Igf1* cKO mice. ***(A,C)*** Mean release profiles (± SEM) of $[DA]_o$ in control (CTR) and *Igf1* cKO animals following either 1p (n = 72) ***(A)*** or 4p 100 Hz (n = 36) ***(C)*** in dorsal and ventral striatal sites. ***(B,D)*** Mean peak evoked (± SEM) of $[DA]_o$ in CTR and *Igf1* cKO animals following either 1p (n = 72) ***(B)*** or 4p 100 Hz (n = 46) ***(D)***. ***(E)*** 4p/1p ratio (± SEM)between control and *Igf1* cKO animals (n = 46).

5.3.2 Dopamine reuptake is not altered in Igf1 cKO animals

As the *Igf1* cKO animals are in a DAT-Cre background, it is possible that reuptake is altered in this genotype in a manner independent to the knockout. To assess whether DA uptake is altered in these animals, several different analyses were employed. The average area under curve was calculated for 1p and 4p- evoked release transients and was not significantly different between both genotypes, as assessed with unpaired t-tests (**Figure 5.2B 1p -** Dorsal striatum control vs *Igf1* cKO: unpaired t-test: t(142) = 0.7429, p = 0.4587, n = 72; Ventral striatum control vs *Igf1* cKO: unpaired t-test: t(142) = 0.2014, p = 0.8407, n = 72; **4p -** Dorsal striatum control vs *Igf1* cKO: unpaired t-test: t(70) = 0.6565, p = 0.5136, n = 36; Ventral striatum control vs *Igf1* cKO: unpaired t-test: t(70) = 0.5203, p = 0.5319, n = 36). Furthermore, comparing the falling phases of the mean DA release transients from dorsal sites of the two genotypes did not reveal a significant difference (**Figure 5.2C**; One phase decay: control: k = 2.652, *Igf1* cKO: k = 2.748, p = 0.2197). These results suggest that uptake is not significantly different between the two genotypes.

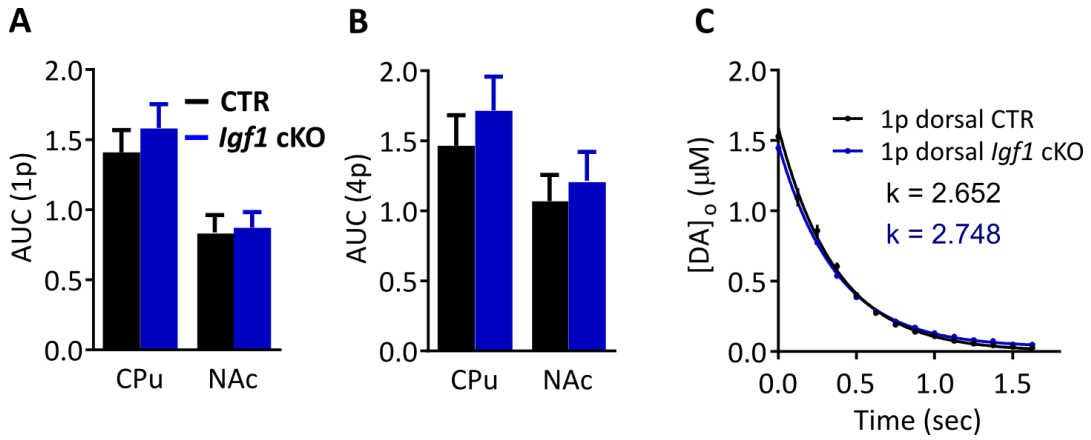

Figure 5.2 – Striatal dopamine uptake is not significantly altered in *Igf1* cKO animals. *(A,B)* Area under curve (AUC) values (± SEM) for 1p-evoked DA transients (n = 72) ***(A)*** or 4p-evoked transients (n = 36) ***(B)***. ***(C)*** Mean decay phases of concentration-matched 1p-evoked DA transients in dorsal striatum).

5.3.3 Striatal dopamine content is not altered in Igf1 cKO animals

As factors relating to release and reuptake are not different between *Igf1* cKO and control animals, we also assessed striatal DA content. Striatal punches obtained from recorded slices were then analysed for DA content with HPLC. Striatal DA content was not significantly different between genotypes (**Figure 5.3** Dorsal striatum control vs *Igf1* cKO: unpaired t-test: $t(5) = 0.7429$, $p = 0.4587$, n = 6; Ventral striatum control vs *Igf1* cKO: unpaired t-test: $t(5) = 0.2014$, $p = 0.8407$, n = 6).

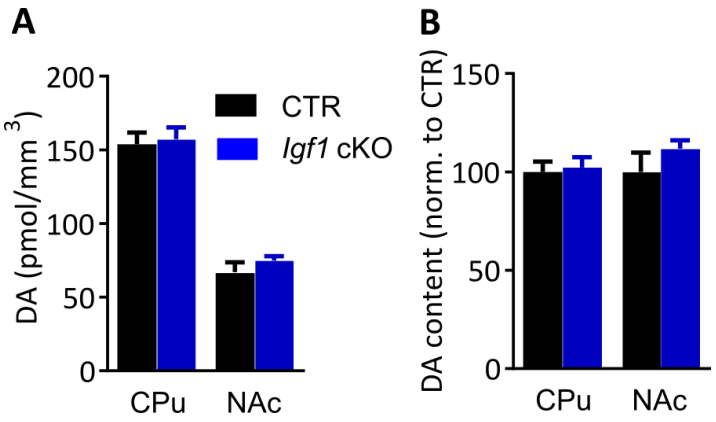

Figure 5.3 – Striatal dopamine content is unchanged in *Igf1* cKO mice. ***(A,B)*** Striatal DA content (± SEM) in control (CTR) and *Igf1* cKO animals. DA is expressed as pmol/mm^3 ***(A)*** or normalised to control ***(B)***, n = 6.

5.4 Discussion

In this chapter I have explored the role of conditionally knocking out IGF-1 in striatal DA release. While IGF-1 has been demonstrated to modulate DA neuron function at the level of the soma, had not been established previously whether knocking out IGF-1 affected striatal DA release. The data presented in this chapter indicates that axonal DA release or striatal DA content is apparently unaffected by the conditional knock-out of IGF-1 in DA neurons.

It is important to note that the genetic strategy used to knock-out IGF-1 from DA neurons is not ideal for drawing conclusions from FCV data. Selective ablation of IGF-1 from DA neurons is accomplished by expressing Cre under the control of the DAT promoter, which would then delete IGF-1 from DA neurons by Cre-dependent recombination of a floxed *Igf1* gene. The control genotype contains solely the floxed *Igf1* gene. Consequently, the difference between control animals and *Igf1* cKO is the absence or presence of Cre recombinase in DA neurons, respectively. Expression of Cre recombinase in DA neurons has been demonstrated to reduce DAT expression (Bäckman et al., 2006), potentially decreasing reuptake rates which could result in slower transient kinetics. This is a confounding factor which could potentially change release levels independent of the *Igf1* cKO. To tackle this, it would be of interest to control for the Slc6a3$^{CreERT2/+}$ transgene by designing the experiment to have the same genotype for control and *Igf1* cKO animals. However, this would require that some animals undergo the tamoxifen treatment, while others are treated only with vehicle. Tamoxifen and its metabolites have been shown to interact at multiple points in the DA metabolic pathway and release machinery, ultimately impacting on DA release levels (Baksi et al., 1985; Chaurasia et al., 1998; Mikelman et al., 2017, 2018).

The transients represented in this chapter (see **Figure 5.1A**) appear to show that *Igf1* cKO transients are slightly wider than their control counterparts. Reduced DAT activity could result in a higher peak for the same $[DA]_o$. In this case, using transient peaks as a measure of released DA would not be very appropriate to assess changes in DA.

To further interrogate whether DA release/uptake is altered in these animals, several different analyses were employed. The concentration-matched declining phases of transients were aligned and compared between each genotype. No significant difference was found between both genotypes. Another method to assess differences between transients from both genotypes would be to compare the area-under-curve (AUC) for the transients. Rather than just comparing the peak DA, the AUC also accounts for differences in other phases of the transient. The average AUC was calculated for 1p- and 4p- evoked release transients and was also not significantly different between both genotypes.

Despite these analyses not exposing a significant difference in the DA transients from both genotypes, it is possible that *Igf1* cKO animals have altered DA release which is corrected for by a change in DAT function/expression.

These results suggest that the clearance, and consequently uptake of DA, is unchanged in *Igf1* cKO in addition to release levels and DA content. The overall lack of change in striatal DA release appears to localise the effects of the hypodopaminergic phenotype identified by Dr Ang's group to the somatodendritic region of midbrain DA neurons. This is particularly supported by IGF-1 immunolabelling data presented in the collaborative publication: in cultured midbrain DA neurons IGF-1 immunolabelling was detected in dendritic processes but not in axons. It is likely that the reduced excitability of midbrain DA neurons is the prominent cause of the behavioural deficits seen *in vivo* (Pristerà et al., 2019).

In this chapter we have demonstrated that knocking out IGF-1 does not appear to alter striatal DA release. Peak levels of 1p and 4p evoked $[DA]_o$ are unchanged, as is the 4p/1p ratio. Further analysis of the acquired FCV data did not reveal a difference in the release/reuptake mechanisms. In addition, there is no change in striatal DA content. Due to allied data present in the publication (Pristerà et al., 2019), this suggests that the deficits seen in *Igf1* cKO animals are due to a reduction in midbrain DA neuron excitability. However, confounds in the design of this experiment make it difficult to assert this claim.

6. General discussion

In addition to cell body activity in the midbrain, striatal DA release is powerfully modulated by local mechanisms which can alter how ascending signals are converted into DA output. As DA is a crucial striatal signal in influencing striatal processing and basal ganglia function, unravelling the role of this regulation is important to understand how the DA signal is modified to regulate behaviour. In addition, exploring the modulation of DA by local factors could also reveal a role for these factors in diseases with DA dysregulation, building a more complete picture of the aetiology behind these disorders and providing novel therapeutic targets.

The main aim of this thesis was to explore how local striatal factors can modulate striatal DA release. In **Chapter 3**, I described how striatal GABA receptors can modulate DA release, and that an endogenous GABA tone in striatal slices supresses DA release. **Chapter 4** details several methods I attempted to implement to study striatal ACh, a powerful modulator of DA release. In **Chapter 5**, I discuss set of experiments where I assess whether conditionally knocking out IGF-1 from midbrain DA neurons impacts on striatal DA release. In this chapter, I will discuss the main findings presented in the experimental chapters and their implications.

6.1 Modulation of striatal DA release by GABA receptors

The striatum is a densely GABAergic region, striatal GABA neurons include MSNs (~95% of total neurons) as well as interneurons (~2-3%) including FSIs and LTSIs, amongst others (Gittis and Kreitzer, 2012). A single nigrostriatal DA axon can cover ~3% of striatal

volume, (Matsuda et al., 2009), potentially encompassing ~70,000 GABAergic neurons (Oorschot, 1996).

In **Chapter 3** I demonstrate that striatal DA release is suppressed by $GABA_A$ and $GABA_B$ receptors, and activation of these receptors slightly alters the frequency filtering of DA release. This is consistent with previous studies which demonstrate a modulation of DA release with GABA receptor ligands (Ronken et al., 1993; Smolders et al., 1995; Schmitz et al., 2002; Avshalumov et al., 2003; Pitman et al., 2014). These effects are suggested to be due to GABA receptors expressed on DA axons, as they are still present when co-applied with an nAChR blocker and glutamate receptor blockers and are present with optogenetically-evoked release. We further demonstrated that, within acute striatal slices, DA release is suppressed by an endogenous GABA tone which has been previously described in other striatal neurons (Santhakumar et al., 2010). I therefore propose that this GABA tone acts on $GABA_A$ and $GABA_B$ receptors located on DA axons. However, these results are not conclusive regarding the presence of GABA receptors on DA axons, and future works will need to fully confirm using electron microscopy or molecular approaches whether $GABA_A$ and $GABA_B$ receptors are expressed on DA axons. Leading on from this question, it could be important to assess what specific subunits $GABA_A$ subunits would be expressed on DA axons. Expression of different $GABA_A$ subunits confer different properties to the receptor. For example, α4, α5, and δ subunit-containing $GABA_A$ receptors have high affinity for GABA and a low degree of desensitisation, and are well adapted for tonic signalling (Ade et al., 2008; Janssen et al., 2009). It would be expected that if $GABA_A$ receptors are expressed on DA axons and are important in tonic signalling, they would express subunits with properties to match this function.

The role of this tonic GABA inhibition of DA release is not understood. Several studies on axonal $GABA_A$ receptors have shown that tonic activation can promote shunting inhibition (Wall, 1995; Westberg et al., 2000; Verdier et al., 2003) and branch-point failure (Zhang and Jackson, 1993, 1995; Jackson and Zhang, 1995; Ruiz et al., 2003; Alle and Geiger, 2007). When activated, $GABA_B$ receptors can open inwardly rectifying K^+ channels (Newberry and Nicoll, 1984; Andrade et al., 1986) or inhibit Ca^{2+} influx via N or P/Q-type Ca^{2+} channels, leading to decreased neurotransmitter release (Harrison, 1990; Scholz and Miller, 1991; Bettler et al., 2004). This tonic GABA tone DA axons may therefore act to inhibit DA axons and reduce action potential propagation through the axonal arbour. Further experiments should determine if tonic activation of these receptors promotes some of the mechanisms described above, leading to a change in AP propagation across the DA arbour and different patterns of DA release. Interestingly, this tonic GABAergic inhibition of DA release is found to be enhanced in the dorsal striatum of SNCA-OVX animals, with a corresponding downregulation of GAT-1 and GAT-3 expression in the dorsal striatum, but not the NAc (Roberts et al., 2019).

The presence of a GABA tone on DA neurons appears to create an additional layer of modulation acting on DA release. Altering $[K^+]_o$ powerfully changes STP of DA release, and this no longer occurs when GABA receptors are antagonising (Condon et al., 2018). This suggests that local factors that mediate a change in K^+ conductance can more differentially alter STP of DA release, dependent on the activation or inactivation of GABA receptors, and therefore provide a further layer of filtering of DA activity. Future experiments should aim to target the specific mechanism underlying the changes in K^+ dependent STP.

6.2 Interrogating striatal cholinergic circuits in PD

Despite being only ~1% of striatal neurons, ChIs powerfully modulate striatal DA release. Early observations from PD showed that antimuscarinic drugs could be used to ameliorate PD symptoms, suggesting PD is a hypodopaminergic and hypercholinergic disorder. Classically, this led to a suggestion that ACh and DA act in opposition, but published data has been inconclusive regarding this.

6.2.1 The SNCA-OVX;ChAT-Cre line

To further study ChI function in the PD state, we implemented a new transgenic cross: *SNCA*-OVX;ChAT-Cre. These animals allow for the selective genetic targeting to ChIs. We showed that *SNCA*-OVX;ChAT-Cre animals show normal DA deficits, and could in fact prove a valuable tool in exploring the DA/ACh axis in PD in the future. The ability to genetically target ChIs within a PD context allows for several questions to be addressed.

Selective expression of ChR on ChIs would allow to optically drive ChIs within a PD context. One question which would be relevant to study is whether ChI-evoked DA release is different between *SNCA*-OVX;ChAT-Cre or *Snca*$^{-/-}$;ChAT-Cre. Changes to striatal nAChRs have been described with loss of DA axons, resulting in differential receptor subtype loss depending on the extent of damage (Quik et al., 2004; Bordia et al., 2007). A predominant loss of the α6α4β2β3 nAChRs occur with moderate lesioning, a decrease in the α6β2β3 subtypes with greater nigrostriatal damage, and a decrease in the α4β2 subtypes only with very severe degeneration. Different subtype compositions confer different ligand-binding and conductance properties. This could impact on how ACh impacts on DA release, and it could

be possible to assess whether ACh-evoked DA release is altered in our parkinsonian model by using an optogenetic approach to evoke ACh-evoked DA release.

ChIs could also be induced to express a calcium sensor to measure intracellular calcium transients. Fluorescent calcium indicators are an important tool used to detect and measure Ca^{2+} and can be used to image and measure changes in Ca^{2+} concentrations associated with neural activity. This could be used to assess how this population functions in freely-moving animals, allowing to assess whether ChI activity is differently altered. Fluorescent calcium indicators are an important tool used to detect and measure calcium and can be used to image and measure changes in Ca^{2+} concentrations associated with neural activity.

This cross could also allow for a chemogenetic approach targeting ChIs. With chemogenetics, designer receptors exclusively activated by designer drugs (DREADDs) are used to activate or inhibit targeted neurons, rather than opsins. The most commonly used stimulatory DREADD is hM3Dq, a modified human M3 muscarinic receptor that has low affinity for the native ACh, but high affinity for the synthetic ligand clozapine-N-oxide (CNO) (Armbruster et al., 2007). When hM3Dq is activated with local or systemic administration of CNO, targeted neurons undergo burst firing (Alexander et al., 2009). For neuronal inhibition, the Gi-coupled a modified human M4 muscarinic receptor hM4Di is often used to silence targeted neurons with CNO (Urban and Roth, 2015). It would be interesting to attempt to manipulate ChIs *in vivo*, and attempt to correct some the motor deficits in PD.

6.2.2 ChI number and function in Parkinson's disease

We also implemented a new immunohistochemical technique for assessing changes in ChI number and activity. *SNCA*-OVX;ChAT-Cre animals show higher ChI numbers, but reduced S6rp signal in comparison to controls.

Our data suggests that ChI numbers are higher in the striatum of *SNCA*-OVX;ChAT-Cre animals. This suggests that the striatum in the PD context could be hypercholinergic. While anticholinergic drugs have been used for symptomatic relief (Katzenschlager et al., 2003), anatomical data has not been conclusive in identifying an increase in cholinergic markers. Higher ChI cell number could lead to higher striatal amounts of ACh, which could impact on striatal DA release. A higher amount of striatal ACh could impact on nAChRs that are susceptible to desensitization following sustained administration of ligands such as nicotine (Pidoplichko et al., 1997; Zhou et al., 2001; Mansvelder and McGehee, 2002; Quick and Lester, 2002; Wooltorton et al., 2003; Giniatullin et al., 2005). Nicotine, when applied to the brain at concentrations seen in smokers, readily desensitizes β2*-nAChRs in the VTA and in the striatum (Pidoplichko et al., 1997; Zhou et al., 2001; Mansvelder and McGehee, 2002). This nAChR desensitization is critical to the outcome on presynaptic nAChR control of DA release in striatum. Inactive nAChRs, as when desensitised by nicotine or blocked by DHβE, result in frequency filtering of DA release (Rice and Cragg, 2004). Whether a higher ChI cell number results in increased levels of ACh, and this distorts the intended DA signal is not yet known.

We also demonstrated that ChIs have reduced s6RP signal, indicating a reduction in global activity. Several studies have shown that in more acute models of PD or DA denervation, ChI function is altered. Loss of DA axons has been shown to downregulate M4 receptors and disrupt a barium-sensitive component of a slow afterhyperpolarization current

(sAHP), lead to elevated striatal ACh release and allowing continuous firing at higher rates during sustained excitation (Ding et al., 2006; Sanchez et al., 2011). A more recent study, however, suggests a loss of ChI function due to a reduction in ACh availability and HCN channel expression (McKinley et al., 2019). The inconsistencies in the published literature may be due to the use of vastly different animal models of PD. Putting our data together, it appears that a compensatory mechanism may be in place where in parkinsonism an increase in ChIs could lead to a reduction in their activity, or vice versa. What impact these changes may have on the processing of information within the striatum is not yet known.

6.2.3 Choline detection

Finally, we attempted to implement a method for the electrochemical detection of choline. Fully understanding the striatal ACh system is crucial, as dysregulation of this system has been linked to many disorders beyond PD, such as addiction and Alzheimer's disease (Francis et al., 1999; Williams and Adinoff, 2008). However, due to the difficulties in directly measuring this neurotransmitter, ACh neurotransmittion is poorly understood. Microdialysis, one of the more commonly used methods to detect ACh has poor spatial and temporal resolution. Patch-clamp recordings have excellent sensitivity and temporal resolution, but the approach is limited by the number of cells that can be recorded simultaneously and the prominent desensitization of cholinergic currents (Dani and Bertrand, 2007). More recently developed FRET sensors and cell-based fluorescent sensors (CNiFERs) for ACh allow for real-time imaging for ACh. However, CNiFERs have been demonstrated to have low sensitivity to ACh (Ziegler et al., 2011; Markovic et al., 2012), or require invasive cell transplantation methods (Nguyen et al., 2010; Muller et al., 2014).

While we were capable of obtaining putative Ch signals with the probes, these were infrequently seen and difficult to verify. Consequently, due to the sensitivity of the probes to DA, and the difficulties in adapting these *in vivo* probes to our *in vitro* paradigm, the implementation of Ch detection was not pursued further. One main reason for abandoning this approach is due to the development of genetically encoded probes for the detection ACh

During my doctoral research, a family of genetically encoded G-protein-coupled receptor activation-based sensors for ACh (GACh) were developed (Jing et al., 2018). GACh sensors were constructed by coupling a circularly permutated green fluorescent protein with an mAChR. These sensors have sub-micromolar sensitivity, specificity comparable to endogenous mAChRs, high signal-to-noise ratio, sub-second kinetics, and photostability suitable real-time assays of ACh signals. The GACh sensors were validated in cultured HEK293T cells and cortical neurons, in tissue slices prepared from multiple brain regions, in the olfactory system of living Drosophila, and in the visual cortex of freely behaving mice *in vivo*. While still preliminary, this technique offers great potential to assess ACh dynamics, but still needs to be verified within acute striatal slices. Furthermore, it is worth noting that this technique requires expression of a genetically modified membrane protein which could have an impact on the normal functioning of striatal cells.

6.3 The role of IGF-1 in striatal DA release

The results obtained in **Chapter 5** suggest that axonal DA release or striatal DA content is apparently unaffected by the conditional knock-out of IGF-1 in DA neurons. Conditional knock-out of IGF-1 results in a hypodopaminergic phenotype, a loss of TH activity and a reduction of somatodendritic function that includes hypoexcitability of midbrain DA neurons.

Our data shows that there was no loss of DA release per pulse in striatum, suggesting that the hypodopaminergic phenotype is not due to a compromise in striatal DA release per pulse, but rather due to changes in DA neuron excitability. The overall lack of change in striatal DA release appears to localise the effects of the hypodopaminergic phenotype to the somatodendritic region of midbrain DA neurons. This is particularly supported by IGF-1 immunolabelling data presented in the publication this data contributed to: in cultured midbrain DA neurons IGF-1 immunolabelling was detected in dendritic processes but not in axons (Pristerà et al., 2019). It is likely that the reduced excitability of midbrain DA neurons is the prominent cause of the behavioural deficits seen *in vivo*.

6.4 Concluding remarks

In conclusion, the data presented in this thesis demonstrates a role for GABA and GABA receptors in modulating striatal DA release. Further data demonstrate the verification of a transgenic mouse line cross that allows for the genetic targeting of ChIs. Immunohistochemical data suggests that there is an increased number of ChIs, and a decrease in their global activity. We also attempted to implement a method for the electrochemical detection of Ch, a proxy of ACh. Finally, data in this thesis demonstrated that, while a conditional knock out of IGF-1 can cause a hypodopaminergic phenotype in mice, this is not due to a DA deficit in the striatum.

References

Abeliovich A, Schmitz Y, Fariñas I, Choi-Lundberg D, Ho W-H, Castillo PE, Shinsky N, Verdugo JMG, Armanini M, Ryan A, Hynes M, Phillips H, Sulzer D, Rosenthal A (2000) Mice Lacking α-Synuclein Display Functional Deficits in the Nigrostriatal Dopamine System. Neuron 25:239–252.

Ade KK, Janssen MJ, Ortinski PI, Vicini S (2008) Differential Tonic GABA Conductances in Striatal Medium Spiny Neurons. J Neurosci 28:1185–1197.

Adrover MF, Shin JH, Alvarez VA (2014) Glutamate and Dopamine Transmission from Midbrain Dopamine Neurons Share Similar Release Properties But Are Differentially Affected by Cocaine. J Neurosci 34:3183–3192.

Agus ZS, Kelepouris E, Dukes I, Morad M (2017) Cytosolic magnesium modulates calcium channel activity in mammalian ventricular cells. Am J Physiol Physiol 256:C452–C455.

Albin RL, Young AB, Penney JB (1989) The functional anatomy of basal ganglia disorders. Trends Neurosci 12:366–375.

Albin RL, Young AB, Penney JB (1995) The functional anatomy of disorders of the basal ganglia. Trends Neurosci 18:63–64.

Alcantara AA, Chen V, Herring BE, Mendenhall JM, Berlanga ML (2003) Localization of dopamine D2 receptors on cholinergic interneurons of the dorsal striatum and nucleus accumbens of the rat. Brain Res 986:22–29.

Alexander GE, Crutcher MD (1990) Functional architecture of basal ganglia circuits: neural substrates of parallel processing. Trends Neurosci 13:266–271.

Alexander GM, Rogan SC, Abbas AI, Armbruster BN, Pei Y, Allen JA, Nonneman RJ, Hartmann J, Moy SS, Nicolelis MA, McNamara JO, Roth BL (2009) Remote control of neuronal activity in transgenic mice expressing evolved G protein-coupled receptors. Neuron 63:27–39.

Alle H, Geiger JRP (2007) GABAergic Spill-Over Transmission onto Hippocampal Mossy Fiber Boutons.

Ammari R, Lopez C, Fiorentino H, Gonon F, Hammond C (2009) A mouse juvenile or adult slice with preserved functional nigro-striatal dopaminergic neurons. Neuroscience 159:3–6.

Andrade R, Malenka RC, Nicoll RA (1986) A G protein couples serotonin and GABAB receptors to the same channels in hippocampus. Science 234:1261–1265.

Anwar S, Peters O, Millership S, Ninkina N, Doig N, Connor-Robson N, Threlfell S, Kooner G, Deacon RM, Bannerman DM, Bolam JP, Chandra SS, Cragg SJ, Wade-Martins R, Buchman VL (2011) Functional alterations to the nigrostriatal system in mice lacking all three members of the synuclein family. J Neurosci 31:7264–7274.

Aosaki T, Tsubokawa H, Ishida A, Watanabe K, Graybiel AM, Kimura M (1994) Responses of

tonically active neurons in the primate's striatum undergo systematic changes during behavioral sensorimotor conditioning. J Neurosci 14:3969–3984.

Apicella P (2002) Tonically active neurons in the primate striatum and their role in the processing of information about motivationally relevant events. Eur J Neurosci 16:2017–2026.

Apicella P (2007) Leading tonically active neurons of the striatum from reward detection to context recognition. Trends Neurosci 30:299–306.

Aransay A, RodrÃ-guez-LÃ³pez C, GarcÃ-a-Amado M, ClascÃ¡ F, Prensa L (2015) Long-range projection neurons of the mouse ventral tegmental area: a single-cell axon tracing analysis. Front Neuroanat 9:59.

Arbuthnott GW, Wickens J (2007) Space, time and dopamine. Trends Neurosci 30:62–69.

Armbruster BN, Li X, Pausch MH, Herlitze S, Roth BL (2007) Evolving the lock to fit the key to create a family of G protein-coupled receptors potently activated by an inert ligand. Proc Natl Acad Sci 104:5163–5168.

Armstrong-James M, Millar J (1979) Carbon fibre microelectrodes. J Neurosci Methods 1:279–287.

Augood SJ, Herbison AE, Emson PC (1995) Localization of GAT-1 GABA transporter mRNA in rat striatum: cellular coexpression with GAD67 mRNA, GAD67 immunoreactivity, and parvalbumin mRNA. J Neurosci 15:865–874.

Averbeck BB, Lehman J, Jacobson M, Haber SN (2014) Estimates of projection overlap and zones of convergence within frontal-striatal circuits. J Neurosci 34:9497–9505.

Avshalumov M V., Chen BT, Marshall SP, Pena DM, Rice ME, Peña DM, Rice ME (2003) Glutamate-dependent inhibition of dopamine release in striatum is mediated by a new diffusible messenger, H2O2. J Neurosci 23:2744–2750.

Avshalumov M V., Rice ME (2003) Activation of ATP-sensitive K+ (KATP) channels by H2O2 underlies glutamate-dependent inhibition of striatal dopamine release. Proc Natl Acad Sci 100:11729–11734.

Avshalumov M V, Patel JC, Rice ME (2008) AMPA receptor-dependent H2O2 generation in striatal medium spiny neurons but not dopamine axons: one source of a retrograde signal that can inhibit dopamine release. J Neurophysiol 100:1590–1601.

Ayadi A El, Zigmond MJ, Smith AD (2016) IGF-1 protects dopamine neurons against oxidative stress: association with changes in phosphokinases. Exp Brain Res 234:1863–1873.

Baba M, Nakajo S, Tu PH, Tomita T, Nakaya K, Lee VM, Trojanowski JQ, Iwatsubo T (1998) Aggregation of alpha-synuclein in Lewy bodies of sporadic Parkinson's disease and dementia with Lewy bodies. Am J Pathol 152:879–884.

Bäckman CM, Malik N, Zhang Y, Shan L, Grinberg A, Hoffer BJ, Westphal H, Tomac AC (2006) Characterization of a mouse strain expressing Cre recombinase from the 3' untranslated region of the dopamine transporter locus. Genesis 44:383–390.

Baimel C, Lau BK, Qiao M, Borgland SL (2017) Projection-Target-Defined Effects of Orexin

and Dynorphin on VTA Dopamine Neurons. Cell Rep 18:1346–1355.

Baker KL, Bolger FB, Lowry JP (2015) A microelectrochemical biosensor for real-time in vivo monitoring of brain extracellular choline. Analyst 140:3738–3745.

Baker KL, Bolger FB, Lowry JP (2017) Development of a microelectrochemical biosensor for the real-time detection of choline. Sensors Actuators, B Chem 243:412–420.

Baksi SN, Hughes MJ, Light KE (1985) Alteration of dopamine metabolism in different brain regions of the rabbit by estradiol and tamoxifen. Neuroscience 14:1053–1059.

Bao L, Avshalumov M V., Patel JC, Lee CR, Miller EW, Chang CJ, Rice ME (2009) Mitochondria Are the Source of Hydrogen Peroxide for Dynamic Brain-Cell Signaling. J Neurosci 29:9002–9010.

Baptista MJ, O'Farrell C, Daya S, Ahmad R, Miller DW, Hardy J, Farrer MJ, Cookson MR (2003) Co-ordinate transcriptional regulation of dopamine synthesis genes by α-synuclein in human neuroblastoma cell lines. J Neurochem 85:957–968.

Barbeau A (1962) The Pathogenesis of Parkinson's Disease: A New Hypothesis. Can Med Assoc J 87:802–807.

Bath BD, Michael DJ, Trafton BJ, Joseph JD, Runnels PL, Wightman RM (2000) Subsecond adsorption and desorption of dopamine at carbon-fiber microelectrodes. Anal Chem 72:5994–6002.

Bean BP (2007) The action potential in mammalian central neurons. Nat Rev Neurosci 8:451–465.

Beatty JA, Sullivan MA, Morikawa H, Wilson CJ (2012) Complex autonomous firing patterns of striatal low-threshold spike interneurons. J Neurophysiol 108:771–781.

Beaulieu J-M, Gainetdinov RR (2011) The Physiology, Signaling, and Pharmacology of Dopamine Receptors Sibley DR, ed. Pharmacol Rev 63:182–217.

Beck KD, Powell-Braxtont L, Widmer HR, Valverde J, Hefti F (1995) Igf1 gene disruption results in reduced brain size, CNS hypomyelination, and loss of hippocampal granule and striatal parvalbumin-containing neurons. Neuron 14:717–730.

Beckstead MJ, Grandy DK, Wickman K, Williams JT (2004) Vesicular Dopamine Release Elicits an Inhibitory Postsynaptic Current in Midbrain Dopamine Neurons. Neuron 42:939–946.

Beckstead RM, Domesick VB, Nauta WJH (1979) Efferent connections of the substantia nigra and ventral tegmental area in the rat. Brain Res 175:191–217.

Bekris LM, Yu C-E, Bird TD, Tsuang DW (2010) Review Article: Genetics of Alzheimer Disease. J Geriatr Psychiatry Neurol 23:213–227.

Bendor J, Lizardi-Ortiz JE, Westphalen RI, Brandstetter M, Hemmings HC, Sulzer D, Flajolet M, Greengard P (2010) AGAP1/AP-3-dependent endocytic recycling of M5 muscarinic receptors promotes dopamine release. EMBO J 29:2813–2826.

Bennett BD, Wilson CJ (1999) Spontaneous activity of neostriatal cholinergic interneurons in

vitro. J Neurosci 19:5586–5596.

Berggård T, Miron S, Önnerfjord P, Thulin E, Akerfeldt KS, Enghild JJ, Akke M, Linse S (2002) Calbindin D28k exhibits properties characteristic of a Ca2+ sensor. J Biol Chem 277:16662–16672.

Bernard V, Bolam JP (1998) Subcellular and subsynaptic distribution of the NR1 subunit of the NMDA receptor in the neostriatum and globus pallidus of the rat: Co-localization at synapses with the GluR2/3 subunit of the AMPA receptor. Eur J Neurosci 10:3721–3736.

Berrios J, Stamatakis AM, Kantak PA, McElligott ZA, Judson MC, Aita M, Rougie M, Stuber GD, Philpot BD (2016) Loss of UBE3A from TH-expressing neurons suppresses GABA co-release and enhances VTA-NAc optical self-stimulation. Nat Commun 7:10702.

Bertran-Gonzalez J, Chieng BC, Laurent V, Valjent E, Balleine BW (2012) Striatal Cholinergic Interneurons Display Activity-Related Phosphorylation of Ribosomal Protein S6. PLoS One 7.

Besson M-J, Graybiel AM, Nastuk MA (1988) [3H]SCH 23390 binding to D1 dopamine receptors in the basal ganglia of the cat and primate: Delineation of striosomal compartments and pallidal and nigral subdivisions. Neuroscience 26:101–119.

Bettler B, Kaupmann K, Mosbacher J, Gassmann M, Structure M (2004) Molecular structure and physiological functions of GABA(B) receptors. Physiol Rev 84:835–867.

Bevan MD, Booth PA, Eaton SA, Bolam JP (1998) Selective innervation of neostriatal interneurons by a subclass of neuron in the globus pallidus of the rat. J Neurosci 18:9438–9452.

Bhisitkul RB, Villa JE, Kocsis JD (1987) Axonal GABA receptors are selectively present on normal and regenerated sensory fibers in rat peripheral nerve. Exp brain Res 66:659–663.

Binda F, Bossi E, Giovannardi S, Forlani G, Peres A (2002) Temperature effects on the presteady-state and transport-associated currents of GABA cotransporter rGAT1. FEBS Lett 512:303–307.

Björklund A, Dunnett SB (2007) Dopamine neuron systems in the brain: an update. Trends Neurosci 30:194–202.

Bolam JP, Hanley JJ, Booth PA, Bevan MD (2000) Synaptic organisation of the basal ganglia. J Anat 196 (Pt 4:527–542.

Bolam JP, Wainer BH, Smith AD (1984) Characterization of cholinergic neurons in the rat neostriatum. A combination of choline acetyltransferase immunocytochemistry, Golgi-impregnation and electron microscopy. Neuroscience 12:711–718.

Borden L (1996) GABA transporter heterogeneity: pharmacology and cellular localization. Neurochem Int 29:335–356.

Bordia T, Grady SR, McIntosh JM, Quik M (2007) Nigrostriatal damage preferentially decreases a subpopulation of alpha6beta2* nAChRs in mouse, monkey, and Parkinson's

disease striatum. Mol Pharmacol 72:52–61.

Bowery NGG, Hudson ALL, Price GWW (1987) GABAA and GABAB receptor site distribution in the rat central nervous system. Neuroscience 20:365–383.

Boyes J, Bolam JP (2003) The subcellular localization of GABA B receptor subunits in the rat substantia nigra. Neuroscience 18:3279–3293.

Branda CS, Dymecki SM (2004) Talking about a revolution: The impact of site-specific recombinases on genetic analyses in mice. Dev Cell 6:7–28.

Brazhnik E, Shah F, Tepper JM (2008) GABAergic afferents activate both GABAA and GABAB receptors in mouse substantia nigra dopaminergic neurons in vivo. J Neurosci 28:10386–10398.

Brickley SG, Mody I (2012) Extrasynaptic GABAA Receptors: Their Function in the CNS and Implications for Disease. Neuron 73:23–34.

Brimblecombe KR, Cragg SJ (2015) Substance P Weights Striatal Dopamine Transmission Differently within the Striosome-Matrix Axis. J Neurosci 35:9017–9023.

Britt JP, McGehee DS (2008) Presynaptic Opioid and Nicotinic Receptor Modulation of Dopamine Overflow in the Nucleus Accumbens. J Neurosci 28:1672–1681.

Brody DL, Yue DT (2000) Release-independent short-term synaptic depression in cultured hippocampal neurons. J Neurosci 20:2480–2494.

Bucher D, Goaillard JM (2011) Beyond faithful conduction: Short-term dynamics, neuromodulation, and long-term regulation of spike propagation in the axon. Prog Neurobiol 94:307–346.

Bugiani O, Perdelli F, Salvarani S, Leonardi A, Mancardi GL (1980) Loss of striatal neurons in Parkinson's disease: a cytometric study. Eur Neurol 19:339–344.

Burmeister JJ, Palmer M, Gerhardt GA (2003) Ceramic-based multisite microelectrode array for rapid choline measures in brain tissue. Anal Chim Acta 481:65–74.

Burnstock G (2004) Cotransmission. Curr Opin Pharmacol 4:47–52.

Cachope R, Mateo Y, Mathur BN, Irving J, Wang H-L, Morales M, Lovinger DM, Cheer JF (2012) Selective Activation of Cholinergic Interneurons Enhances Accumbal Phasic Dopamine Release: Setting the Tone for Reward Processing. Cell Rep 2:33–41.

Calabresi P, Centonze D, Gubellini P, Pisani A, Bernardi G (2000) Acetylcholine-mediated modulation of striatal function. Trends Neurosci 23:120–126.

Calabresi P, Picconi B, Tozzi A, Di Filippo M (2007) Dopamine-mediated regulation of corticostriatal synaptic plasticity. Trends Neurosci 30:211–219.

Calabresi P, Saiardi A, Pisani A, Baik JH, Centonze D, Mercuri NB, Bernardi G, Borrelli E (1997) Abnormal synaptic plasticity in the striatum of mice lacking dopamine D2 receptors. J Neurosci 17:4536–4544.

Cao P, Maximov A, Südhof TC (2011) Activity-dependent IGF-1 exocytosis is controlled by the Ca 2+-sensor synaptotagmin-10. Cell 145:300–311.

Carlezon WA, Devine DP, Wise RA (1995) Habit-forming actions of nomifensine in nucleus accumbens. Psychopharmacology (Berl) 122:194–197.

Carter AG, Soler-Llavina GJ, Sabatini BL (2007) Timing and Location of Synaptic Inputs Determine Modes of Subthreshold Integration in Striatal Medium Spiny Neurons. J Neurosci 27:8967–8977.

Cass WA, Zahniser NR (1991) Potassium Channel Blockers Inhibit D_2 Dopamine, but Not A_1 Adenosine, Receptor-Mediated Inhibition of Striatal Dopamine Release. J Neurochem 57:147–152.

Cepeda C, Galvan L, Holley SM, Rao SP, André VM, Botelho EP, Chen JY, Watson JB, Deisseroth K, Levine MS, Andre VM, Botelho EP, Chen JY, Watson JB, Deisseroth K, Levine MS (2013) Multiple sources of striatal inhibition are differentially affected in Huntington's disease mouse models. J Neurosci 33:7393–7406.

Chai H, Diaz-Castro B, Shigetomi E, Monte E, Octeau JC, Yu X, Cohn W, Rajendran PS, Vondriska TM, Whitelegge JP, Coppola G, Khakh BS (2017) Neural Circuit-Specialized Astrocytes: Transcriptomic, Proteomic, Morphological, and Functional Evidence. Neuron 95:531-549.e9.

Chan CS, Guzman JN, Ilijic E, Mercer JN, Rick C, Tkatch T, Meredith GE, Surmeier DJ (2007) 'Rejuvenation' protects neurons in mouse models of Parkinson's disease. Nature 447:1081–1086.

Chang HT, Kita H (1992) Interneurons in the rat striatum: relationships between parvalbumin neurons and cholinergic neurons. Brain Res 574:307–311.

Charara A, Heilman C, Levey A. I, Smith Y (1999) Pre- and postsynaptic localization of GABA(B) receptors in the basal ganglia in monkeys. Neuroscience 95:127–140.

Charlety PJ, Grenhoff J, Chergui K, De la Chapelle B, Buda M, Svensson TH, Chouvet G (1991) Burst firing of mesencephalic dopamine neurons is inhibited by somatodendritic application of kynurenate. Acta Physiol Scand 142:105–112.

Chartier-Harlin M-C, Kachergus J, Roumier C, Mouroux V, Douay X, Lincoln S, Levecque C, Larvor L, Andrieux J, Hulihan M, Waucquier N, Defebvre L, Amouyel P, Farrer M, Destée A (2004) α-synuclein locus duplication as a cause of familial Parkinson's disease. Lancet 364:1167–1169.

Chaurasia CS, Chen CE, Rubin J, Dewey SL (1998) Effects of tamoxifen on striatal dopamine and 5-hydroxytryptamine release in freely moving male rats: An in-vivo microdialysis investigation. J Pharm Pharmacol 50:1377–1385.

Chen E, Lallai V, Sherafat Y, Grimes NP, Pushkin AN, Fowler JP, Fowler CD (2018) Altered Baseline and Nicotine-Mediated Behavioral and Cholinergic Profiles in ChAT-Cre Mouse Lines. J Neurosci 38:2177–2188.

Chen Q, Veenman L, Knopp K, Yan Z, Medina L, Song WJ, Surmeier DJ, Reiner A (1998) Evidence for the preferential localization of glutamate receptor-1 subunits of AMPA receptors to the dendritic spines of medium spiny neurons in rat striatum. Neuroscience 83:749–761.

Chergui K, Suaud-Chagny MF, Gonon F (1994) Nonlinear relationship between impulse flow, dopamine release and dopamine elimination in the rat brainin vivo. Neuroscience 62:641–645.

Chuhma N, Mingote S, Yetnikoff L, Kalmbach A, Ma T, Ztaou S, Sienna A-C, Tepler S, Poulin J-F, Ansorge M, Awatramani R, Kang UJ, Rayport S (2018) Dopamine neuron glutamate cotransmission evokes a delayed excitation in lateral dorsal striatal cholinergic interneurons. Elife 7.

Chuhma N, Zhang H, Masson J, Zhuang X, Sulzer D, Hen R, Rayport S (2004) Dopamine neurons mediate a fast excitatory signal via their glutamatergic synapses. J Neurosci 24:972–981.

Chung CY, Seo H, Sonntag KC, Brooks A, Lin L, Isacson O (2005) Cell type-specific gene expression of midbrain dopaminergic neurons reveals molecules involved in their vulnerability and protection. Hum Mol Genet 14:1709–1725.

Ciccarelli A, Calza A, Panzanelli P, Concas A, Giustetto M, Sassoè-Pognetto M (2012) Organization of GABAergic Synaptic Circuits in the Rat Ventral Tegmental Area Groc L, ed. PLoS One 7:e46250.

Cisek P, Kalaska JF (2010) Neural mechanisms for interacting with a world full of action choices. Annu Rev Neurosci 33:269–298.

Clark D, Chiodo LA (1988) Electrophysiological and pharmacological characterization of identified nigrostriatal and mesoaccumbens dopamine neurons in the rat. Synapse 2:474–485.

Clayton DF, George JM (1998) The synucleins: a family of proteins involved in synaptic function, plasticity, neurodegeneration and disease. Trends Neurosci 21:249–254.

Cohen JY, Haesler S, Vong L, Lowell BB, Uchida N (2012) Neuron-type-specific signals for reward and punishment in the ventral tegmental area. Nature 482:85–88.

Collins AL, Aitken TJ, Greenfield VY, Ostlund SB, Wassum KM (2016) Nucleus Accumbens Acetylcholine Receptors Modulate Dopamine and Motivation. Neuropsychopharmacology 41:2830–2838.

Condon MD, Platt NJ, Roberts BM, Tseu M-Y, Vietti-Michelina S, Threlfell S, Cragg SJ (2018) Plasticity in striatal dopamine release is governed by release-independent depression and the dopamine transporter. bioRxiv:392753.

Congar P, Bergevin A, Trudeau L-E (2002) D2 Receptors Inhibit the Secretory Process Downstream From Calcium Influx in Dopaminergic Neurons: Implication of K^+ Channels. J Neurophysiol 87:1046–1056.

Consolo S, Caltavuturo C, Colli E, Recchia M, Di Chiara G (1999) Different sensitivity of in vivo acetylcholine transmission to D1 receptor stimulation in shell and core of nucleus accumbens. Neuroscience 89:1209–1217.

Contant C, Umbriaco D, Garcia S, Watkins KC, Descarries L (1996) Ultrastructural characterization of the acetylcholine innervation in adult rat neostriatum. Neuroscience 71:937–947.

Cragg SJ (2003) Variable dopamine release probability and short-term plasticity between functional domains of the primate striatum. J Neurosci 23:4378–4385.

Cragg SJ (2006) Meaningful silences: how dopamine listens to the ACh pause. Trends Neurosci 29:125–131.

Cragg SJ, Rice ME (2004) DAncing past the DAT at a DA synapse. Trends Neurosci 27:270–277.

Crittenden JR, Graybiel AM (2011) Basal Ganglia Disorders Associated with Imbalances in the Striatal Striosome and Matrix Compartments. Front Neuroanat 5:59.

Cui G, Jun SB, Jin X, Pham MD, Vogel SS, Lovinger DM, Costa RM (2014) Concurrent activation of striatal direct and indirect pathways during action initiation. Nature 494:238–242.

Damsma G, Robertson GS, Tham CS, Fibiger HC (1991) Dopaminergic regulation of striatal acetylcholine release: importance of D1 and N-methyl-D-aspartate receptors. J Pharmacol Exp Ther 259.

Dani JA, Bertrand D (2007) Nicotinic acetylcholine receptors and nicotinic cholinergic mechanisms of the central nervous system. Annu Rev Pharmacol Toxicol 47:699–729.

Darbin O, Wichmann T (2008) Effects of Striatal GABA $_A$ -Receptor Blockade on Striatal and Cortical Activity in Monkeys. J Neurophysiol 99:1294–1305.

Day JJ, Roitman MF, Wightman RM, Carelli RM (2007) Associative learning mediates dynamic shifts in dopamine signaling in the nucleus accumbens. Nat Neurosci 10:1020–1028.

Deisseroth K (2015) Optogenetics: 10 years of microbial opsins in neuroscience. Nat Neurosci 18:1213–1225.

DeLong MR (1990) Primate models of movement disorders of basal ganglia origin. Trends Neurosci 13:281–285.

DeLong MR, Wichmann T (2007) Circuits and circuit disorders of the basal ganglia. Arch Neurol 64:20–24.

Descarries L, Bérubé-Carrière N, Riad M, Bo GD, Mendez JA, Trudeau L-É (2008) Glutamate in dopamine neurons: Synaptic versus diffuse transmission. Brain Res Rev 58:290–302.

Descarries L, Gisiger V, Steriade M (1997) Diffuse transmission by acetylcholine in the CNS. Prog Neurobiol 53:603–625.

Descarries L, Mechawar N (2000) Ultrastructural evidence for diffuse transmission by monoamine and acetylcholine neurons of the central nervous system. In, pp 27–47.

Ding J, Guzman JN, Tkatch T, Chen S, Goldberg J a, Ebert PJ, Levitt P, Wilson CJ, Hamm HE, Surmeier DJ (2006) RGS4-dependent attenuation of M4 autoreceptor function in striatal cholinergic interneurons following dopamine depletion. Nat Neurosci 9:832–842.

Dodson PD, Dreyer JK, Jennings KA, Syed ECJ, Wade-Martins R, Cragg SJ, Bolam JP, Magill PJ

(2016) Representation of spontaneous movement by dopaminergic neurons is cell-type selective and disrupted in parkinsonism. Proc Natl Acad Sci 113:201515941.

Doig NM, Moss J, Bolam JP (2010) Cortical and Thalamic Innervation of Direct and Indirect Pathway Medium-Sized Spiny Neurons in Mouse Striatum. J Neurosci 30:14610–14618.

Dorsey ER et al. (2018) Global, regional, and national burden of Parkinson's disease, 1990–2016: a systematic analysis for the Global Burden of Disease Study 2016. Lancet Neurol 17:939–953.

Dreyer JK, Herrik KF, Berg RW, Hounsgaard JD (2010) Influence of Phasic and Tonic Dopamine Release on Receptor Activation. J Neurosci 30:14273–14283.

Dubé L, Smith AD, Bolam JP (1988) Identification of synaptic terminals of thalamic or cortical origin in contact with distinct medium-size spiny neurons in the rat neostriatum. J Comp Neurol 267:455–471.

Dubois B, Pillon B (1997) Cognitive deficits in Parkinson's disease. J Neurol 244:2–8.

Durieux PF, Schiffmann SN, de Kerchove d'Exaerde A (2012) Differential regulation of motor control and response to dopaminergic drugs by D1R and D2R neurons in distinct dorsal striatum subregions. EMBO J 31:640–653.

Durkin MM, Smith KE, Borden LA, Weinshank RL, Branchek TA, Gustafson EL (1995) Localization of messenger RNAs encoding three GABA transporters in rat brain: an in situ hybridization study. Brain Res Mol Brain Res 33:7–21.

Duvoisin RC (1967) Cholinergic-anticholinergic antagonism in parkinsonism. Arch Neurol 17:124–136.

Dvorzhak A, Myakhar O, Unichenko P, Kirmse K, Kirischuk S (2010) Estimation of ambient GABA levels in layer I of the mouse neonatal cortex in brain slices. J Physiol 588:2351–2360.

Ehringer H, Hornykiewicz O (1960) [Distribution of noradrenaline and dopamine (3-hydroxytyramine) in the human brain and their behavior in diseases of the extrapyramidal system]. Klin Wochenschr 38:1236–1239.

Elghaba R, Vautrelle N, Bracci E (2016) Mutual Control of Cholinergic and Low-Threshold Spike Interneurons in the Striatum. Front Cell Neurosci 10:111.

Exley R, Cragg SJ (2008) Presynaptic nicotinic receptors: a dynamic and diverse cholinergic filter of striatal dopamine neurotransmission. Br J Pharmacol 153 Suppl:S283-97.

Exley R, McIntosh JM, Marks MJ, Maskos U, Cragg SJ (2012) Striatal α5 nicotinic receptor subunit regulates dopamine transmission in dorsal striatum. J Neurosci 32:2352–2356.

Farrant M, Nusser Z (2005) Variations on an inhibitory theme: Phasic and tonic activation of GABAAreceptors. Nat Rev Neurosci 6:215–229.

Feng LR, Federoff HJ, Vicini S, Maguire-Zeiss KA (2010) α-Synuclein mediates alterations in membrane conductance: a potential role for α-synuclein oligomers in cell vulnerability. Eur J Neurosci 32:10–17.

Fenno LE et al. (2014) Targeting cells with single vectors using multiple-feature Boolean logic. Nat Methods 11:763–772.

Fernandez AM, Torres-Alemán I (2012) The many faces of insulin-like peptide signalling in the brain. Nat Rev Neurosci 13:225–239.

Ficková M, Dahmen N, Fehr C, Hiemke C (1999) Quantitation of GABA transporter 3 (GAT3) mRNA in rat brain by competitive RT-PCR. Brain Res Brain Res Protoc 4:341–350.

Fisher SD, Robertson PB, Black MJ, Redgrave P, Sagar MA, Abraham WC, Reynolds JNJ (2017) Reinforcement determines the timing dependence of corticostriatal synaptic plasticity in vivo. Nat Commun 8:334.

Floresco SB, West AR, Ash B, Moore H, Grace AA (2003) Afferent modulation of dopamine neuron firing differentially regulates tonic and phasic dopamine transmission. Nat Neurosci 6:968–973.

Flotow H, Thomas G (1992) Substrate recognition determinants of the mitogen-activated 70K S6 kinase from rat liver. J Biol Chem 267:3074–3078.

Foster DJ, Gentry PR, Lizardi-Ortiz JE, Bridges TM, Wood MR, Niswender CM, Sulzer D, Lindsley CW, Xiang Z, Conn PJ (2014) M5 Receptor Activation Produces Opposing Physiological Outcomes in Dopamine Neurons Depending on the Receptor's Location. J Neurosci 34:3253–3262.

Francis PT, Palmer AM, Snape M, Wilcock GK (1999) The cholinergic hypothesis of Alzheimer's disease: a review of progress. J Neurol Neurosurg Psychiatry 66:137–147.

Freeze BS, Kravitz A V, Hammack N, Berke JD, Kreitzer AC (2013) Control of basal ganglia output by direct and indirect pathway projection neurons. J Neurosci 33:18531–18539.

Fuchs J, Nilsson C, Kachergus J, Munz M, Larsson EM, Schüle B, Langston JW, Middleton F a., Ross O a., Hulihan M, Gasser T, Farrer MJ (2007) Phenotypic variation in a large Swedish pedigree due to SNCA duplication and triplication. Neurology 68:916–922.

Gangarossa G, Guzman M, Prado VF, Prado MAM, Daumas S, El Mestikawy S, Valjent E (2016) Role of the atypical vesicular glutamate transporter VGLUT3 in l-DOPA-induced dyskinesia. Neurobiol Dis 87:69–79.

Gangarossa G, Perroy J, Valjent E (2013) Combinatorial topography and cell-type specific regulation of the ERK pathway by dopaminergic agonists in the mouse striatum. Brain Struct Funct 218:405–419.

Garris PA, Christensen JR, Rebec G V, Wightman RM (1997) Real-time measurement of electrically evoked extracellular dopamine in the striatum of freely moving rats. J Neurochem 68:152–161.

Gerfen C, Engber T, Mahan L, Susel Z, Chase T, Monsma F, Sibley D (1990) D1 and D2 dopamine receptor-regulated gene expression of striatonigral and striatopallidal neurons. Science (80-) 250:1429–1432.

Gerfen CR, Baimbridge KG, Thibault J (1987a) The neostriatal mosaic: III. Biochemical and developmental dissociation of patch-matrix mesostriatal systems. J Neurosci 7:3935–

3944.

Gerfen CR, Bolam JP (2010) The Neuroanatomical Organization of the Basal Ganglia. Handb Behav Neurosci 20:3–28.

Gerfen CR, Herkenham M, Thibault J (1987b) The neostriatal mosaic: II. Patch- and matrix-directed mesostriatal dopaminergic and non-dopaminergic systems. J Neurosci 7:3915–3934.

Giniatullin R, Nistri A, Yakel JL (2005) Desensitization of nicotinic ACh receptors: shaping cholinergic signaling. Trends Neurosci 28:371–378.

Gispert S, Del Turco D, Garrett L, Chen A, Bernard DJ, Hamm-Clement J, Korf H-W, Deller T, Braak H, Auburger G, Nussbaum RL (2003) Transgenic mice expressing mutant A53T human alpha-synuclein show neuronal dysfunction in the absence of aggregate formation. Mol Cell Neurosci 24:419–429.

Gittis AH, Kreitzer AC (2012) Striatal microcircuitry and movement disorders. Trends Neurosci 35:557–564.

Gonon F, Burie JB, Jaber M, Benoit-Marand M, Dumartin B, Bloch B (2000) Geometry and kinetics of dopaminergic transmission in the rat striatum and in mice lacking the dopamine transporter. In: Progress in brain research, pp 291–302.

Gonon F, Cespuglio R, Ponchon JL, Buda M, Jouvet M, Adams RN, Pujol JF (1978) [In vivo continuous electrochemical determination of dopamine release in rat neostriatum]. C R Acad Sci Hebd Seances Acad Sci D 286:1203–1206.

Grace AA, Bunney BS (1984a) The control of firing pattern in nigral dopamine neurons: Burst Firing Pattern. J Neurosci 4:2877–2890.

Grace AA, Bunney BS (1984b) The control of firing pattern in nigral dopamine neurons: single spike firing. J Neurosci 4:2866–2876.

Gras C, Amilhon B, Lepicard ÈM, Poirel O, Vinatier J, Herbin M, Dumas S, Tzavara ET, Wade MR, Nomikos GG, Hanoun N, Saurini F, Kemel M-L, Gasnier B, Giros B, Mestikawy S El (2008) The vesicular glutamate transporter VGLUT3 synergizes striatal acetylcholine tone. Nat Neurosci 11:292–300.

Graveland GA, Difiglia M (1985) The frequency and distribution of medium-sized neurons with indented nuclei in the primate and rodent neostriatum. Brain Res 327:307–311.

Graybiel AM, Aosaki T, Flaherty AW, Kimura M (1994) The basal ganglia and adaptive motor control. Science 265:1826–1831.

Graybiel AM, Ragsdale CW (1978) Histochemically distinct compartments in the striatum of human, monkeys, and cat demonstrated by acetylthiocholinesterase staining. Proc Natl Acad Sci 75:5723–5726.

Gunaydin LA, Yizhar O, Berndt A, Sohal VS, Deisseroth K, Hegemann P (2010) Ultrafast optogenetic control. Nat Neurosci 13:387–392.

Guo Q, Wang D, He X, Feng Q, Lin R, Xu F, Fu L, Luo M (2015) Whole-Brain Mapping of Inputs to Projection Neurons and Cholinergic Interneurons in the Dorsal Striatum Arenkiel B,

ed. PLoS One 10:e0123381.

Guzmán JN, Hernández A, Galarraga E, Tapia D, Laville A, Vergara R, Aceves J, Bargas J (2003) Dopaminergic modulation of axon collaterals interconnecting spiny neurons of the rat striatum. J Neurosci 23:8931–8940.

Hafizi S, Kruk ZL, Stamford JA (1990) Fast cyclic voltammetry: improved sensitivity to dopamine with extended oxidation scan limits. J Neurosci Methods 33:41–49.

Harrison NL (1990) On the presynaptic action of baclofen at inhibitory synapses between cultured rat hippocampal neurones. J Physiol 422:433–446.

Hartung H, Threlfell S, Cragg SJ (2011) Nitric oxide donors enhance the frequency dependence of dopamine release in nucleus accumbens. Neuropsychopharmacology 36:1811–1822.

He Y, Zorumski CF, Mennerick S (2002) Contribution of presynaptic Na(+) channel inactivation to paired-pulse synaptic depression in cultured hippocampal neurons. J Neurophysiol 87:925–936.

Heien MLA V, Phillips PEM, Stuber GD, Seipel AT, Wightman RM (2003) Overoxidation of carbon-fiber microelectrodes enhances dopamine adsorption and increases sensitivity. Analyst 128:1413–1419.

Henselmans JM, Stoof JC (1991) Regional differences in the regulation of acetylcholine release upon D2 dopamine and N-methyl-D-aspartate receptor activation in rat nucleus accumbens and neostriatum. Brain Res 566:1–7.

Hermans A, Keithley RB, Kita JM, Sombers LA, Wightman RM (2008) Dopamine detection with fast-scan cyclic voltammetry used with analog background subtraction. Anal Chem 80:4040–4048.

Hernández-López S, Bargas J, Surmeier DJ, Reyes A, Galarraga E (1997) D1 receptor activation enhances evoked discharge in neostriatal medium spiny neurons by modulating an L-type Ca2+ conductance. J Neurosci 17:3334–3342.

Hersch S, Gutekunst C, Rees H, Heilman C, Levey A (1994) Distribution of m1-m4 muscarinic receptor proteins in the rat striatum: light and electron microscopic immunocytochemistry using subtype- specific antibodies. J Neurosci 14:3351–3363.

Hjorth J, Blackwell KT, Hellgren Kotaleski J (2009) Gap Junctions between Striatal Fast-Spiking Interneurons Regulate Spiking Activity and Synchronization as a Function of Cortical Activity. J Neurosci 29:5276–5286.

Hnasko TS, Chuhma N, Zhang H, Goh GY, Sulzer D, Palmiter RD, Rayport S, Edwards RH (2010) Vesicular Glutamate Transport Promotes Dopamine Storage and Glutamate Corelease In Vivo. Neuron 65:643–656.

Holly EN, Davatolhagh MF, Choi K, Alabi OO, Vargas Cifuentes L, Fuccillo M V. (2019) Striatal Low-Threshold Spiking Interneurons Regulate Goal-Directed Learning. Neuron 103:92-101.e6.

Hoover DB, Muth EA, Jacobowitz DM (1978) A mapping of the distribution of acetylcholine,

choline acetyltransferase and acetylcholinesterase in discrete areas of rat brain. Brain Res 153:295–306.

Hornykiewicz O (1998) Biochemical aspects of Parkinson's disease. Neurology 51:S2-9.

Howe MW, Dombeck DA (2016) Rapid signalling in distinct dopaminergic axons during locomotion and reward. Nature 535:505–510.

Hyland BI, Reynolds JNJ, Hay J, Perk CG, Miller R (2002) Firing modes of midbrain dopamine cells in the freely moving rat. Neuroscience 114:475–492.

Iacopino A, Christakos S, German D, Sonsalla PK, Altar CA (1992) Calbindin-D28K-containing neurons in animal models of neurodegeneration: possible protection from excitotoxicity. Mol Brain Res 13:251–261.

Ikemoto S (2007) Dopamine reward circuitry: Two projection systems from the ventral midbrain to the nucleus accumbens–olfactory tubercle complex. Brain Res Rev 56:27–78.

Imperato A, Angelucci L, Casolini P, Zocchi A, Puglisi-Allegra S (1992) Repeated stressful experiences differently affect limbic dopamine release during and following stress. Brain Res 577:194–199.

Izzo PN, Bolam JP (1988) Cholinergic synaptic input to different parts of spiny striatonigral neurons in the rat. J Comp Neurol 269:219–234.

Jackman SL, Beneduce BM, Drew IR, Regehr WG (2014) Achieving high-frequency optical control of synaptic transmission. J Neurosci 34:7704–7714.

Jackson MB, Zhang SJ (1995) Action potential propagation and propagation block by GABA in rat posterior pituitary nerve terminals. J Physiol 483:597–611.

Janezic S et al. (2013) Deficits in dopaminergic transmission precede neuron loss and dysfunction in a new Parkinson model. Proc Natl Acad Sci 110:E4016–E4025.

Janssen MJ, Ade KK, Fu Z, Vicini S (2009) Dopamine modulation of GABA tonic conductance in striatal output neurons. J Neurosci 29:5116–5126.

Jennings KA, Platt NJ, Cragg SJ (2015) The impact of a parkinsonian lesion on dynamic striatal dopamine transmission depends on nicotinic receptor activation. Neurobiol Dis 82:262–268.

Jing M et al. (2018) A genetically encoded fluorescent acetylcholine indicator for in vitro and in vivo studies. Nat Biotechnol 36:726–737.

Joel D, Weiner I (1994) The organization of the basal ganglia-thalamocortical circuits: open interconnected rather than closed segregated. Neuroscience 63:363–379.

Jones EA, Wang JQ, McGinty JF (2001a) Intrastriatal GABAA receptor blockade does not alter dopamine D1/D2 receptor interactions in the intact rat striatum. Neuroscience 102:381–389.

Jones IW, Bolam JP, Wonnacott S (2001b) Presynaptic Localisation of the Nicotinic Acetylcholine Receptor 2 Subunit Immunoreactivity in Rat Nigrostriatal Dopaminergic

Neurones. J Comp Neurol 439:235–247.

Kalivas PW, McFarland K, Bowers S, Szumlinski K, Xi Z-X, Baker D (2003) Glutamate transmission and addiction to cocaine. Ann N Y Acad Sci 1003:169–175.

Kappeler L, De Magalhaes Filho C, Dupont J, Leneuve P, Cervera P, Périn L, Loudes C, Blaise A, Klein R, Epelbaum J, Le Bouc Y, Holzenberger M (2008) Brain IGF-1 receptors control mammalian growth and lifespan through a neuroendocrine mechanism. PLoS Biol 6:2144–2153.

Katzenschlager R, Sampaio C, Costa J, Lees A (2003) Anticholinergics for symptomatic management of Parkinson's disease. Cochrane database Syst Rev:CD003735.

Kawaguchi Y (1993) Physiological, morphological, and histochemical characterization of three classes of interneurons in rat neostriatum. J Neurosci 13:4908–4923.

Kawaguchi Y, Wilson CJ, Emson PC (1990) Projection subtypes of rat neostriatal matrix cells revealed by intracellular injection of biocytin. J Neurosci 10:3421–3438.

Kawano M, Kawasaki A, Sakata-Haga H, Fukui Y, Kawano H, Nogami H, Hisano S (2006) Particular subpopulations of midbrain and hypothalamic dopamine neurons express vesicular glutamate transporter 2 in the rat brain. J Comp Neurol 498:581–592.

Kayed R, Head E, Thompson JL, McIntire TM, Milton SC, Cotman CW, Glabe CG (2003) Common Structure of Soluble Amyloid Oligomers Implies Common Mechanism of Pathogenesis. Science (80-) 300:486–489.

Keithley RB, Takmakov P, Bucher ES, Belle AM, Owesson-White CA, Park J, Wightman RM (2011) Higher sensitivity dopamine measurements with faster-scan cyclic voltammetry. Anal Chem 83:3563–3571.

Kemp JM, Powell TP (1971) The connexions of the striatum and globus pallidus: synthesis and speculation. Philos Trans R Soc Lond B Biol Sci 262:441–457.

Kim J-I, Ganesan S, Luo SX, Wu Y-W, Park E, Huang EJ, Chen L, Ding JB (2015) Aldehyde dehydrogenase 1a1 mediates a GABA synthesis pathway in midbrain dopaminergic neurons. Science 350:102–106.

Kimura R, Ushiyama N, Fujii T, Kawashima K (2003) Nicotine-induced Ca2+ signaling and down-regulation of nicotinic acetylcholine receptor subunit expression in the CEM human leukemic T-cell line. Life Sci 72:2155–2158.

Kirmse K, Dvorzhak A, Kirischuk S, Grantyn R (2008) GABA transporter 1 tunes GABAergic synaptic transmission at output neurons of the mouse neostriatum. J Physiol 586:5665–5678.

Kirmse K, Kirischuk S (2006) Ambient GABA Constrains the Strength of GABAergic Synapses at Cajal-Retzius Cells in the Developing Visual Cortex. J Neurosci 26:4216–4227.

Kirmse K, Kirischuk S, Grantyn R (2009) Role of GABA transporter 3 in GABAergic synaptic transmission at striatal output neurons. Synapse 63:921–929.

Kita H, Kosaka T, Heizmann CW (1990) Parvalbumin-immunoreactive neurons in the rat neostriatum: a light and electron microscopic study. Brain Res 536:1–15.

Knight ZA, Tan K, Birsoy K, Schmidt S, Garrison JL, Wysocki RW, Emiliano A, Ekstrand MI, Friedman JM (2012) Molecular profiling of activated neurons by phosphorylated ribosome capture. Cell 151:1126–1137.

Knowlton BJ, Mangels JA, Squire LR (1996) A neostriatal habit learning system in humans. Science 273:1399–1402.

Koganemaru G, Abe H, Kuramashi A, Ebihara K, Matsuo H, Funahashi H, Yasuda K, Ikeda T, Nishimori T, Ishida Y (2014) Effects of cabergoline and rotigotine on tacrine-induced tremulous jaw movements in rats. Pharmacol Biochem Behav 126:103–108.

Koós T, Tepper JM (1999) Inhibitory control of neostriatal projection neurons by GABAergic interneurons. Nat Neurosci 2:467–472.

Koos T, Tepper JM, Wilson CJ (2004) Comparison of IPSCs Evoked by Spiny and Fast-Spiking Neurons in the Neostriatum. J Neurosci 24:7916–7922.

Kosillo P, Zhang Y-F, Threlfell S, Cragg SJ (2016) Cortical Control of Striatal Dopamine Transmission via Striatal Cholinergic Interneurons. Cereb Cortex:1–10.

Kravitz A V., Freeze BS, Parker PRL, Kay K, Thwin MT, Deisseroth K, Kreitzer AC (2010) Regulation of parkinsonian motor behaviours by optogenetic control of basal ganglia circuitry. Nature 466:622–626.

Kreitzer AC, Malenka RC (2007) Endocannabinoid-mediated rescue of striatal LTD and motor deficits in Parkinson's disease models. Nature 445:643–647.

Kreitzer AC, Malenka RC (2008) Striatal Plasticity and Basal Ganglia Circuit Function. Neuron 60:543–554.

Kubota Y, Kawaguchi Y (2000) Dependence of GABAergic synaptic areas on the interneuron type and target size. J Neurosci 20:375–386.

Kullmann DM, Ruiz A, Rusakov DM, Scott R, Semyanov A, Walker MC (2005) Presynaptic, extrasynaptic and axonal GABA A receptors in the CNS: Where and why? Prog Biophys Mol Biol 87:33–46.

Kume-Kick J, Rice ME (1998) Dependence of dopamine calibration factors on media Ca2+ and Mg2+ at carbon-fiber microelectrodes used with fast-scan cyclic voltammetry. J Neurosci Methods 84:55–62.

Kurz A, Double KL, Lastres-Becker I, Tozzi A, Tantucci M, Bockhart V, Bonin M, García-Arencibia M, Nuber S, Schlaudraff F, Liss B, Fernández-Ruiz J, Gerlach M, Wüllner U, Lüddens H, Calabresi P, Auburger G, Gispert S (2010) A53T-Alpha-Synuclein Overexpression Impairs Dopamine Signaling and Striatal Synaptic Plasticity in Old Mice Pazin MJ, ed. PLoS One 5:e11464.

Labouèbe G, Liu S, Dias C, Zou H, Wong JCY, Karunakaran S, Clee SM, Phillips AG, Boutrel B, Borgland SL (2013) Insulin induces long-term depression of ventral tegmental area dopamine neurons via endocannabinoids. Nat Neurosci 16:300–308.

Lacey MG, Mercuri NB, North RA (1988) On the potassium conductance increase activated by GABAB and dopamine D2 receptors in rat substantia nigra neurones. J Physiol

401:437–453.

Lacey MG, Mercuri NB, North RA (1989) Two cell types in rat substantia nigra zona compacta distinguished by membrane properties and the actions of dopamine and opioids. J Neurosci 9:1233–1241.

Lansman JB (1986) Blockade of current through single calcium channels by Cd2+, Mg2+, and Ca2+. Voltage and concentration dependence of calcium entry into the pore. J Gen Physiol 88:321–347.

Lashuel HA, Petre BM, Wall J, Simon M, Nowak RJ, Walz T, Lansbury PT (2002) Alpha-synuclein, especially the Parkinson's disease-associated mutants, forms pore-like annular and tubular protofibrils. J Mol Biol 322:1089–1102.

Laviv T, Riven I, Dolev I, Vertkin I, Balana B, Slesinger PA, Slutsky I (2010) Basal GABA Regulates GABABR Conformation and Release Probability at Single Hippocampal Synapses. Neuron 67:253–267.

Lavoie B, Parent A (1991) Dopaminergic neurons expressing calbindin in normal and parkinsonian monkeys. Neuroreport 2:601–604.

Lavoie B, Smith Y, Parent A (1989) Dopaminergic innervation of the basal ganglia in the squirrel monkey as revealed by tyrosine hydroxylase immunohistochemistry. J Comp Neurol 289:36–52.

Le Feuvre Y, Fricker D, Leresche N (1997) $GABA_A$ receptor-mediated IPSCs in rat thalamic sensory nuclei: patterns of discharge and tonic modulation by $GABA_B$ autoreceptors. J Physiol 502:91–104.

Le Moine C, Normand E, Bloch B (1991) Phenotypical characterization of the rat striatal neurons expressing the D1 dopamine receptor gene. Proc Natl Acad Sci U S A 88:4205–4209.

Lee S, Kim K, Zhou ZJ (2010) Role of ACh-GABA Cotransmission in Detecting Image Motion and Motion Direction. Neuron 68:1159–1172.

Lim SAO, Kang UJ, McGehee DS (2014) Striatal cholinergic interneuron regulation and circuit effects. Front Synaptic Neurosci 6:1–23.

Liu J-L, Grinberg A, Westphal H, Sauer B, Accili D, Karas M, LeRoith D (1998) Insulin-Like Growth Factor-I Affects Perinatal Lethality and Postnatal Development in a Gene Dosage-Dependent Manner: Manipulation Using the Cre/loxP System in Transgenic Mice. Mol Endocrinol 12:1452–1462.

Liu Z, Chen Z, Shang C, Yan F, Shi Y, Zhang J, Qu B, Han H, Wang Y, Li D, Südhof TC, Cao P (2017) IGF1-Dependent Synaptic Plasticity of Mitral Cells in Olfactory Memory during Social Learning. Neuron 95:106-122.e5.

Lokwan SJ, Overton PG, Berry MS, Clark D (1999) Stimulation of the pedunculopontine tegmental nucleus in the rat produces burst firing in A9 dopaminergic neurons. Neuroscience 92:245–254.

Lopes EF, Roberts BM, Siddorn RE, Clements MA, Cragg SJ (2019) Inhibition of Nigrostriatal

Dopamine Release by Striatal GABAA and GABAB Receptors. J Neurosci 39:1058–1065.

Lozovaya N, Eftekhari S, Cloarec R, Gouty-Colomer LA, Dufour A, Riffault B, Billon-Grand M, Pons-Bennaceur A, Oumar N, Burnashev N, Ben-Ari Y, Hammond C (2018) GABAergic inhibition in dual-transmission cholinergic and GABAergic striatal interneurons is abolished in Parkinson disease. Nat Commun 9.

Luo R, Partridge JG, Vicini S (2013) Distinct roles of synaptic and extrasynaptic GABAAreceptors in striatal inhibition dynamics. Front Neural Circuits 7:186.

Madisen L et al. (2012) A toolbox of Cre-dependent optogenetic transgenic mice for light-induced activation and silencing. Nat Neurosci 15:793–802.

Mansvelder HD, McGehee DS (2002) Cellular and synaptic mechanisms of nicotine addiction. J Neurobiol 53:606–617.

Mapelli L, Rossi P, Nieus T, D'Angelo E (2009) Tonic Activation of GABA $_B$ Receptors Reduces Release Probability at Inhibitory Connections in the Cerebellar Glomerulus. J Neurophysiol 101:3089–3099.

Mardinly AR, Spiegel I, Patrizi A, Centofante E, Bazinet JE, Tzeng CP, Mandel-Brehm C, Harmin DA, Adesnik H, Fagiolini M, Greenberg ME (2016) Sensory experience regulates cortical inhibition by inducing IGF1 in VIP neurons. Nature 531:371–375.

Marinelli M, McCutcheon JE (2014) Heterogeneity of dopamine neuron activity across traits and states. Neuroscience 282:176–197.

Markovic D, Holdich J, Al-Sabah S, Mistry R, Krasel C, Mahaut-Smith MP, Challiss RAJ (2012) FRET-based detection of M1 muscarinic acetylcholine receptor activation by orthosteric and allosteric agonists. PLoS One 7:e29946.

Marques O, Outeiro TF (2012) Alpha-synuclein: from secretion to dysfunction and death. Cell Death Dis 3:e350–e350.

Martel P, Leo D, Fulton S, Bérard M, Trudeau LE (2011) Role of Kv1 potassium channels in regulating dopamine release and presynaptic D2 receptor function. PLoS One 6.

Matamales M, Götz J, Bertran-Gonzalez J (2016) Quantitative Imaging of Cholinergic Interneurons Reveals a Distinctive Spatial Organization and a Functional Gradient across the Mouse Striatum. PLoS One 11:e0157682.

Matsuda W, Furuta T, Nakamura KC, Hioki H, Fujiyama F, Arai R, Kaneko T (2009) Single Nigrostriatal Dopaminergic Neurons Form Widely Spread and Highly Dense Axonal Arborizations in the Neostriatum. J Neurosci 29:444–453.

Maurice N, Mercer J, Chan CS, Hernandez-Lopez S, Held J, Tkatch T, Surmeier DJ (2004) D2 Dopamine Receptor-Mediated Modulation of Voltage-Dependent Na+ Channels Reduces Autonomous Activity in Striatal Cholinergic Interneurons. J Neurosci 24:10289–10301.

Mayorga A (1997) Tremulous Jaw Movements Produced by Acute Tacrine Administration: Possible Relation to Parkinsonian Side Effects. Pharmacol Biochem Behav 56:273–279.

McFarlane C, Warner DS, Dexter F (1995) Interactions between NMDA and AMPA glutamate

receptor antagonists during halothane anesthesia in the rat. Neuropharmacology 34:659–663.

McGeer PL, McGeer EG (1971) Cholinergic Enzyme Systems in Parkinson's Disease. Arch Neurol 25:265–268.

McGregor MM, Nelson AB (2019) Circuit Mechanisms of Parkinson's Disease. Neuron 101:1042–1056.

McKinley JW, Shi Z, Kawikova I, Hur M, Bamford IJ, Sudarsana Devi SP, Vahedipour A, Darvas M, Bamford NS (2019) Dopamine Deficiency Reduces Striatal Cholinergic Interneuron Function in Models of Parkinson's Disease. Neuron.

Melchior JR, Ferris MJ, Stuber GD, Riddle DR, Jones SR (2015) Optogenetic versus electrical stimulation of dopamine terminals in the nucleus accumbens reveals local modulation of presynaptic release. J Neurochem 134:833–844.

Mendez JA, Bourque M-J, Bo GD, Bourdeau ML, Danik M, Williams S, Lacaille J-C, Trudeau L-E (2008) Developmental and Target-Dependent Regulation of Vesicular Glutamate Transporter Expression by Dopamine Neurons. J Neurosci 28:6309–6318.

Merighi A, Salio C, Ferrini F, Lossi L (2011) Neuromodulatory function of neuropeptides in the normal CNS. J Chem Neuroanat 42:276–287.

Mesulam MM, Mufson EJ, Levey AI, Wainer BH (1984) Atlas of cholinergic neurons in the forebrain and upper brainstem of the macaque based on monoclonal choline acetyltransferase immunohistochemistry and acetylcholinesterase histochemistry. Neuroscience 12:669–686.

Michailova A, McCulloch A (2001) Model study of ATP and ADP buffering, transport of Ca 2+ and Mg 2+ , and regulation of ion pumps in ventricular myocyte. Biophys J 81:614–629.

Middleton FA, Strick PL (2000) Basal ganglia and cerebellar loops: motor and cognitive circuits. Brain Res Brain Res Rev 31:236–250.

Mikelman SR, Guptaroy B, Gnegy ME (2017) Tamoxifen and its active metabolites inhibit dopamine transporter function independently of the estrogen receptors. J Neurochem 141:31–36.

Mikelman SR, Guptaroy B, Schmitt KC, Jones KT, Zhen J, Reith MEA, Gnegy ME (2018) Tamoxifen Directly Interacts with the Dopamine Transporter. J Pharmacol Exp Ther 367:119–128.

Millar J, Stamford JA, Kruk ZL, Wightman RM (1985) Electrochemical, pharmacological and electrophysiological evidence of rapid dopamine release and removal in the rat caudate nucleus following electrical stimulation of the median forebrain bundle. Eur J Pharmacol.

Mingote S, Chuhma N, Kalmbach A, Thomsen GM, Wang Y, Mihali A, Sferrazza C, Zucker-Scharff I, Siena A-C, Welch MG, Lizardi-Ortiz J, Sulzer D, Moore H, Gaisler-Salomon I, Rayport S (2017) Dopamine neuron dependent behaviors mediated by glutamate cotransmission. Elife 6.

Mingote S, Chuhma N, Kusnoor S V., Field B, Deutch AY, Rayport S (2015) Functional Connectome Analysis of Dopamine Neuron Glutamatergic Connections in Forebrain Regions. J Neurosci 35:16259–16271.

Mirenowicz J, Schultz W (1994) Importance of unpredictability for reward responses in primate dopamine neurons. J Neurophysiol 72:1024–1027.

Mirenowicz J, Schultz W (1996) Preferential activation of midbrain dopamine neurons by appetitive rather than aversive stimuli. Nature 379:449–451.

Mitchell SJ, Silver RA (2018) GABA Spillover from Single Inhibitory Axons Suppresses Low-Frequency Excitatory Transmission at the Cerebellar Glomerulus. J Neurosci 20:8651–8658.

Miyashita T, Shao YR, Chung J, Pourzia O, Feldman DE (2013) Long-term channelrhodopsin-2 (ChR2) expression can induce abnormal axonal morphology and targeting in cerebral cortex. Front Neural Circuits 7:8.

Morris G, Arkadir D, Nevet a, Vaadia E, Bergman H (2004) Coincident but distinct messages of midbrain dopamine and striatal tonically active neurons. Neuron 43:133–143.

Muller A, Joseph V, Slesinger PA, Kleinfeld D (2014) Cell-based reporters reveal in vivo dynamics of dopamine and norepinephrine release in murine cortex. Nat Methods 11:1245–1252.

Nagel G, Brauner M, Liewald JF, Adeishvili N, Bamberg E, Gottschalk A (2005) Light activation of channelrhodopsin-2 in excitable cells of Caenorhabditis elegans triggers rapid behavioral responses. Curr Biol 15:2279–2284.

Nagel G, Szellas T, Huhn W, Kateriya S, Adeishvili N, Berthold P, Ollig D, Hegemann P, Bamberg E (2003) Channelrhodopsin-2, a directly light-gated cation-selective membrane channel. Proc Natl Acad Sci U S A 100:13940–13945.

Nair-Roberts RG, Chatelain-Badie SD, Benson E, White-Cooper H, Bolam JP, Ungless MA (2008) Stereological estimates of dopaminergic, GABAergic and glutamatergic neurons in the ventral tegmental area, substantia nigra and retrorubral field in the rat. Neuroscience 152:1024–1031.

Nauta HJW (1979) A proposed conceptual reorganization of the basal ganglia and telencephalon. Neuroscience 4:1875–1881.

Nauta WJH, Smith GP, Faull RLM, Domesick VB (1978) Efferent connections and nigral afferents of the nucleus accumbens septi in the rat. Neuroscience 3:385–401.

Nelson AB, Hammack N, Yang CF, Shah NM, Seal RP, Kreitzer AC (2014) Striatal Cholinergic Interneurons Drive GABA Release from Dopamine Terminals. Neuron 82:63–70.

Nelson AB, Kreitzer AC (2014) Reassessing Models of Basal Ganglia Function and Dysfunction. Annu Rev Neurosci 37:117–135.

Newberry NR, Nicoll RA (1984) Direct hyperpolarizing action of baclofen on hippocampal pyramidal cells. Nature 308:450–452.

Ng CH, Wang XS, Ong WY (2000) A light and electron microscopic study of the GABA

transporter GAT-3 in the monkey basal ganglia and brainstem. J Neurocytol 29:595–603.

Ng TK, Yung KK (2000) Distinct cellular distribution of GABA(B)R1 and GABA(A)alpha1 receptor immunoreactivity in the rat substantia nigra. Neuroscience 99:65–76.

Nguyen Q-T, Schroeder LF, Mank M, Muller A, Taylor P, Griesbeck O, Kleinfeld D (2010) An in vivo biosensor for neurotransmitter release and in situ receptor activity. Nat Neurosci 13:127–132.

Nicholson LF, Faull RL, Waldvogel HJ, Dragunow M (1992) The regional, cellular and subcellular localization of GABAA/benzodiazepine receptors in the substantia nigra of the rat. Neuroscience 50:355–370.

Nicola SM (2007) The nucleus accumbens as part of a basal ganglia action selection circuit. Psychopharmacology (Berl) 191:521–550.

Nisenbaum ES, Wilson CJ (1995) Potassium currents responsible for inward and outward rectification in rat neostriatal spiny projection neurons. J Neurosci 15:4449–4463.

Nordberg A, Nyberg P, Windblad B (1985) Topographic distribution of choline acetyltransferase activity and muscarinic and nicotinic receptors in Parkinson brains. Neurochem Pathol 3:223–236.

Nygård O, Nilsson L (1990) Translational dynamics. Interactions between the translational factors, tRNA and ribosomes during eukaryotic protein synthesis. Eur J Biochem 191:1–17.

Obeso JA, Rodríguez-Oroz MC, Benitez-Temino B, Blesa FJ, Guridi J, Marin C, Rodriguez M (2008) Functional organization of the basal ganglia: therapeutic implications for Parkinson's disease. Mov Disord 23 Suppl 3:S548-59.

Oorschot DE (1996) Total number of neurons in the neostriatal, pallidal, subthalamic, and substantia nigral nuclei of the rat basal ganglia: A stereological study using the cavalieri and optical disector methods. J Comp Neurol 366:580–599.

Ott BR, Lannon MC (1992) Exacerbation of parkinsonism by tacrine. Clin Neuropharmacol 15:322–325.

Packard MG (1999) Glutamate infused posttraining into the hippocampus or caudate-putamen differentially strengthens place and response learning. Proc Natl Acad Sci U S A 96:12881–12886.

Packard MG, McGaugh JL (1996) Inactivation of hippocampus or caudate nucleus with lidocaine differentially affects expression of place and response learning. Neurobiol Learn Mem 65:65–72.

Pakhotin P, Bracci E (2007) Cholinergic Interneurons Control the Excitatory Input to the Striatum. J Neurosci 27:391–400.

Paladini CA, Tepper JM (1999) GABA(A) and GABA(B) antagonists differentially affect the firing pattern of substantia nigra dopaminergic neurons in vivo. Synapse 32:165–176.

Pancani T, Bolarinwa C, Smith Y, Lindsley CW, Conn PJ, Xiang Z (2014) M4 mAChR-Mediated

Modulation of Glutamatergic Transmission at Corticostriatal Synapses. ACS Chem Neurosci 5:318–324.

Paquet M, Smith Y (2003) Group I metabotropic glutamate receptors in the monkey striatum: subsynaptic association with glutamatergic and dopaminergic afferents. J Neurosci 23:7659–7669.

Parikh V, Kozak R, Martinez V, Sarter M (2007) Prefrontal acetylcholine release controls cue detection on multiple timescales. Neuron 56:141–154.

Patel JC, Witkovsky P, Coetzee WA, Rice ME (2011) Subsecond regulation of striatal dopamine release by pre-synaptic K ATP channels. J Neurochem 118:721–736.

Patriarchi T, Cho JR, Merten K, Howe MW, Marley A, Xiong W, Folk RW, Broussard GJ, Liang R, Jang MJ, Zhong H, Dombeck D, von Zastrow M, Nimmerjahn A, Gradinaru V, Williams JT, Tian L (2018) Ultrafast neuronal imaging of dopamine dynamics with designed genetically encoded sensors. Science 360:1–15.

Paumier KL, Luk KC, Manfredsson FP, Kanaan NM, Lipton JW, Collier TJ, Steece-Collier K, Kemp CJ, Celano S, Schulz E, Sandoval IM, Fleming S, Dirr E, Polinski NK, Trojanowski JQ, Lee VM, Sortwell CE (2015) Intrastriatal injection of pre-formed mouse α-synuclein fibrils into rats triggers α-synuclein pathology and bilateral nigrostriatal degeneration. Neurobiol Dis 82:185–199.

Phillips PEM, Stuber GD, Heien MLA V., Wightman RM, Carelli RM (2003) Subsecond dopamine release promotes cocaine seeking. Nature 422:614–618.

Picconi B, Centonze D, Håkansson K, Bernardi G, Greengard P, Fisone G, Cenci MA, Calabresi P (2003) Loss of bidirectional striatal synaptic plasticity in L-DOPA–induced dyskinesia. Nat Neurosci 6:501–506.

Pidoplichko VI, DeBiasi M, Williams JT, Dani JA (1997) Nicotine activates and desensitizes midbrain dopamine neurons. Nature 390:401–404.

Pissadaki EK, Bolam JP (2013) The energy cost of action potential propagation in dopamine neurons: clues to susceptibility in Parkinson's disease. Front Comput Neurosci 7:13.

Pitman KA, Puil E, Borgland SL (2014) GABA(B) modulation of dopamine release in the nucleus accumbens core. Eur J Neurosci 40:3472–3480.

Platt NJ, Gispert S, Auburger G, Cragg SJ (2012) Striatal Dopamine Transmission Is Subtly Modified in Human A53Tα-Synuclein Overexpressing Mice Smith W, ed. PLoS One 7:e36397.

Plotkin JL, Day M, Surmeier DJ (2011) Synaptically driven state transitions in distal dendrites of striatal spiny neurons. Nat Neurosci 14:881–888.

Poulin JF, Zou J, Drouin-Ouellet J, Kim KYA, Cicchetti F, Awatramani RB (2014) Defining midbrain dopaminergic neuron diversity by single-cell gene expression profiling. Cell Rep 9:930–943.

Prensa L, Parent A (2001) The nigrostriatal pathway in the rat: A single-axon study of the relationship between dorsal and ventral tier nigral neurons and the striosome/matrix

striatal compartments. J Neurosci 21:7247–7260.

Pristerà A, Blomeley C, Lopes E, Threlfell S, Merlini E, Burdakov D, Cragg S, Guillemot F, Ang S-L (2019) Dopamine neuron-derived IGF-1 controls dopamine neuron firing, skill learning, and exploration. Proc Natl Acad Sci U S A 116:3817–3826.

Puche JE, Castilla-Cortázar I (2012) Human conditions of insulin-like growth factor-I (IGF-I) deficiency. J Transl Med 10:1–29.

Puopolo M, Raviola E, Bean BP (2007) Roles of Subthreshold Calcium Current and Sodium Current in Spontaneous Firing of Mouse Midbrain Dopamine Neurons. J Neurosci 27:645–656.

Quick MW, Lester RAJ (2002) Desensitization of neuronal nicotinic receptors. J Neurobiol 53:457–478.

Quik M, Bordia T, Forno L, McIntosh JM (2004) Loss of alpha-conotoxinMII- and A85380-sensitive nicotinic receptors in Parkinson's disease striatum. J Neurochem 88:668–679.

Quinn JJ, Pittenger C, Lee AS, Pierson JL, Taylor JR (2013) Striatum-dependent habits are insensitive to both increases and decreases in reinforcer value in mice. Eur J Neurosci 37:1012–1021.

Ramanathan S, Hanley JJ, Deniau J-M, Bolam JP (2002) Synaptic convergence of motor and somatosensory cortical afferents onto GABAergic interneurons in the rat striatum. J Neurosci 22:8158–8169.

Redgrave P, Rodriguez M, Smith Y, Rodriguez-Oroz MC, Lehericy S, Bergman H, Agid Y, DeLong MR, Obeso JA (2010) Goal-directed and habitual control in the basal ganglia: implications for Parkinson's disease. Nat Rev Neurosci 11:760–772.

Reisine TD, Fields JZ, Yamamura HI (1977) Neurotransmitter receptor alterations in Parkinson's disease. Life Sci 21:335–343.

Reynolds JNJ, Hyland BI, Wickens JR (2001) A cellular mechanism of reward-related learning. Nature 413:67–70.

Reynolds JNJ, Wickens JR (2002) Dopamine-dependent plasticity of corticostriatal synapses. Neural Netw 15:507–521.

Rice ME, Cragg SJ (2004) Nicotine amplifies reward-related dopamine signals in striatum. Nat Neurosci 7:583–584.

Rice ME, Patel JC, Cragg SJ (2011) Dopamine release in the basal ganglia. Neuroscience.

Rieker C, Engblom D, Kreiner G, Domanskyi A, Schober A, Stotz S, Neumann M, Yuan X, Grummt I, Schutz G, Parlato R (2011) Nucleolar Disruption in Dopaminergic Neurons Leads to Oxidative Damage and Parkinsonism through Repression of Mammalian Target of Rapamycin Signaling. J Neurosci 31:453–460.

Rinne JO, Laihinen A, Lönnberg P, Marjamäki P, Rinne UK (1991) A post-mortem study on striatal dopamine receptors in Parkinson's disease. Brain Res 556:117–122.

Rinne UK, Riekkinen P, Sonninen V, Laaksonen H (1973) Brain acetylcholinesterase in

Parkinson’s disease. Acta Neurol Scand 49:215–226.

Rivera A, Alberti I, Martín AB, Narváez JA, De La Calle A, Moratalla R (2002) Molecular phenotype of rat striatal neurons expressing the dopamine D_5 receptor subtype. Eur J Neurosci 16:2049–2058.

Roberts BM, Doig NM, Brimblecombe KR, Lopes EF, Siddorn RE, Threlfell S, Connor-Robson N, Bengoa-Vergniory N, Pasternack N, Wade-Martins R, Magill PJ, Cragg SJ (2019) Astrocytic striatal GABA transporter activity governs dopamine release and shows maladaptive downregulation in early parkinsonism. bioRxiv:0–29.

Rocca WA (2018) The burden of Parkinson’s disease: a worldwide perspective. Lancet Neurol 17:928–929.

Rocha-González HI, Mao S, Alvarez-Leefmans FJ (2008) Na+,K+,2Cl- cotransport and intracellular chloride regulation in rat primary sensory neurons: thermodynamic and kinetic aspects. J Neurophysiol 100:169–184.

Rodd-Henricks ZA, Bell RL, Kuc KA, Murphy JM, McBride WJ, Lumeng L, Li T-K (2002) Effects of ethanol exposure on subsequent acquisition and extinction of ethanol self-administration and expression of alcohol-seeking behavior in adult alcohol-preferring (P) rats: II. Adult exposure. Alcohol Clin Exp Res 26:1642–1652.

Roitman MF, Stuber GD, Phillips PEM, Wightman RM, Carelli RM (2004) Dopamine Operates as a Subsecond Modulator of Food Seeking. J Neurosci 24:1265–1271.

Romo R, Schultz W (1990) Dopamine neurons of the monkey midbrain: contingencies of responses to active touch during self-initiated arm movements. J Neurophysiol 63:592–606.

Ronken E, Mulder AH, Schoffelmeer AN (1993) Interacting presynaptic kappa-opioid and GABAA receptors modulate dopamine release from rat striatal synaptosomes. J Neurochem 61:1634–1639.

Ruberg M, Ploska A, Javoy-Agid F, Agid Y (1982) Muscarinic binding and choline acetyltransferase activity in Parkinsonian subjects with reference to dementia. Brain Res 232:129–139.

Ruiz A, Fabian-Fine R, Scott R, Walker MC, Rusakov DA, Kullmann DM (2003) GABAA receptors at hippocampal mossy fibers. Neuron 39:961–973.

Runnels PL, Joseph JD, Logman MJ, Wightman RM (1999) Effect of pH and surface functionalities on the cyclic voltammetric responses of carbon-fiber microelectrodes. Anal Chem 71:2782–2789.

Ruvinsky I, Meyuhas O (2006) Ribosomal protein S6 phosphorylation: from protein synthesis to cell size. Trends Biochem Sci 31:342–348.

Ruvinsky I, Sharon N, Lerer T, Cohen H, Stolovich-Rain M, Nir T, Dor Y, Zisman P, Meyuhas O (2005) Ribosomal protein S6 phosphorylation is a determinant of cell size and glucose homeostasis. Genes Dev 19:2199–2211.

Sakaba T, Neher E (2003) Direct modulation of synaptic vesicle priming by GABAB receptor

activation at a glutamatergic synapse. Nature 424:775–778.

Sakamoto S, Goto S, Ito H, Hirano A (1992) Striosomal organization of substance P-like immunoreactivity in parkinsonian patients. Neurology 42:1071–1075.

Sakatani K, Chesler M, Hassan AZ (1991) GABAA receptors modulate axonal conduction in dorsal columns of neonatal rat spinal cord. Brain Res.

Salamone JD, Collins-Praino LE, Pardo M, Podurgiel SJ, Baqi Y, Müller CE, Schwarzschild MA, Correa M (2013) Conditional neural knockout of the adenosine A2A receptor and pharmacological A2A antagonism reduce pilocarpine-induced tremulous jaw movements: Studies with a mouse model of parkinsonian tremor. Eur Neuropsychopharmacol 23:972–977.

Salamone JD, Mayorga AJ, Trevitt JT, Cousins MS, Conlan A, Nawab A (1998) Tremulous jaw movements in rats:a model of parkinsonian tremor. Prog Neurobiol 56:591–611.

Sanchez G, Rodriguez MJ, Pomata P, Rela L, Murer MG (2011) Reduction of an afterhyperpolarization current increases excitability in striatal cholinergic interneurons in rat parkinsonism. J Neurosci 31:6553–6564.

Santhakumar V, Jones RT, Mody I (2010) Developmental regulation and neuroprotective effects of striatal tonic GABAA currents. Neuroscience 167:644–655.

Santini E, Heiman M, Greengard P, Valjent E, Fisone G (2009) Inhibition of mTOR signaling in Parkinson's disease prevents L-DOPA-induced dyskinesia. Sci Signal 2:ra36.

Satake W et al. (2009) Genome-wide association study identifies common variants at four loci as genetic risk factors for Parkinson's disease. Nat Genet 41:1303–1307.

Saunders A, Huang KW, Sabatini BL (2016) Globus Pallidus Externus Neurons Expressing parvalbumin Interconnect the Subthalamic Nucleus and Striatal Interneurons Finkelstein DI, ed. PLoS One 11:e0149798.

Schindelin J, Arganda-Carreras I, Frise E, Kaynig V, Longair M, Pietzsch T, Preibisch S, Rueden C, Saalfeld S, Schmid B, Tinevez J-Y, White DJ, Hartenstein V, Eliceiri K, Tomancak P, Cardona A (2012) Fiji: an open-source platform for biological-image analysis. Nat Methods 9:676–682.

Schlösser B, Kudernatsch MB, Sutor B, Bruggencate G ten (1995) δ, μ, and κ opioid receptor agonists inhibit dopamine overflow in rat neostriatal slices. Neurosci Lett 191:126–130.

Schmitz Y, Schmauss C, Sulzer D (2002) Altered dopamine release and uptake kinetics in mice lacking D2 receptors. J Neurosci 22:8002–8009.

Scholz KP, Miller RJ (1991) GABAB receptor-mediated inhibition of Ca2+ currents and synaptic transmission in cultured rat hippocampal neurones. J Physiol 444:669–686.

Schultz W (2006) Behavioral theories and the neurophysiology of reward. Annu Rev Psychol 57:87–115.

Schultz W (2007) Multiple Dopamine Functions at Different Time Courses. Annu Rev Neurosci 30:259–288.

Schultz W, Dayan P, Montague PR (1997) A Neural Substrate of Prediction and Reward. Science (80-) 275:1593–1599.

Schultz W, Romo R (1990) Dopamine neurons of the monkey midbrain: contingencies of responses to stimuli eliciting immediate behavioral reactions. J Neurophysiol 63:607–624.

Seal R, Edwards R (2006) Functional implications of neurotransmitter co-release: glutamate and GABA share the load. Curr Opin Pharmacol 6:114–119.

Sellings LHL, Clarke PBS (2003) Segregation of amphetamine reward and locomotor stimulation between nucleus accumbens medial shell and core. J Neurosci 23:6295–6303.

Senior SL, Ninkina N, Deacon R, Bannerman D, Buchman VL, Cragg SJ, Wade-Martins R (2008) Increased striatal dopamine release and hyperdopaminergic-like behaviour in mice lacking both alpha-synuclein and gamma-synuclein. Eur J Neurosci 27:947–957.

Sgobio C, Wu J, Zheng W, Chen X, Pan J, Salinas AG, Davis MI, Lovinger DM, Cai H (2017) Aldehyde dehydrogenase 1–positive nigrostriatal dopaminergic fibers exhibit distinct projection pattern and dopamine release dynamics at mouse dorsal striatum. Sci Rep 7:5283.

Sharott A, Doig NM, Mallet N, Magill PJ (2012) Relationships between the Firing of Identified Striatal Interneurons and Spontaneous and Driven Cortical Activities In Vivo. J Neurosci 32:13221–13236.

Shi L, Bian X, Qu Z, Ma Z, Zhou Y, Wang KW, Jiang H, Xie J (2013) Peptide hormone ghrelin enhances neuronal excitability by inhibition of Kv7/KCNQ channels. Nat Commun 4:1412–1435.

Shin JH, Adrover MF, Wess J, Alvarez VA (2015) Muscarinic regulation of dopamine and glutamate transmission in the nucleus accumbens. Proc Natl Acad Sci U S A 112:8124–8129.

Simón-Sánchez J et al. (2009) Genome-wide association study reveals genetic risk underlying Parkinson's disease. Nat Genet 41:1308–1312.

Singleton AB et al. (2003) alpha-Synuclein locus triplication causes Parkinson's disease. Science 302:841.

Smith AD, Bolam JP (1990) The neural network of the basal ganglia as revealed by the study of synaptic connections of identical neurones. Trends Neurosci 13:259–265.

Smith ID, Grace AA (1992) Role of the subthalamic nucleus in the regulation of nigral dopamine neuron activity. Synapse 12:287–303.

Smith Y, Bennett BD, Bolam JP, Parent A, Sadikot AF (1994) Synaptic relationships between dopaminergic afferents and cortical or thalamic input in the sensorimotor territory of the striatum in monkey. J Comp Neurol 344:1–19.

Smolders I, De Klippel N, Sarre S, Ebinger G, Michotte Y (1995) Tonic GABA-ergic modulation of striatal dopamine release studied by in vivo microdialysis in the freely moving rat.

Eur J Pharmacol 284:83–91.

Sodickson DL, Bean BP (1996) GABAB receptor-activated inwardly rectifying potassium current in dissociated hippocampal CA3 neurons. J Neurosci 16:6374–6385.

Somogyi P, Bolam JP, Smith AD (1981) Monosynaptic cortical input and local axon collaterals of identified striatonigral neurons. A light and electron microscopic study using the golgi-peroxidase transport-degeneration procedure. J Comp Neurol 195:567–584.

Specht CG, Schoepfer R (2001) Deletion of the alpha-synuclein locus in a subpopulation of C57BL/6J inbred mice. BMC Neurosci 2:11.

Spillantini MG, Crowther RA, Jakes R, Hasegawa M, Goedert M (1998) -Synuclein in filamentous inclusions of Lewy bodies from Parkinson's disease and dementia with Lewy bodies. Proc Natl Acad Sci 95:6469–6473.

Spillantini MG, Schmidt ML, Lee VM, Trojanowski JQ, Jakes R, Goedert M (1997) Alpha-synuclein in Lewy bodies. Nature 388:839–840.

Stensrud MJ, Chaudhry FA, Leergaard TB, Bjaalie JG, Gundersen V (2013) Vesicular glutamate transporter-3 in the rodent brain: Vesicular colocalization with vesicular γ-aminobutyric acid transporter. J Comp Neurol 521:3042–3056.

Stoof JC, Russchen FT, Verheijden PFHM, Hoogland PVJM (1987) A comparative study of the dopamine-acetylcholine interaction in telencephalic structures of the rat and of a reptile, the lizardGekko gecko. Brain Res 404:273–281.

Stouffer MA, Woods CA, Patel JC, Lee CR, Witkovsky P, Bao L, Machold RP, Jones KT, De Vaca SC, Reith MEA, Carr KD, Rice ME (2015) Insulin enhances striatal dopamine release by activating cholinergic interneurons and thereby signals reward. Nat Commun 6:1–12.

Straub C, Saulnier JL, Bègue A, Feng DD, Huang KW, Sabatini BL (2016) Principles of Synaptic Organization of GABAergic Interneurons in the Striatum. Neuron 92:84–92.

Straub C, Tritsch NX, Hagan N a., Gu C, Sabatini BL (2014) Multiphasic Modulation of Cholinergic Interneurons by Nigrostriatal Afferents. J Neurosci 34:8557–8569.

Stuber GD, Hnasko TS, Britt JP, Edwards RH, Bonci A (2010) Dopaminergic Terminals in the Nucleus Accumbens But Not the Dorsal Striatum Corelease Glutamate. J Neurosci 30:8229–8233.

Stuber GD, Klanker M, de Ridder B, Bowers MS, Joosten RN, Feenstra MG, Bonci A (2008) Reward-Predictive Cues Enhance Excitatory Synaptic Strength onto Midbrain Dopamine Neurons. Science (80-) 321:1690–1692.

Suaud-Chagny MF, Chergui K, Chouvet G, Gonon F (1992) Relationship between dopamine release in the rat nucleus accumbens and the discharge activity of dopaminergic neurons during local in vivo application of amino acids in the ventral tegmental area. Neuroscience 49:63–72.

Sulzer D, Cragg SJ, Rice ME (2016) Striatal dopamine neurotransmission: regulation of release and uptake. Basal Ganglia 6:123–148.

Sun BB, Chiu SY (1999) N-type calcium channels and their regulation by GABAB receptors in

axons of neonatal rat optic nerve. J Neurosci 19:5185–5194.

Sun F et al. (2018) A Genetically Encoded Fluorescent Sensor Enables Rapid and Specific Detection of Dopamine in Flies, Fish, and Mice. Cell 174:481-496.e19.

Surmeier DJ, Song WJ, Yan Z (1996) Coordinated expression of dopamine receptors in neostriatal medium spiny neurons. J Neurosci 16:6579–6591.

Surmeier DJ, Sulzer D (2013) The pathology roadmap in Parkinson disease. Prion 7:85–91.

Talan M (1984) Body temperature of C57BL/6J mice with age. Exp Gerontol.

Tan KR, Yvon C, Turiault M, Mirzabekov JJ, Doehner J, Labouèbe G, Deisseroth K, Tye KM, Lüscher C (2012) GABA Neurons of the VTA Drive Conditioned Place Aversion. Neuron 73:1173–1183.

Taschenberger G, Garrido M, Tereshchenko Y, Bähr M, Zweckstetter M, Kügler S (2012) Aggregation of αSynuclein promotes progressive in vivo neurotoxicity in adult rat dopaminergic neurons. Acta Neuropathol 123:671–683.

Taylor TN, Potgieter D, Anwar S, Senior SL, Janezic S, Threlfell S, Ryan B, Parkkinen L, Deltheil T, Cioroch M, Livieratos A, Oliver PL, Jennings K a., Davies KE, Ansorge O, Bannerman DM, Cragg SJ, Wade-Martins R (2014) Region-specific deficits in dopamine, but not norepinephrine, signaling in a novel A30P ??-synuclein BAC transgenic mouse. Neurobiol Dis 62:193–207.

Tecuapetla F, Patel JC, Xenias H, English D, Tadros I, Shah F, Berlin J, Deisseroth K, Rice ME, Tepper JM, Koos T (2010) Glutamatergic signaling by mesolimbic dopamine neurons in the nucleus accumbens. J Neurosci 30:7105–7110.

Tepper JM, Bolam JP (2004) Functional diversity and specificity of neostriatal interneurons. Curr Opin Neurobiol 14:685–692.

Tepper JM, Koós T, Ibanez-Sandoval O, Tecuapetla F, Faust TW, Assous M (2018) Heterogeneity and Diversity of Striatal GABAergic Interneurons: Update 2018. Front Neuroanat 12:91.

Tepper JM, Sawyer SF, Groves PM (1987) Electrophysiologically identified nigral dopaminergic neurons intracellularly labeled with HRP: light-microscopic analysis. J Neurosci 7:2794–2806.

Thivierge J-P, Rivest F, Monchi O (2007) Spiking neurons, dopamine, and plasticity: Timing is everything, but concentration also matters. Synapse 61:375–390.

Threlfell S, Clements M a, Khodai T, Pienaar IS, Exley R, Wess J, Cragg SJ (2010) Striatal muscarinic receptors promote activity dependence of dopamine transmission via distinct receptor subtypes on cholinergic interneurons in ventral versus dorsal striatum. J Neurosci 30:3398–3408.

Threlfell S, Lalic T, Platt NJ, Jennings KA, Deisseroth K, Cragg SJ (2012) Striatal Dopamine Release Is Triggered by Synchronized Activity in Cholinergic Interneurons. Neuron 75:58–64.

Toomey JS, Bhatia S, Moon LT, Orchard EA, Tainter KH, Lokitz SJ, Terry T, Mathis JM, Penman

AD (2012) Pet imaging a MPTP-induced mouse model of Parkinson's disease using the fluoropropyl-dihydrotetrabenazine analog [18F]-DTBZ (AV-133). PLoS One 7:1–8.

Trigo FF, Marty A, Stell BM (2008) Axonal GABAA receptors. Eur J Neurosci 28:841–848.

Tritsch NX, Ding JB, Sabatini BL (2012) Dopaminergic neurons inhibit striatal output through non-canonical release of GABA. Nature 490:262–266.

Tritsch NX, Granger AJ, Sabatini BL (2016) Mechanisms and functions of GABA co-release. Nat Rev Neurosci 17:139–145.

Tritsch NX, Oh WJ, Gu C, Sabatini BL (2014) Midbrain dopamine neurons sustain inhibitory transmission using plasma membrane uptake of GABA, not synthesis. Elife 2014:1–20.

Tsai H-C, Zhang F, Adamantidis A, Stuber GD, Bonci A, de Lecea L, Deisseroth K (2009) Phasic firing in dopaminergic neurons is sufficient for behavioral conditioning. Science 324:1080–1084.

Tunstall MJ, Oorschot DE, Kean A, Wickens JR (2002) Inhibitory Interactions Between Spiny Projection Neurons in the Rat Striatum. J Neurophysiol 88:1263–1269.

Ulrich D, Bettler B (2007) GABAB receptors: synaptic functions and mechanisms of diversity. Curr Opin Neurobiol 17:298–303.

Ungerstedt U (1971) Stereotaxic Mapping of the Monoamine Pathways in the Rat Brain*. Acta Physiol Scand 82:1–48.

Urban DJ, Roth BL (2015) DREADDs (designer receptors exclusively activated by designer drugs): chemogenetic tools with therapeutic utility. Annu Rev Pharmacol Toxicol 55:399–417.

Usiello A, Baik J-H, Rougé-Pont F, Picetti R, Dierich A, LeMeur M, Piazza PV, Borrelli E (2000) Distinct functions of the two isoforms of dopamine D2 receptors. Nature 408:199–203.

Vaaga CE, Borisovska M, Westbrook GL (2014) Dual-transmitter neurons: functional implications of co-release and co-transmission. Curr Opin Neurobiol 29:25–32.

Valjent E, Bertran-Gonzalez J, Bowling H, Lopez S, Santini E, Matamales M, Bonito-Oliva A, Hervé D, Hoeffer C, Klann E, Girault J-A, Fisone G (2011) Haloperidol regulates the state of phosphorylation of ribosomal protein S6 via activation of PKA and phosphorylation of DARPP-32. Neuropsychopharmacology 36:2561–2570.

van Zessen R, Phillips JL, Budygin EA, Stuber GD (2012) Activation of VTA GABA Neurons Disrupts Reward Consumption. Neuron 73:1184–1194.

Van Bockstaele EJ, Pickel VM (1995) GABA-containing neurons in the ventral tegmental area project to the nucleus accumbens in rat brain. Brain Res 682:215–221.

van den Pol AN (2012) Neuropeptide Transmission in Brain Circuits. Neuron 76:98–115.

van der Westhuizen ET, Valant C, Sexton PM, Christopoulos A (2015) Endogenous allosteric modulators of G protein-coupled receptors. J Pharmacol Exp Ther 353:246–260.

Venda LL, Cragg SJ, Buchman VL, Wade-Martins R (2010) α -Synuclein and dopamine at the crossroads of Parkinson ' s disease. Trends Neurosci 33:559–568.

Verdier D, Lund JP, Kolta A (2003) GABAergic Control of Action Potential Propagation along Axonal Branches of Mammalian Sensory Neurons. J Neurosci 23:2002–2007.

Vergara R, Rick C, Hernández-López S, Laville JA, Guzman JN, Galarraga E, Surmeier DJ, Bargas J (2003) Spontaneous Voltage Oscillations in Striatal Projection Neurons in a Rat Corticostriatal Slice. J Physiol 553:169–182.

Vilaró MT, Palacios JM, Mengod G (1990) Localization of m5 muscarinic receptor mRNA in rat brain examined by in situ hybridization histochemistry. Neurosci Lett 114:154–159.

Voorn P, Vanderschuren LJMJ, Groenewegen HJ, Robbins TW, Pennartz CMA (2004) Putting a spin on the dorsal-ventral divide of the striatum. Trends Neurosci 27:468–474.

Waldvogel HJ, Billinton A, White JH, Emson PC, Faull RLM (2004) Comparative cellular distribution of GABAA and GABAB receptors in the human basal ganglia: immunohistochemical colocalization of the alpha 1 subunit of the GABAA receptor, and the GABABR1 and GABABR2 receptor subunits. J Comp Neurol 470:339–356.

Waldvogel HJ, Fritschy JM, Mohler H, Faull RLM (1998) GABA(A) receptors in the primate basal ganglia: An autoradiographic and a light and electron microscopic immunohistochemical study of the α1 and β2,3 subunits in the baboon brain. J Comp Neurol 397:297–325.

Wall NR, De La Parra M, Callaway EM, Kreitzer AC (2013) Differential Innervation of Direct- and Indirect-Pathway Striatal Projection Neurons. Neuron 79:347–360.

Wall PD (1995) Do nerve impulses penetrate terminal arborizations? A pre-presynaptic control mechanism. Trends Neurosci 18:99–103.

Wang L, Shang S, Kang X, Teng S, Zhu F, Liu B, Wu Q, Li M, Liu W, Xu H, Zhou L, Jiao R, Dou H, Zuo P, Zhang X, Zheng L, Wang S, Wang C, Zhou Z (2014) Modulation of dopamine release in the striatum by physiologically relevant levels of nicotine. Nat Commun 5:3925.

Wang Z, Kai L, Day M, Ronesi J, Yin HH, Ding J, Tkatch T, Lovinger DM, Surmeier DJ (2006) Dopaminergic Control of Corticostriatal Long-Term Synaptic Depression in Medium Spiny Neurons Is Mediated by Cholinergic Interneurons. Neuron 50:443–452.

Weiner DM, Levey AI, Brann MR (1990) Expression of muscarinic acetylcholine and dopamine receptor mRNAs in rat basal ganglia. Proc Natl Acad Sci U S A 87:7050.

Westberg K-G, Kolta A, Clavelou P, Sandström G, Lund JP (2000) Evidence for functional compartmentalization of trigeminal muscle spindle afferents during fictive mastication in the rabbit. Eur J Neurosci 12:1145–1154.

Williams MJ, Adinoff B (2008) The role of acetylcholine in cocaine addiction. Neuropsychopharmacology 33:1779–1797.

Wilson CJ, Groves PM (1981) Spontaneous firing patterns of identified spiny neurons in the rat neostriatum. Brain Res 220:67–80.

Wilson CJ, Kawaguchi Y (1996) The Membrane Potential in the Up State of Striatal Neurons is Determined by Voltage-Activated Potassium Currents. In, pp 131–139. Springer,

Boston, MA.

Wójtowicz AM, Dvorzhak A, Semtner M, Grantyn R (2013) Reduced tonic inhibition in striatal output neurons from Huntington mice due to loss of astrocytic GABA release through GAT-3. Front Neural Circuits 7:188.

Woods KA, Camacho-Hübner C, Savage MO, Clark AJ (1996) Intrauterine growth retardation and postnatal growth failure associated with deletion of the insulin-like growth factor I gene. N Engl J Med 335:1363–1367.

Wooltorton JRA, Pidoplichko VI, Broide RS, Dani JA (2003) Differential desensitization and distribution of nicotinic acetylcholine receptor subtypes in midbrain dopamine areas. J Neurosci 23:3176–3185.

Yamada T, McGeer PL, Baimbridge KG, McGeer EG (1990) Relative sparing in Parkinson's disease of substantia nigra dopamine neurons containing calbindin-D28K. Brain Res 526:303–307.

Yan Z, Song W-J, Surmeier DJ (1997) D2 Dopamine Receptors Reduce N-Type Ca2+ Currents in Rat Neostriatal Cholinergic Interneurons Through a Membrane-Delimited, Protein-Kinase-C-Insensitive Pathway. J Neurophysiol 77:1003–1015.

Yan Z, Surmeier DJ (1997) D5 dopamine receptors enhance Zn2+-sensitive GABA(A) currents in striatal cholinergic interneurons through a PKA/PP1 cascade. Neuron 19:1115–1126.

Yasumi M, Sato K, Shimada S, Nishimura M, Tohyama M (1997) Regional distribution of GABA transporter 1 (GAT1) mRNA in the rat brain: comparison with glutamic acid decarboxylase67 (GAD67) mRNA localization. Brain Res Mol Brain Res 44:205–218.

Yetnikoff L, Lavezzi HN, Reichard RA, Zahm DS (2014) An update on the connections of the ventral mesencephalic dopaminergic complex. Neuroscience 282:23–48.

Yin HH, Knowlton BJ (2006) The role of the basal ganglia in habit formation. Nat Rev Neurosci 7:464–476.

Yin HH, Knowlton BJ, Balleine BW (2004) Lesions of dorsolateral striatum preserve outcome expectancy but disrupt habit formation in instrumental learning. Eur J Neurosci 19:181–189.

Yin HH, Mulcare SP, Hilário MRF, Clouse E, Holloway T, Davis MI, Hansson AC, Lovinger DM, Costa RM (2009) Dynamic reorganization of striatal circuits during the acquisition and consolidation of a skill. Nat Neurosci 12:333–341.

Yin HH, Ostlund SB, Knowlton BJ, Balleine BW (2005) The role of the dorsomedial striatum in instrumental conditioning. Eur J Neurosci 22:513–523.

Yorgason JT, Zeppenfeld DM, Williams JT (2017) Cholinergic Interneurons Underlie Spontaneous Dopamine Release in Nucleus Accumbens. J Neurosci 37:2086–2096.

Yu S, Li X, Liu G, Han J, Zhang C, Li Y, Xu S, Liu C, Gao Y, Yang H, Uéda K, Chan P (2007) Extensive nuclear localization of α-synuclein in normal rat brain neurons revealed by a novel monoclonal antibody. Neuroscience 145:539–555.

Yu X, Taylor AMW, Nagai J, Golshani P, Evans CJ, Coppola G, Khakh BS (2018) Reducing

Astrocyte Calcium Signaling In Vivo Alters Striatal Microcircuits and Causes Repetitive Behavior. Neuron 99:1170-1187.e9.

Yung KK, Ng TK, Wong CK (1999) Subpopulations of neurons in the rat neostriatum display GABABR1 receptor immunoreactivity. Brain Res 830:345–352.

Zhang F, Vierock J, Yizhar O, Fenno LE, Tsunoda S, Kianianmomeni A, Prigge M, Berndt A, Cushman J, Polle J, Magnuson J, Hegemann P, Deisseroth K (2011) The microbial opsin family of optogenetic tools. Cell 147:1446–1457.

Zhang H, Sulzer D (2003) Glutamate spillover in the striatum depresses dopaminergic transmission by activating group I metabotropic glutamate receptors. J Neurosci 23:10585–10592.

Zhang H, Sulzer D (2004) Frequency-dependent modulation of dopamine release by nicotine. Nat Neurosci 7:581–582.

Zhang S, Qi J, Li X, Wang H-L, Britt JP, Hoffman AF, Bonci A, Lupica CR, Morales M (2015) Dopaminergic and glutamatergic microdomains in a subset of rodent mesoaccumbens axons. Nat Neurosci 18:386–392.

Zhang SJ, Jackson MB (1993) GABA-activated chloride channels in secretory nerve endings. Science (80-) 259:531–534.

Zhang SJ, Jackson MB (1995) GABAA receptor activation and the excitability of nerve terminals in the rat posterior pituitary. J Physiol 483 (Pt 3:583–595.

Zhou FM, Liang Y, Dani JA (2001) Endogenous nicotinic cholinergic activity regulates dopamine release in the striatum. Nat Neurosci 4:1224–1229.

Ziegler N, Bätz J, Zabel U, Lohse MJ, Hoffmann C (2011) FRET-based sensors for the human M1-, M3-, and M5-acetylcholine receptors. Bioorg Med Chem 19:1048–1054.